DEVELOPING DEFLECTION ACCEPTANCE CRITERIA FOR COMPACTED, OPEN-GRADED AGGREGATE BASES FOR PERMEABLE PAVEMENTS USING LIGHTWEIGHT DEFLECTOMETER

PROJECT FINAL REPORT-REVISED

PREPARED FOR

INTERLOCKING CONCRETE PAVEMENT INSTITUTE FOUNDATION

PRINCIPAL INVESTIGATOR
DEBAKANTA (DEB) MISHRA, PH.D., P.E.

GRADUATE RESEARCH ASSISTANT
RATUL MONDAL
MD. FAZLE RABBI

SCHOOL OF CIVIL AND ENVIRONMENTAL ENGINEERING
OKLAHOMA STATE UNIVERSITY

SCHOOL OF
CIVIL AND ENVIRONMENTAL ENGINEERING
College of Engineering, Architecture and Technology

FEBRUARY 2022

TABLE OF CONTENTS

LIST OF FIGURES

LIST OF TABLES

CHAPTER 1: INTRODUCTION

Unbound aggregate pavement (base/subbase) layers are usually constructed using locally available aggregate materials to avoid material transportation costs. As these layers primarily rely on aggregate-interlock for their shear strength and modulus properties, degree of compaction largely governs their behavior under loading. Traditionally, dense-graded aggregates are used to construct pavement base/subbase layers, which serve as a major load-bearing layer in conventional flexible pavement structures. However, mechanical properties (such as shear strength and resilient modulus) of dense-graded aggregate layers tend to be significantly affected under fluctuating moisture conditions. The shear strength of these layers may be substantially reduced under high moisture conditions, making them prone to severe permanent deformation or even shear failure. Moreover, recurrent freeze–thaw cycles can drastically undermine the stability (under loading) of a well-compacted dense-graded base/subbase layer. For use in unbound granular pavement layers, Open-Graded Aggregate (OGA) materials can have numerous benefits over their dense-graded counterparts. The low fines content, for example, results in better drainage characteristics making the layer much less susceptible to moisture-induced and freeze–thaw-related damage. Furthermore, OGA layers often have larger top-sizes, which contributes to increased shear strength under well-compacted conditions.

Despite their numerous benefits, long- and short-term performance of OGA materials as base/subbase layers has not been investigated thoroughly. Limited number of research publications have focused on the performance of OGA materials as base/subbase layers. One of the most likely explanations involves the lack of standard compaction and construction specifications for these materials. OGA materials present significant challenges when it comes to density-based compaction control. Although the compaction process is similar to that for dense-graded aggregate layers (vibratory compaction), large void-spaces in the aggregate matrix make in-situ density measurements virtually impossible; conventional density verification techniques such as the nuclear density gauge are impractical. Setting a precise target during field compaction is quite challenging in such situations. Rather than attempting to satisfy any target compaction-control criterion, the current practice is to compact these layers using recipe-based approaches. For example, some highway agency specifications require these layers to be compacted “to the engineer’s satisfaction”. Some others, on the other hand, specify a certain number of passes of a vibratory roller compactor before an OGA layer is considered to be ‘satisfactorily compacted’. Obviously, such compaction specifications do not ensure adequate performance of the layer under loading and need to be updated. Deflection-based compaction control can be a suitable alternative for such layers as it would also give an indication regarding layer performance under loading. This research report documents findings from a recently completed research study conducted in collaboration between the Interlocking Concrete Pavement Institute Foundation (ICPIF) and Oklahoma State University, aimed at developing a deflection-based compaction control protocol for OGA base/subbase courses.

RESEARCH OBJECTIVE AND SCOPE

The primary objective of this research was to develop a mechanics-based compaction assessment protocol for OGA base/subbase courses used under permeable pavements. This was accomplished by studying the packing characteristics of two different OGA materials, conforming to ASTM # 4 and ASTM # 57 specifications, respectively, under different compaction conditions. Portable Impulse Plate Load Test

Devices (PIPLTD), such as the Light Weight Deflectometer (LWD) were used as the deflection measurement device of choice in this study. Technically, an LWD, as defined in ASTM E2583, must have a load cell to measure the load levels applied by each drop. A PIPLTD, on the other hand, is a more generic category (refer to ASTM E2835) and does not have a requirement regarding load cells. The current research effort uses devices of both types (with and without load cells). Therefore, the devices used in the current study, technically fall under the PIPLTD category. Nevertheless, as it is common in the engineering community, both device types have been referred to in this report as LWDs. Multiple LWD units were utilized in this research effort to ensure the research results, as well as developed compaction protocols were device-agnostic. This study used an integrated approach including extensive laboratory testing, numerical modeling, and full-scale pavement testing to accomplish the overall research objectives.

The laboratory testing phase in this study involved aggregate testing at two different scales (or two phases) to evaluate how the behavior of OGA materials could be affected by testing boundary conditions. The first phase involved small-scale testing inside conventional and custom-made Proctor molds. The objective was to develop a laboratory testing protocol that can be used by state or local highway agencies to establish target compaction conditions for OGA materials of interest. These laboratory test results can then be used as references during field construction. The second phase of laboratory testing involved intermediate-scale specimens inside a wooden box of dimensions: 1.2 m x 1.2 m x 1.2 m. OGA materials were placed in this box to construct layers of different thicknesses and were compacted using different number of passes of a vibratory plate compactor. LWD tests were conducted after each compactive effort to track the evolution of packing in the aggregate layer, and the subsequent effect on LWD-measured surface deflections. The objective of intermediate-scale laboratory testing was to assess how they compared against the small-scale results, and whether the intermediate-scale test set-up was sufficiently large to eliminate boundary conditions during testing. If free from boundary effects, the intermediate-scale test results can give a picture of the expected OGA layer behavior in the field under different compaction conditions.

The field-testing effort involved construction a full-scale pavement section with multiple test cells, where OGA materials were used to construct base/subbase layers of different thicknesses, and their compaction behavior was studied through LWD testing after different number of vibratory roller passes. The test cells were constructed to represent different thickness combinations commonly used in the construction of permeable pavements. Different lift thicknesses were incorporated into the construction plan to identify any effect of lift thickness on compaction evolution in OGA materials. The subgrade conditions were varied by targeting a certain degree of compaction for half of the cells, and not specifying any subgrade compaction criteria for the remainder. Similarly, a geotextile was placed at the subgrade-subbase interface for half of the cells, with no geotextile placement for the remainder. LWD testing was carried out on the subgrade as well as the aggregate lifts after each pass of the compactor to study how the LWD-measured surface deflections were affected by different construction variables.

This project also involved a numerical modeling task to study the compaction evolution in OGA materials using the Discrete Element Method (DEM). The DEM work involved simulation of LWD tests on OGA materials placed in a custom-made large Proctor mold. Results from the DEM work has been included as a stand-alone research manuscript that will be submitted to a journal (see Appendix A of this report).

Successful completion of this multi-phased study and implementation of the newly developed compaction control methodology will facilitate the construction of better-performing pavement base/subbase courses using OGA materials. This research's primary outcome was a recommended testing approach for compaction control of pavement base/subbase layers using OGA materials.

CHAPTER 2: LITERATURE REVIEW

Pavement unbound layers, e.g. subgrade, subbase and base, provide foundation support during the surface layer construction, and impart strength and stability to the pavement structure under repetitive vehicular loading. As the subgrade and base/subbase layers are mostly constructed using locally available soils and aggregates, stability of these layers greatly depends on construction practices, particularly the degree of compaction. Quality Control and Quality Assurance (QC/QA) practices for unbound pavement layer construction have traditionally been based on target density values. These target density values are calculated as certain percentages of the maximum achievable densities established for the given materials through laboratory testing. The most common examples of laboratory compaction tests include: the standard and modified compaction methods, also referred to as the Proctor methods. In-place densities of the unbound layers being constructed are determined using nuclear density gauges (NDG) or other accepted methods (e.g. the sand cone method). The in-place densities are then compared against the target density values established through laboratory testing.

However, such density-based compaction control has several limitations. For example, the NDG utilizes a probe with a radioactive source, and requires adherence to complex safety regulations for , storage and transportation. On the other hand, the sand cone method is time-consuming, and is not expedient. Moreover, density is not a mechanistic property directly used in the design and analysis of pavements. Although several researchers in the past have correlated higher densities to unbound layer stiffness or resilient modulus improvements (Rowshanzamir 1995; Tutumluer and Seyhan 1998), mechanistic-empirical (M-E) pavement design methods do not consider soil/aggregate layer density as a mechanistic input parameter.

The resilient modulus on the other hand, governs the nature of stress dissipation and resulting strains in a soil/aggregate layer under loading, and is therefore an essential input for mechanistic analysis and performance prediction of a pavement structure. This fact alone has made the alternative of measuring in-situ layer modulus very attractive for pavement designers. Nevertheless, now the primary challenge is developing related construction specifications that incorporate the determination of field modulus values for soil subgrades and pavement layers.

The need for developing specifications for compaction control is more critical for OGA materials where traditional density measurement approaches such as the ‘backscatter’ mode of nuclear density gauges presents some potential for variability from the nature of the test. Also, it is important to note that it is ‘nearly impossible’ to insert the probe of a nuclear density gauge into an OGA layer. By contrast, compaction control specifications developed based on deflection (or stiffness) criteria can be particularly useful. Ultimately, the ‘stability’ of a constructed unbound layer is reflected through the amount of deformation (elastic or plastic) it undergoes under loading.

Therefore, compaction specifications based on deflection criteria can be more easily related to pavement performance under loading compared to density-based specifications. Adoption of deflection-based compaction control specifications will be particularly beneficial to the design and construction of better-performing pavement unbound layers. The Light-Weight Deflectometer (LWD) is one such device that

can be used to measure in-place deflections and layer modulus, and can be used for compaction quality assurance without excessive delay to construction activities.

THE LIGHT WEIGTH DEFLECTOMETER AND ITS WORKING PRINCIPLE

The Lightweight Deflectometer (LWD was first developed in Germany with the aim of easily measuring the in-situ modulus of highway materials. In the US, several state Departments of Transportation (DOTs) such as Florida, Indiana, and Minnesota have recently adopted compaction control specifications for dense-graded aggregate base layers using LWDs. Recently, Schwartz et al. (2017) developed a new specification for consideration by the American Association of State Highway and Transportation Officials (AASHTO) for using LWDs for compaction control of subgrades and dense-graded aggregate layers.

Basic Features of an LWD

Different types of LWDs are available and show similarities in the mechanics of their operation irrespective of minor design and operational differences. Because of its light weight, portability, and ease of operation, the LWD has become a device of choice for in-situ layer modulus measurement on soils and aggregates. Researchers in the past have reported that LWD devices from different manufacturers give slightly different results depending on their inherent design and operational differences (Puppala 2008; Ryden and Mooney 2009; Vennapusa and White 2007). The LWD is also referred to as a portable falling weight deflectometer (PFWD) because of similarities in operational principles between the two devices. Figure 1 shows the schematic diagram of a typical LWD device; The equipment has three major components: (1) drop weight, (2) loading plate, and (3) geophone. The weight release, a fix-and-release mechanism at the top helps to hold the drop weight at a certain height before being dropped. A buffer system is used on top of the loading plate for facilitating uniform transmission of the stress pulse generated from the dropping mass.

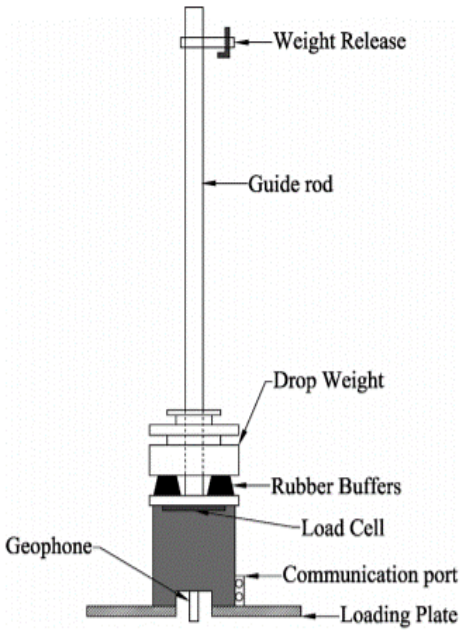

Figure 1. Schematic of a typical LWD device (Vennapusa and White 2007)

Some of the original LWD devices used around the world were Prima 100, the TRL Foundation Tester (Rogers et al. 1995), The German Dynamic Plate Bearing Test (GDP) (Kudla et al. 1991), and the Loadman (Gros 1993). Inherent features of these devices, and their adequacy for in-situ layer modulus measurement were studied by several researchers (Flemming et al. 2000; Mooney et al. 2009 and George 2006). These earlier versions of LWDs used a velocity transducer (or geophone) for deflection measurement through single integration of the velocity measured on the surface of the layer being tested.

Over the years, several other companies have started producing LWD systems commercially. The devices that are readily available in the US are those manufactured by Dynatest Corporation, Olson Engineering, or Zorn Instruments. Table 1 lists the typical features of these LWDs used by researchers and/or practitioners. Among several differences between the devices as listed in Table 1, it should be noted that the Zorn does not directly measure the load being applied by the dropping mass. The Dynatest and the Olson devices, on the other hand, use load cells to measure the applied forces.

Table 1. Features of LWDs Most Commonly Used in the United States

Manufacturer	Dynatest	Olson	Zorn
Plate Style	Annulus	Plate	Plate
Plate Dia (mm)	150, 200, 300	100, 150, 200, 300	100, 150, 200, 300
Drop Mass (kg)	10, 15, 20	3.6, 10, 15, 20	5, 10, 15
Drop Height (m)	Variable	600mm (max)	5 (kg) 35cm, 10 and15 (kg) 72cm and 54cm (200mm dia). All are Nominal Exact Height is Set by Calibration
Damper	Rubber	Steel Spring	Steel Spring
Force Measurement	Yes	Yes (Load cell)	No (Based on Calibration of Drop Height)
Plate Response Sensor	Geophone	Geophone	Accelerometer
Impulse time, ms	15-30	16 nominal (15-20)	15.5 (nominal)
Max Load (kN)	1-25	1.7-13.8	3.5 - 10.5
Contact Stress	User Defined	User Selectable	Varies by Height and Weight
Poisson's Ratio	User Defined	User Selectable	Fixed -0.5

LWD Working Principle

The LWD is a dynamic plate load testing device which can be used to determine the modulus of pavement unbound materials such as subgrade soils or base aggregates. This system applies a pulse load to a disk-shaped steel or aluminum plate. Once the drop weight is released, it hits a spring-dashpot unit which is attached to the plate in contact with ground. The plate and the ground move together in a coupled model which is analogous to a two degree-of-freedom mass-spring-damper system. Figure 2 presents a schematic illustrating the mechanics of interaction between the LWD and the ground surface during impulse-based modulus measurement.

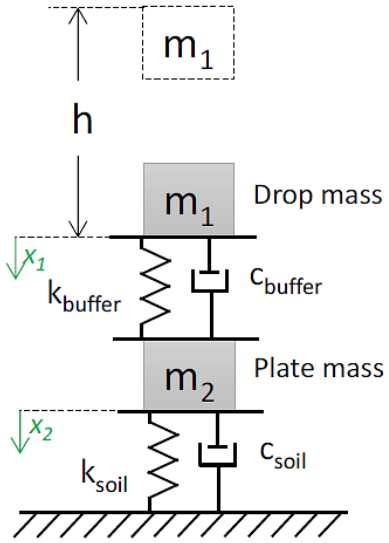

Figure 2. Two degrees of freedom system representing LWD-ground movement (Schwartz et al. 2017)

The velocity sensor/geophone measures the ground movement and load cell measures the load imparted by the falling weight. LWDs have different types of sensors at different locations. The maximum displacement of the ground surface after each drop is calculated by means of double/single integration of the acceleration/velocities. Some of the LWDs available in the market (e.g. the one manufactured by Dynatest) provide additional geophones to measure the surface deflection at fixed radial offsets from the center of the loading plate. Figure 3 shows example load- and deflection- time histories obtained during LWD testing of geomaterials (soils or aggregates).

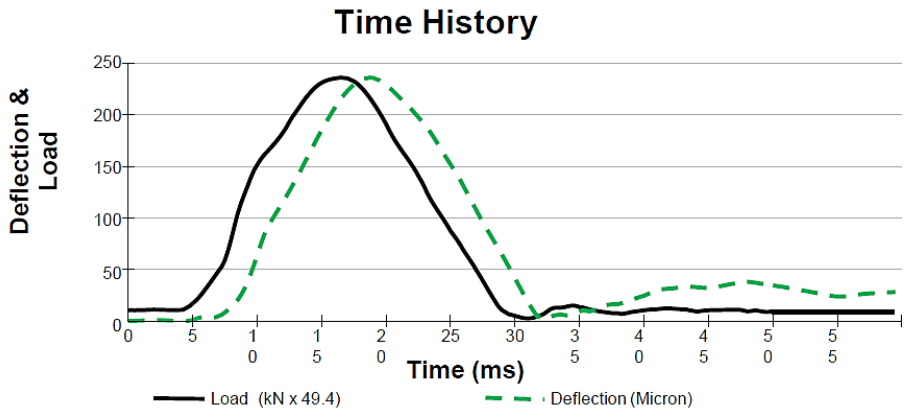

Figure 3. Example of load and deflection time history obtained during LWD testing of geomaterials

Modulus Calculation Technique

A velocity sensor/geophone measures the ground movement, and a load cell measures the load applied by the falling weight. One of the LWDs (Zorn) used in this study does not have a load cell to directly measure the force being applied through the dropped weight. Rather, a pre-established calibration is used

to "estimate" the force based on the drop height. The recorded maximum surface displacement corresponding to the maximum applied force is used to calculate the surface layer modulus. The formula used to calculate the modulus of the LWD tested layer is derived from using Boussinesq's principle (see Equation 1).

$$E = \frac{2 \times k_s \times \left(1 - \nu^2\right)}{A \times r_0} \text{ ----------(1)}$$

In Equation-1, A is the stress distribution factor, ν is the Poisson's ratio, r is the plate radius, and k_s is the stiffness of material which is the ratio between peak load and peak deflection values measured under a particular drop of the mass. Equation (1) was developed assuming the test medium to be linear-elastic, isotropic, homogenous, and semi-infinite. The shape factor to determine the contact stress distribution between the plate and soil is assumed with the Poisson's ratio. The stress distribution under the plate can be defined as a function of plate rigidity and soil types (Terzaghi et al. 1996). White et al. (2007) listed the shape factor values for different conditions. Figure 4 shows the stress distribution characteristics for different types of soils and loading plates. *Unfortunately, no such shape factor was found in the literature for OGA materials.*

Plate Type	Soil Type	Stress Distribution		Shape factor (*f*)
Rigid	Clay (elastic material)	Inverse Parabolic	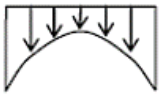	π/2
Rigid	Cohesionless sand	Parabolic	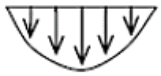	8/3
Rigid	Material with intermediate characteristics	Inverse Parabolic to Uniform	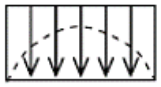	π/2 to 2
Flexible	Clay (elastic material)	Uniform	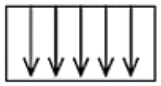	2
Flexible	Cohesionless Sand	Parabolic	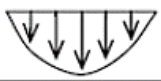	8/3

Figure 4. Stress distribution factors for estimating LWD modulus value (White et al. 2007)

Schwartz et al. (2017) performed LWD tests directly on Proctor molds to establish target field modulus values at a given soil moisture content. He used LWD plate diameters that were slightly smaller than the diameter of the Proctor mold. In this case, the equation used to measure the modulus of dense-graded aggregate materials inside the mold was derived from the theory of elasticity for a cylinder (elastic material) with a constrained lateral deflection, as shown in Equation-2.

$$E = \left(1 - \frac{2 \times \nu^2}{1 - \nu}\right) \times \frac{4H}{\pi D^2} \times k \quad \text{----------(2)}$$

Here, ν is the Poisson's ratio, H is the mold's height, D is the plate or mold diameter, k is soil stiffness (ratio of peak force to peak deflection).

LWD-measured modulus values in a Proctor mold can be different from the resilient modulus test results for three reasons: (a) different stress paths in the two tests (See Figure 4); (b) assumption of Poisson's ratio during LWD-based calculations; and (c) difference in the type of strain being measured: resilient strain measured for M_R calculations, vs. total strain measured during LWD measurements. During resilient modulus testing, a constant confining pressure is applied throughout the test. With that, axial deviator stress is applied, which increases the confining pressure (σ_3) to total axial stress (σ_1). On the other hand, during LWD testing on mold, both confining pressure (σ_3) and total axial stress (σ_1) start from zero and rapidly rise to its maximum value. These differences are illustrated in Figure 5. Although those tests are different, researchers correlated the M_r with LWD lab modulus for the dense-graded aggregates materials (Schwartz et al., 2017, Jibon et al., 2020).

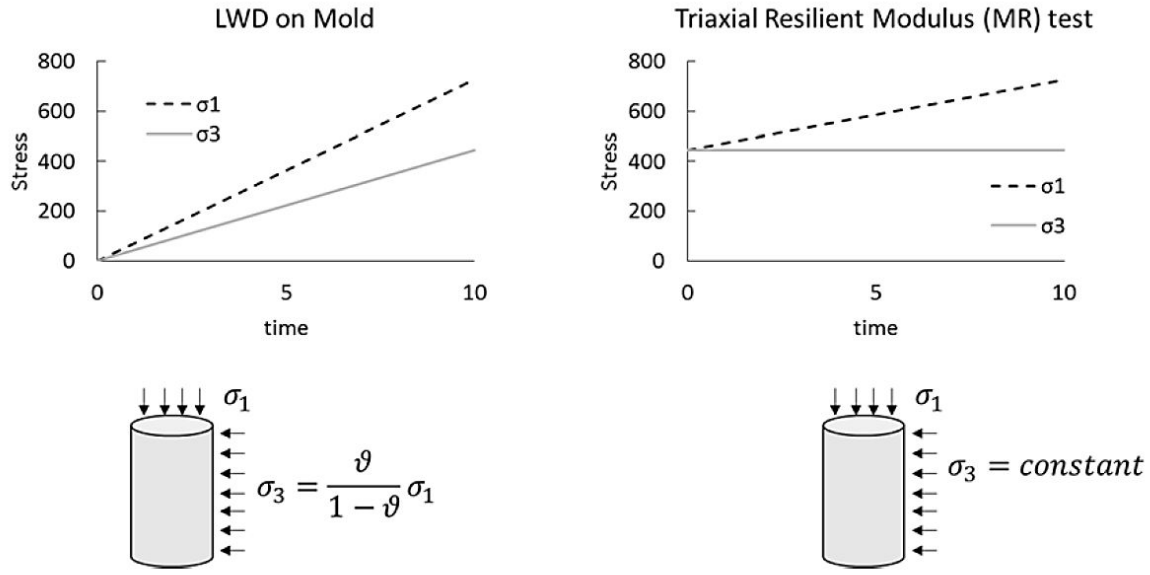

Figure 5. Stress path difference in LWD test on mold versus M_R (Schwartz et al. 2017)

ESTABLISHING BENCHMARK VALUES FOR FIELD LWD TESTING

LWD testing of a geomaterial provides a deflection value either through direct measurement or through single/double integration of geophone/accelerometer measurements. The deflection of the layer can be used to calculate a layer modulus value. However, to justify use in mechanistic-empirical pavement design and analysis approaches, it is important for the LWD-measured modulus values to be first compared against more standard methods of modulus measurement. Several research efforts in the past have focused on large- or small-scale tests in the laboratory to establish the modulus values for soils and

aggregates, which can then be used as references/benchmarks against which to compare the LWD measurements.

Unbound materials subjected to traffic-induced stress pulses experience elastic and plastic deformations which are commonly known as 'resilient' and 'permanent' deformations in pavement applications, respectively. The response of a typical unbound material after being subjected to one cycle of pulsed loading is shown in Figure 6 (Mishra 2012). These resilient and plastic components of total strain depend on several factors such as number and magnitude of traffic load applications, speed of traffic operation, thickness of underlaying and overlaying layers, quality of materials etc. The accumulation of plastic strain gradually decreases with the number of load applications for typical unbound materials during the pavement service life.

Generally, well-compacted unbound layers become stable during the construction phase, and all subsequent loadings lead to elastic deformations. Ideally, a well-constructed pavement layer does not accumulate any permanent deformation during repeated traffic loadings which is a key assumption inherent to mechanistic empirical pavement design. Pavement ME considers only elastic response of materials for predicting critical pavement response parameters.

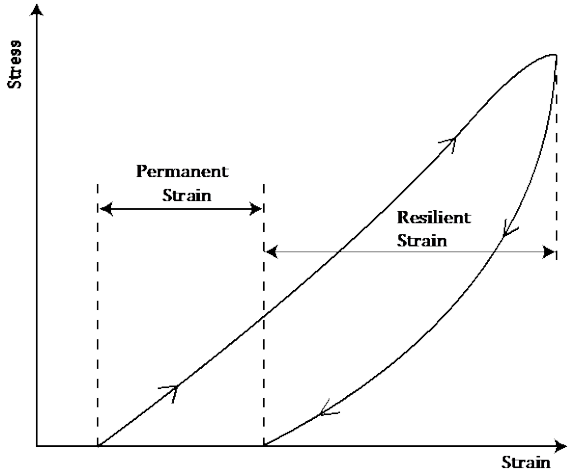

Figure 6. Stress strain response of unbound material under one cycle of loading (Mishra, 2012)

Resilient Modulus is a fundamental material property defined as the ratio of peak deviatoric stress to recoverable strain under repeated loading.

Figure 7 shows a typical stress-strain plot to define the concept of resilient modulus. Soil characterization under repeated loading helps understand material behavior under different stress fields, and facilitates accurate, mechanics-based pavement analysis for pavement response calculation. The resilient modulus of unbound materials is determined in laboratory through repeated load triaxial testing. AASHTO T-307 is the most commonly used laboratory testing procedure to establish the resilient modulus values for soils and aggregates. Cylindrical test specimens are subjected to fifteen different combinations of axial and confining stresses during this test, and the resilient modulus values corresponding to each stress state are calculated.

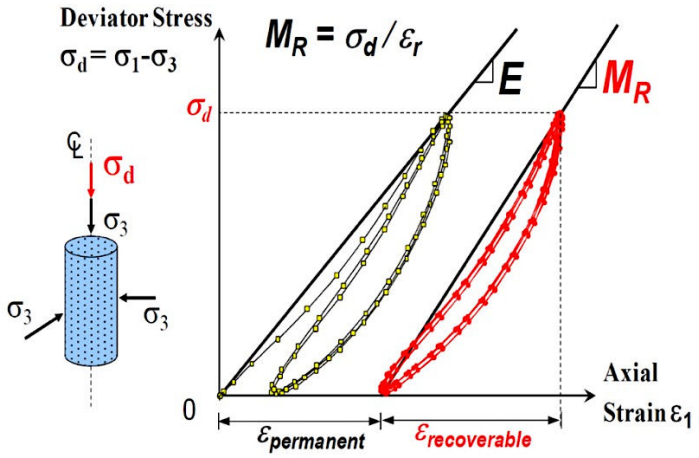

Figure 7. Graphical representation for defining Resilient Modulus of unbound materials (Tutumluer, 2013)

It is important to note that the resilient modulus of a soil or aggregate is not a constant value and is dependent on the stress states applied to the specimen. Typically, unbound aggregates exhibit stress-hardening behavior, whereas subgrade soils exhibit stress-softening behavior. Therefore, if the resilient modulus value of a constructed soil or aggregate layer is to be measured in the field, the stress-dependent nature of these materials must be considered. If an LWD is used in the field to measure the in-place modulus values, the LWD-measured modulus has to be compared/correlated to the resilient modulus of the same material measured in the laboratory.

The resilient modulus value of a soil/aggregate is significantly affected by several factors including moisture content, particle size distribution, type and amount of fines, etc. (Lekarp et al. 2000; Hopkins et al. 2004; Gupta et al. 2007 and Cary and Zapata 2010). However, routine resilient modulus testing is performed at optimum moisture content only in accordance with AASHTO T-307. Schwartz et al. (2014) evaluated the predictive capabilities of nine resilient modulus constitutive models and empirical predictive models for cohesive and non-cohesive soils. Statistical analysis of accuracy and bias of the predicted moduli at different moisture and density conditions showed that the accuracy of prediction was far away from acceptable. Accordingly, these constitutive models cannot be used to estimate target modulus values for LWD-based compaction quality control (Schwartz et al. 2014).

LWD Testing on a Proctor Mold

As the repeated load triaxial testing to determine resilient modulus is time consuming and complex in nature. Most of the State DOTs do not perform repeated load triaxial tests on a regular basis. Therefore, this requires an alternative way to establish the resilient modulus values of unbound materials in the laboratory. Nazarian et al. (2014) conducted a survey of highway agencies (or departments of transportation) of all US states and Canadian provinces and reported that only seven (7) agencies out of the twenty-seven (27) respondents, reported using repeated load triaxial testing to establish the resilient modulus values of soils and aggregates. That survey results from respondents are shown in Figure 8.

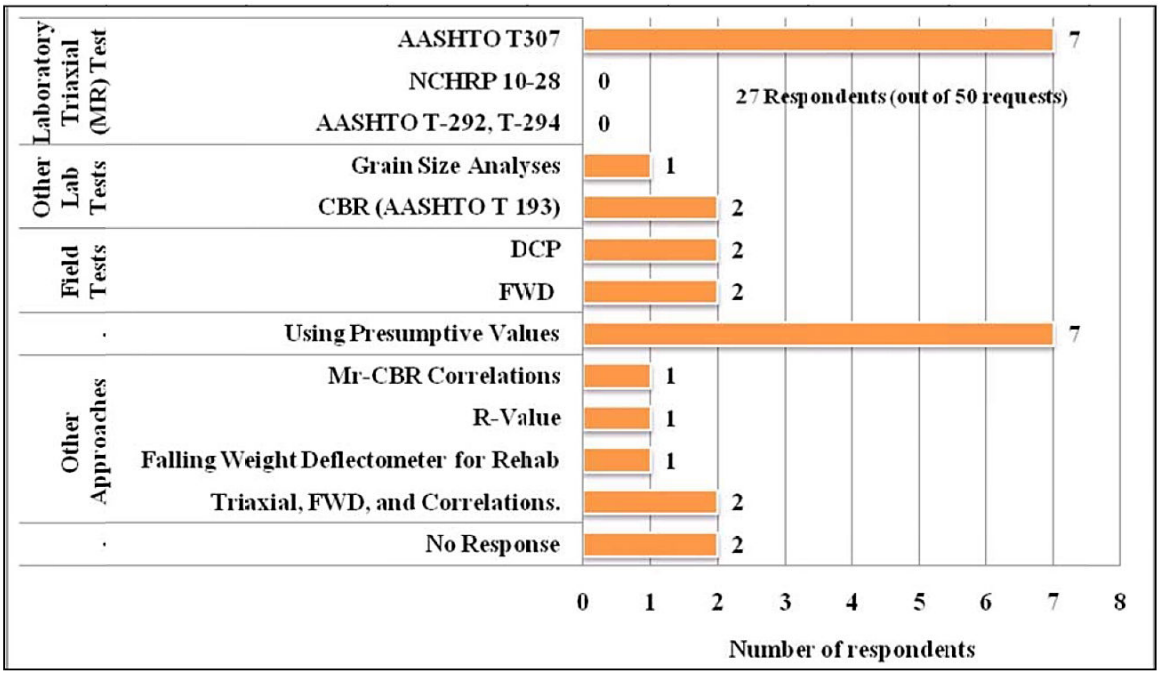

Figure 8. Different methods used by state DOTs to establish modulus values for pavement unbound materials (Nazarian et al. 2014)

Selecting Target Moduli from LWD Test on Mold

Schwartz et al. (2017) explains the procedure to establish a target field modulus value to facilitate LWD-based compaction quality control of soil and aggregate layers. They compacted specimens inside a 150-mm diameter Proctor mold under 3 to 6 different moisture conditions as per AASHTO T-99. LWD testing was conducted on the specimen after compaction and a modulus value corresponding to each moisture content was established. They studied the stress dependency and moisture dependency of the materials during this effort. Table 2 shows the different drop heights which were considered during LWD testing on the molds to evaluate stress dependency of the materials.

Table 2. Different Drop Heights for LWD Tests on Proctor Mold (Schwartz et al. 2017)

Drop Height	Zorn (cm)	Dynatest (cm)	Olson (cm)
h7	2.5	2.5	2.5
h8	5.1	5.1	5.1
h9	7.6	7.6	7.6
h10	10.2	10.2	10.2
h11	12.7	12.7	12.7
h12	31.8	17.8	21.6

A total of 6 drops at each drop height was performed. The maximum load applied by each LWD and the corresponding peak deformation for last three drops were averaged, and the modulus values were

calculated using Equation (5). The Coefficient of Variation (COV) of deflection values from the last three drops were calculated; any data with COV > 10% was excluded from target moduli calculations.

The results from the LWD testing in Proctor molds can be plotted similar to the typical moisture-density curves (see Figure 9). As seen from the figure, the LWD-measured modulus values vary with compaction moisture content, and the modulus vs. moisture curve follows a bell-shaped curve just like a typical moisture-density curve. This "modulus growth curve" can be used as a reference, and a certain percentage of the peak modulus value can be used as a threshold value while checking compaction quality in the field. It should be noted that Schwartz et al. (2017) advised the practice of caution while performing LWD tests on Proctor molds with compaction moisture contents significantly greater than the Optimum Moisture Content (OMC). Such high moisture contents can result in substantial permanent deformation and excessive drainage of water from the mold. Moreover, the LWD drop weight can create excessive pore water pressures resulting in very high LWD modulus values.

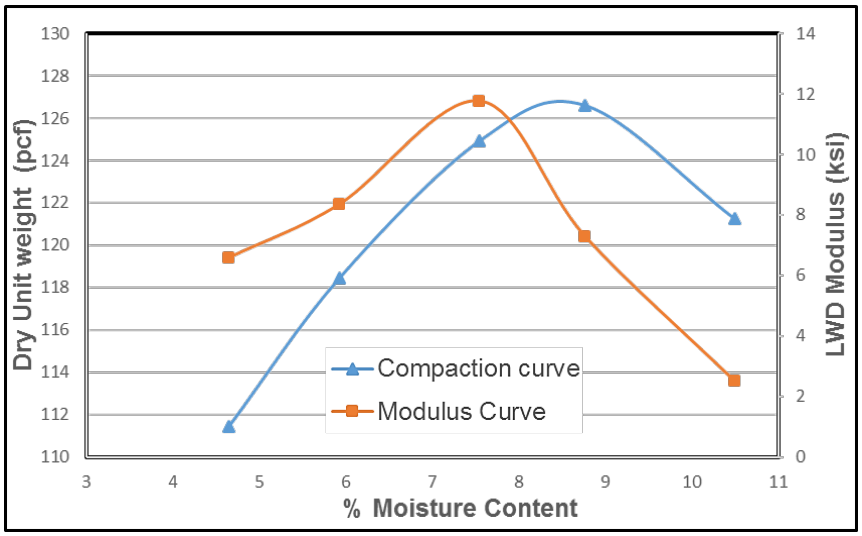

Figure 9. Variation of LWD modulus on mold and dry density with moisture content for a typical soil type

Free-Free Resonant Column Test

Another approach available to establish reference modulus values for soils and aggregates in the laboratory involves the performance of the Resonant Column Test. In this test, a cylindrical specimen of the aggregate/soil is impacted with a hammer mounted with load cell and an accelerometer placed on top of the specimen. When an impulse load is applied to specimen, seismic energy with a wide range of frequency propagate within the specimen. Energy associated with one or more frequencies are trapped and resonate depending on dimension and stiffness of specimen. Modulus of the specimen can be easily determined using following Equation (6) if the resonant frequency is known (Richart et al. 1970).

$$E_{FFRC} = \rho \times \left(2 \times f_L \times L\right)^2 \text{ ----------(3)}$$

Where, f_L is resonant frequency, ρ is wet density of specimen, L is length of specimen and E_{FFRC} is the Free-Free Resonant Column (FFRC) modulus. Nazarian et al. (2003a) reported that modulus values

obtained from FFRC tests can be directly related to seismic modulus values measured using the Portable Seismic Pavement Analyzer (PSPA) without a complex transfer function for analyzing other soil or base types. Nazarian et al. (2014) conducted FFRC tests on every specimen prepared for resilient modulus testing. Performing both tests simultaneously will allow highway agencies to develop a database for construction quality control (Nazarian et al. 2003b).

Selecting Target Moduli from Structural Model

Nazarian et al. (2014) discussed a detailed procedure to establish field target modulus values using a calibrated structural model. The first step in this approach involves repeated load triaxial testing to establish the resilient modulus properties in the laboratory and fitting the test results with commonly used stress-dependent resilient modulus equations. The model parameters thus established can then be used to calculate a representative resilient modulus value under typical stress states experienced by geomaterials during LWD testing. They determined the target surface deflection values for an LWD using by assuming a nominal load of 1200 lbs applied to an 8-inch diameter plate.

FIELD EVALUATION AND VERIFICATION

Once the target modulus values have been established through extensive laboratory testing, the next step involves testing either in large-scale test pits or in actual constructed pavement sections. The objective is to assess the practicality and repeatability of the test devices in actual construction practice, to estimate spatial variability of moisture, density and modulus, and to validate the process of target modulus determination under actual field conditions. Schwartz et al. (2017), for the purpose of field verification, selected a particular project in the field, and performed all relevant soil/aggregate testing in the laboratory. Each site was approximately 50-200 feet long. The testing locations used along a compacted lane are shown in
Figure 10. These compacted lanes were dived into three sub-lanes and LWD tests were performed in the middle of each sub lane at 5 to 10 ft. intervals.

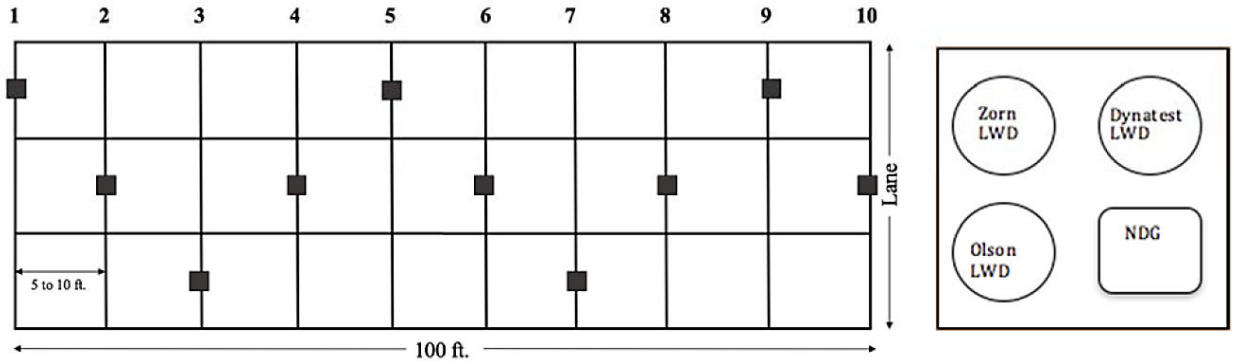

Figure 10. Layout of test station along a compacted lane and station plan (Schwartz et al. 2017)

Besides the LWD tests, nuclear density gauge and moisture content tests were also carried out. The moisture content measurements helped to control moisture during construction. Note that several researchers in the past have reported significant effects of moisture content on modulus values (Richter 2006; Cary and Zapata 2010; Seikmeier 2011and Mazari et al. 2014). Therefore, moisture content measurements are critical to facilitating appropriate interpretation of the LWD measurements.

COMPARING THE PERFORMANCES OF DIFFERENT LWDS

Schwartz et al. (2017) compared the performances of different LWD types used in their study. LWD tests were performed at different locations within a test section, including edge, center, and different offset locations. The testing spots were always 1.5m to 3m away from the edge of the road to avoid any boundary effects during testing. The standard deviation in moduli measurements by Zorn, Olson and Dynatest LWDs were calculated to show the spatial variability in measured modulus values. They reported highest spatial variability for the Dynatest LWD at the selected sites. The COV for the Dynatest LWD varied between 15 to 95% for subgrade soils, and 14 to 86% for the base materials. Among the three LWDs, the Zorn LWD showed lowest variability which was 10 to 80% for subgrade soils, and 12 to 39% for the base materials.

Table 3 lists the modulus values measured using the different LWDs, and their corresponding spatial variabilities. The Dynatest LWD was found to be the most sensitive to the drying of the compacted surface due to evaporation of moisture as increasing trends in moduli with passing time were recorded.

Table 3. Variation in Moduli Measurement for Different LWDs (Schwartz et al. 2017)

		Zorn LWD		**Dynatest LWD**		**Olson LWD**	
Layer	**Parameter**	**Modulus [MPa]**	**COV [%]**	**Modulus [MPa]**	**COV [%]**	**Modulus [MPa]**	**COV [%]**
Subgrade	Min.	10.4	10.2	11.2	15.2	19.3	15.5
	Max.	82.2	80.2	355.9	95.0	101.5	71.5
	Avg.	39.7	33.1	96.5	54.8	51.8	34.8
Base	Min.	35.1	12.5	45.6	13.9	46.8	11.2
	Max.	73.3	38.8	152.3	85.7	82.8	33.6
	Avg.	56.6	21.5	97.9	35.9	63.5	25.9

The LWD testing was performed on OGAs in the following sequence to investigate the effect of additional compaction imposed by LWD drops and repeatability in modulus measurements.

(a) Six drops from half height or lowered drop height
(b) Six drops from full height on the same location as step a without moving the LWD plate
(c) Six drops from the same half height on the same location as step a without moving the LWD plates.

In each of cases, three seating drops followed by three measuring drops protocol were used to determine the modulus values. The moduli measured from step a were referred to as “first half height drop moduli” and moduli measured from step c were referred to as “second half height drop moduli”. Table 4 lists the correlation between first half height drop and second half height drop moduli along with the average Percent Compaction (PC) values at each site.

Table 4. Correlation between Moduli at First Half Height Drop and Second Half Height Drop for Olson LWD (Schwartz et al. 2017)

Location and Soil Type	Round of Testing	Correlation (intercept=0)	R^2	Average % PC
Virginia, Phenix subgrade	1st	y = 0.9685x	0.478	96.8
MD 5 subgrade	1st	y = 1.2132x	0.956	98.6
	2nd	y = 1.0497x	0.890	98.4
	3rd	y = 1.0667x	0.877	98.8
MD 337, deep GAB layer	1st	y = 1.1383x	-0.196	98.0
MD 404 subgrade	1st	y = 1.2735x	0.993	N/A
MD 404 GAB	1st	y = 1.2326x	0.755	90.2
New York embankment (local subgrade)	Lift 1, 1st	y = 1.2481x	-0.279	84.8
	Lift 2, 1st	y = 1.4127x	0.299	83.2
	Lift 2, 2nd	y = 1.1566x	0.369	83.2
Indiana, cement modified subgrade	1st	y = 1.0217x	0.916	N/A
Indiana, GAB	1st	y = 1.158x	0.934	N/A
Missouri, GAB	1st	y = 1.1556x	0.786	100.0
	2nd	y = 1.0318x	0.924	99.5

Summary of the correlation equations ($y = ax$) with the corresponding coefficient of determination (R^2) values have been listed in Table 4; y and x represent modulus values from second half drop height and first half drop height, respectively. For the Olson LWD, the second half-height modulus values were 3% to 15% more than the first half-height modulus for well-compacted layers; this range changed to more than 15% for under-compacted locations. The Zorn LWD exhibited very good correlation between the moduli from first and second half height drops, as expected. For the Zorn LWD, the moduli of second half-height were 2% to 20% greater than the moduli of first half-height for well-compacted sites with Percentage Compaction (PC) greater than 95%. The Dynatest LWD exhibited fairly good correlation between these two modulus values for well-compacted sites; however, the correlation was poor for under-compacted sites.

ESTABLISHING ACCEPTANCE CRITERIA FOR LWD TESTS

Researcher have recommended that each State DOT should conduct local calibration to find the acceptance criteria for E_{field}/E_{target} (also known as modular ratio) for their local materials. A framework was proposed by Schwartz et al. (2017) to find the acceptable limits of modular ratio. A material should be rejected when a considerable number of field tests produce modular ratios outside of the acceptable limits. The acceptable modular ratio value also depends on different types of LWDs. For example, for the Zorn LWD, $E_{field}/E_{target} = 1$ was taken as the threshold value to separate under-compacted layers from well-compacted ones. The corresponding threshold limits were approximately 0.5 for the Dynatest LWD and 0.8 for the Olson LWD. Schwartz et al. (2017) recommended the following steps to establish threshold values for E_{field}/E_{target}

(a) Perform LWD testing on Proctor molds in the laboratory to determine the E_{target} value.
(b) Before achieving Maximum Dry Density (MDD) in the field, measure E_{field} after a few passes of the compactor.
(c) Measure E_{field} after achieving MDD.
(d) Determine the E_{field} /E_{target} for both passing and failing conditions.
(e) Estimate the threshold which separates the field to target ratio for passing and failing conditions.

If a considerable number of field Q/A tests produce modulus ratios outside the acceptable limit, the materials should be rejected. The Percentage Within Limit (PWL) methodology can be implemented to establish acceptance criteria as per AASHTO R 9-05 based on quality index Q. This quality index can be calculated using the following equation.

$$Q = \frac{\bar{X} - LSL}{S} \quad \text{----------(4)}$$

Where $\bar{X}$ is the sample mean for the lot/sublot, LSL is the lower specification limit and S is the sample standard deviation for the lot/sublot. After determining quality index (Q), the required PWL can be estimated from the PWL estimation table for a given target sample size. If the estimated PWL is less than the minimum number required by the agency, an appropriate remedial measure should be adopted for the lots including removal and replacement, corrective action or reduced pay factor.

REQUIRED SAMPLING FREQUENCY FOR LWD TESTS

Before a given agency can develop and adopt an LWD-based compaction control specification, it is important to decide on the minimum number of LWD tests that need to be performed for a given project. Schwartz et al. (2017) proposed a methodology to decide on the minimum number of LWD tests that should be performed. Based on the standard deviation data captured in field during the verification phase, they calculated the allowable error, and compared with corresponding error in the NDG data. The minimum required sample size was calculated based on a t-distribution parameter as shown in the following equation:

$$n = \left(\frac{t \times s}{e} \right)^2 \quad \text{----------(5)}$$

Where s is the sample standard deviation, t is the value from a standard Student's distribution table for each confidence level and degree of freedom, and e is the acceptable error. They recommended that each agency should calculate the minimum required testing based on the modulus standard deviation data for their materials and their selected LWD devices. However, the following recommendations were also made.

- For subgrade, base and subbase compaction: divide each lane mile into 4 sublots per lift and perform a minimum of 10 LWD tests in each sublots at random locations;
- For road embankment materials (1 ft. or more below the top of subgrade): Divide each lane mile into 4 sublots per lift and perform a minimum of 5 LWD test per sublots at random locations.
-

ASTM STANDARDS CONCERNING LWD TESTING OF SOILS AND AGGREGATES

Currently, the following two ASTM standards available concerning LWD testing on aggregates and soils:

(1) ASTM E2583, "*Standard Test Method for Measuring Deflection with a Light Weight Deflectometer*." This test method measures the deflection of a paved or unpaved surface with a Light Weight Deflectometer. A load cell shall be used to measure the load being applied upon each drop of the falling mass. This specification is often called a specification for a geophone-type LWD. The Olson and Dynatest LWD types have load cells to directly measure the impact load magnitudes and satisfy the ASTM E2583 requirements.

(2) ASTM E2835, "Standard Test Method for Measuring Deflection using a Portable Impulse Plate Load Test Device." This method measures the deflection of a load plate resting on a soil or aggregate layer. A velocity transducer or accelerometers is used to measure the vertical plate deflection at the center of the loading plate. As this specification does not require the device to directly measure the load being applied, the falling weight is dropped from pre-calibrated fixed heights to standardize the amount of load being applied from one test to another. The Zorn LWD does not have a load cell and meets the ASTM E2835 requirements. Note that most of the states in the US that have implemented LWD testing into practice, primarily follow this test method; the Zorn LWD is the device that is most commonly used by state DOTs.

The two specifications vary in several important aspects. For example, ASTM E2583 specifies that the load pulse should have a time of loading between 20 and 40 msecs. ASTM E2835, on the other hand, requires the load pulse to be between 10 and 30 msecs. It is important to note that even for the same peak load level, if the pulse durations are different, it is quite possible the surface deflections to be different because of the nature in which energy is transferred from the plate to the underlying layer. The two specifications also differ in terms of the required precision in the recorded data. ASTM E2583 requires the precision of the deflection sensor to be within ± 2 μm (0.08 mils), whereas ASTM E2835 requires the deflection sensor precision to be within ±40 μm (1.6 mils). Accordingly, a device meeting ASTM E2835 can be as much as 20 times less precise than a device meeting ASTM E2583 requirements. These differences must be kept in mind while the two device types are being compared.

AVAILABLE CONSTRUCTION SPECIFICATIONS UTILIZING LWD TESTING

This section briefly summarizes currently available specifications used by state highway agencies in the US concerning LWD testing on constructed soil and aggregate layers.

Indiana DOT Specification

Indiana test method (ITM No. 514-15T) details a procedure to determine allowable deflection of dense-graded aggregate layers using an LWD. This specification also includes how to determine the roller type, pattern and number of passes of the roller for the compaction of recycled materials by testing using a Dynamic Cone Penetrometer (DCP). A control test section, with approximate dimensions of 100 ft. x 20 ft. is recommended to be constructed, with the depth being same as a typically allowed lift thickness. The subgrade shall be proof rolled before constructing test section per Indiana DOT specifications. The moisture content of the test section is required to be within 3% of the optimum moisture content, on the dry side.

The repeated roller applications are required to facilitate compaction until no further stiffness increment is observed in field. The obtained stiffness value at this point reaches a maximum value and considered as a peak stiffness. The LWD device used for in-place modulus/stiffness measurement should meet the following requirements: 10kg ± 0.1 kg falling weight with a 5kg ± 0.25 kg guide rod, lock pin and spring assembly. The drop height shall be fixed per manufacturer recommendations and should generate a maximum of 7.07 kN force. Loading plate should be made of steel having 300 mm in diameter and 20 mm in thickness. The maximum vertical deflection should be measured by an accelerometer attached to the center of the plate. The maximum allowable deflection after compaction should be established by the following method:

- Compact the test section with 4 roller applications in a vibratory mode without any stopping and turning
- Conduct 10 LWD tests following the ASTM E2835-11 standard on the test sections at the location shown in Figure 11 and average the test results found from 10 locations. After conducting each test, mark the location for further testing.

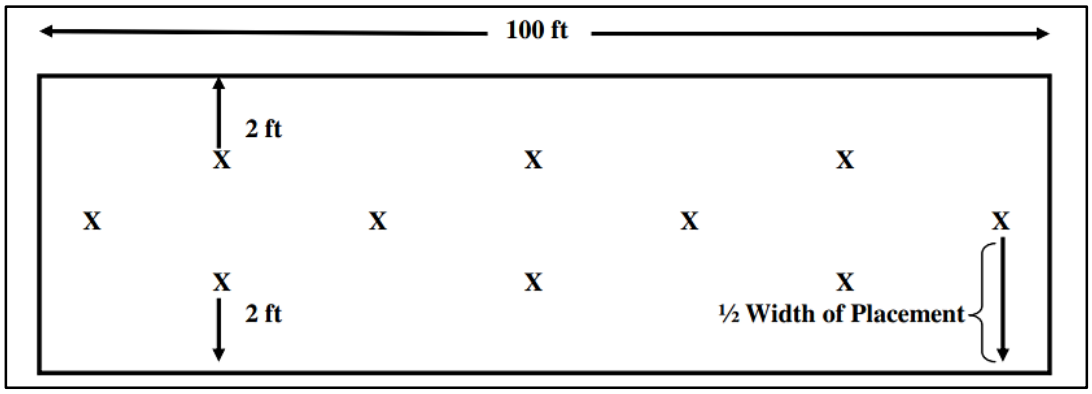

Figure 11. Plan view of approximate location of the LWD tests in test section as specified by Indiana DOT (ITM No. 514-15T 2015)

- Apply the one additional roller pass and conduct the LWD tests at exactly same 10 locations. Find the average of the performed 10 LWD test results.
- The compaction is considered to have attained the peak value when the difference between average LWD test results from 4 and 5 roller application is less than 0.02 mm. If the difference is greater than 0.02 mm, an additional roller pass is performed and the procedure should be repeated until the difference becomes less than 0.02 mm.
- The maximum allowable deflection for construction quality control is the lowest average of 10 LWD test values.

Zhao et al. (2018) conducted extensive in-situ LWD testing in Indiana and found that a minimum of 5 LWD tests were required for a small area of compaction, whereas at least 8 to 10 LWD tests were required for a large area of compaction. The Coefficient of Variation (COV) of LWD test results were within 20% to 35%. The COV of 20% or less indicated low variation, a COV of 20% to 35% indicated normal variation and a COV greater than 35% was taken to indicate excessive variation between the test results.

Minnesota DOT Specification

Embacher (2008) reported that the Minnesota DOT (MnDOT) has been utilizing LWDs for quality control of embankment and pavement foundation construction works to facilitate stiffness-based mechanistic pavement design. Individual MnDOT districts have in their inventory the Zorn ZFG 2000 models used for compaction quality control following the ASTM E2835 test method standard. The Minnesota DOT specifications recommend building control strips to identify target LWD deflection values to be adopted. Control strips (300 ft. long x 32 ft. wide; maximum thickness = 4 ft.) are required to be constructed for each type or source of soil. A total of six LWD drops (three seating drops followed by the average value from three measuring drops) are recommended at each testing location. Minimum of three locations at 25-ft. spacing should be considered for LWD testing between each compaction pass.

Once the target LWD modulus value has been established from the control strip testing, it is used as the benchmark to compare results from the actual pavement section against. LWD-measured modulus values from the constructed pavement section should be at least 90% of the target modulus value established through the control group testing. If the modulus measured from testing of the actual pavement section is greater than 120% of the target modulus, then reconstruction of control strip is suggested to re-establish the target modulus. MnDOT also recommends recalibration of the LWD units annually or after 10,000 measurements.

In the field, onsite verification of the equipment can be performed by checking the repeatability of deflection measurements under individual drops. This is carried out by performing three seating drops followed by nine testing drops on a verification pad laid on top of a concrete floor. The difference between maximum and minimum deflection values obtained from the nine load pulses should be less than 0.04 mm. If this criterion is not satisfied, recalibration of the LWD should be considered.

Nebraska DOT Specification

Nebraska DOT standard test method designated as NDT T2835, titled “Deflection Measurement of Soils using a Light Weight Deflectometer (LWD)”, is a modified version of the ASTM E2835 specification, and outlines the procedure for LWD testing on soils. The requirements for LWD are as follows: (1) 10 kg falling weight with 720 mm drop height; (2) guide rod to allow free fall of the weight; (3) a steel spring buffer system for transmitting the load to plate resting on the layer being tested; and (4) a 300-mm diameter loading plate for distributing the load imparted from the falling weight to the layer being tested. Repeatability of the LWD test results are required to be checked for newly purchased units, after a particular unit has gone through recalibration, after observing questionable test results, as well as after 10,000 test measurements. The verification is carried out by performing nine LWD drops on a test pad having a bare, sound concrete surface with a minimum thickness of 6 inches. The difference between the maximum and minimum deflection values recorded under these nine drops shall be less than 0.04 mm. The difference between mean deflection value calculated from the nine drops and the deflection recorded under an individual drop shall be less than 0.02 mm. If these criteria are not met, the LWD units is required to be submitted for recalibration.

For on-site measurements, it is recommended that LWD testing should be performed immediately after compaction when air temperature is in the range of 32 to 120 degrees Fahrenheit. Before LWD testing is performed at a particular location, a test area at least 1.5 times larger than the diameter of the loading

plate should be prepared, and a smooth and level spot be prepared by removing any disturbed or additional materials from the surface. After preparation of test spot, six falling weight drops are executed, and the average deflection from the last three drops is recorded. The specification requires the tester to move approximately 1.5 ft. longitudinally from a particular test spot if any of the following conditions occur during testing: (1) sliding of load plate; (2) failing to catch the falling weight after rebound; or (3) the weight is dropped from a height that is different from the calibrated height. Cho et al. (2011) reported that the Nebraska DOT was considering the quantification and acceptance of soil compaction based on LWD-measured deflection or modulus values.

Wisconsin DOT Study for Specification Development

Titi (2012) recommended a protocol for LWD-based compaction control for the Wisconsin DOT by evaluating the quality of the constructed base layers. The field-testing phase consisted of in-place density measurements using the sand cone method, LWD testing, and DCP testing. A control section, 300-ft. long and of the same width as the base layer was compacted to the required density, and LWD tests were performed in accordance with ASTM E2583 test protocol. 10 different test locations per 100 ft of the control section were selected to perform LWD tests. The average deflection value from 10 LWD tests was used to compute the allowable deflection value. The study recommended that for QC/QA in the field, contractors should perform 10 LWD tests for each 1,000 ton of compacted aggregate with minimum of five tests per day. The average deflection from all LWD tests should be equal to or less than the maximum allowable deflection obtained from LWD tests on control section.

UK Specification

British Standards BS1924-2 and BS1377-7 (BS1924-2:2018) describe the method to determine in-situ material dynamic stiffness or resistance to vertical deformation. The LWD equipment described in these specifications has the following features: (1) 300-mm diameter plate capable of uniform distribution of pulsed load, and that allows the measurement of deflection under the plate center; (2) a load cell to measure the applied load with a precision not less than 0.1 kN; (3) a mass of 10 kg and falling along a guide shaft; (4) a deflection sensor capable of measuring maximum vertical deflections with a precision of ± 2 μm; and (5) a spring element buffer system to generate transient load pulses of 15 ms to 30 ms duration. Note that smaller plates of 100 mm, 150 mm and 200 mm in diameter can also be used to achieve high target stress values. However, the zone of influence is significantly reduced compared to 300 mm standard plate (Frost et al. 2010).

The British standards specify three seating drops from a certain test height to achieve target stress values of 100±5 kPa. The LWD plate should remain stable after performing the seating drops; otherwise, a new test location needs to be selected, and the process needs to be restated. Once adequate “seating” of the load plate has been achieved, three measuring drops are performed, and the mean of test output is used to calculate the normalized surface modulus. The test results are considered to be “non-compliant” for any of the following reasons: (a) the rebound portion of the deflection pulse is greater than or equal to 20% of the peak deflection value; (b) non-standard pulse shapes due to shear failure of material and/or when permanent deformation under the plate is greater than 10 mm after completion of testing; or (3) if application of the repeated loading during LWD Testing causes water to rise to the surface of the test location.

STUDIES ON OPEN GRADED AGGREGATE LAYERS

Most of the studies reported it the literature focusing on LWD testing of geomaterials deal with testing on soils or dense-graded aggregate only. Not many studies have focused on LWD testing of OGA base courses or other coarse-graded aggregates such as railroad ballast. It is important to note that development of LWD-based compaction quality control specifications for such materials will significantly benefit the engineering community.

As previously noted, the open-graded nature of layers precludes density measurements using the nuclear density gauge. As a result, the specification, construction and compaction of such layers often follows a method approach. For example, freshly constructed railroad ballast layers are usually not tested for density. Similarly, OGA base courses and other such coarse aggregate layers used in pavement applications are often compacted "to the satisfaction of the engineer" or by specifying a "minimum" number of passes by compaction equipment exerting a specified force. Although the development of LWD-based compaction quality control specifications for such layers would be greatly beneficial, reliable LWD testing on such layers is not trivial. Due to the uneven nature of the surface for these layers, it may not be easy to prepare a smooth surface for LWD testing. If the LWD loading plate fails to establish uniform contact with the layer being tested, the test results may not be reliable. Point-based deflection measurement approaches, such as the one in the Dynatest LWD include a central geophone that protrudes through the center of the annular plate and measures the displacement of the underlying surface under the dropping mass. This is not appropriate for testing aggregate and soil layers because movement of a particular aggregate particle under the protruding geophone may be interpreted as unreasonably high (or low) deflection values under the dropping mass. In such cases, it is important to measure the surface deflection using the entire plate as one unit, e.g., the accelerometer-based plate deflection measurement in the Zorn device, the geophone-based plate deflection measurement in the Olson device, or by plugging the annular hole in the Dynatest device. This section summarizes the limited number of studies that have focused on LWD testing of OGA bases or similar coarse-grained aggregate layers such as railroad ballast.

While developing construction protocols, Smith et al. (2018) conducted LWD testing on OGA base layers used in permeable interlocking concrete pavements. Compaction specification based on a specific number of roller passes or minimum of 95% Proctor density likely do not provide consistent results for OGA aggregates. Specifically, OGA aggregates for permeable interlocking concrete pavement (PICP) have little to no fines ($\leq$ 2% passing the No. 200 sieve) and typically have density values between 95 to 120 pcf (1522 – 1922 kg/m^3). Porosities should be at least 30% for water storage (Smith 2017). Jointing, bedding, base and subbase aggregates used in vehicular PICP applications should be crushed with minimum 90% fractured faces and a maximum LA abrasion values of < 40.

Performing LWD testing with a 300-mm diameter plate on these aggregates, Smith et al. (2018) observed that the deflection results were significantly affected by the depth of the subbase layer. Higher deflections were found for 300-mm thick ASTM #2 subbase layers compared to those with a 100-mm thick #57 base on this subbase. LWD-measured deflection values decreased substantially by changing the thickness of the subbase layer from 300 to 400 mm.

Other testing was conducted on an area of uncompacted clay soil subgrade with geotextile under a 150-mm thick ASTM #2 subbase supporting a 100 mm thick #57 base. Smith et al. (2018) investigated the

effect of number of drops on the LWD-measured deflections. They observed that increasing the number of drops beyond 6 further compacted the compacted aggregate layers. Specifically, drops 4 to 6 had a deflection range from 0.523 to 3.760-mm deflection whereas the range was reduced from 0.019 to 0.094 mm during drops 16 to 18. All measurements were taken in the same locations. This test section had only a 150 mm thick subbase layer, whereas a 300 mm thick subbase layer was required to avoid the influence of soil subgrade. Smith et al. (2018) suggested to conduct further research to find the optimal number of LWD drops, the effect of saturated soil subgrade on deflection results, and also the effect of geotextile presence at the subgrade interface on the LWD-measured deflections.

Li et al. (2011) found that wet conditions lead to softer subgrade conditions and higher shear stress/strength ratios on top of subgrade; accordingly, thicker subbase layers need to be constructed to achieve lower deflection values.

As already discussed, the railroad ballast layer is in many ways similar to OGA base courses and presents some challenges as far as LWD testing is concerned. It is interesting to note that during the early days of LWD development in Germany in the 1980s, LWDs were used to measure the "dynamic elastic modulus" of open graded railroad ballast with soils and roadway base course aggregates. Zorn's LWD user manual lists modulus acceptance criteria for the ballast layers in German railroads (Zorn 2011).

Tamrakar and Nazarian (2019) conducted LWD tests on fouled railroad ballast to characterize its permanent deformation and stiffness behavior. A container made of polyethylene pipe with 900 mm diameter, 700 mm height and 25 mm thickness was considered in this study to simulate ballast layer and subgrade in a container. The material profile consists of 100 mm pea gravel at bottom, 300 mm thick subgrade in the middle and 300 mm thick ballast layer on top. A Zorn LWD with 100 mm diameter plate was used to perform LWD tests on top of the ballast layer following the ASTM-recommended procedure.

Figure 12a shows a photograph of LWD testing on top of the ballast layer built inside the cylindrical container; Figure 12b shows typical deflection time histories obtained during the testing. Tamarkar and Nazarian (2019) reported that the LWD measurements were significantly affected by the presence of the underlying soft subgrade layer. This led to lower modulus values reported by the LWD compared to those reported by using the Portable Seismic Pavement Analyzer (PSPA). This clearly emphasizes the importance of considering the depth of influence during LWD testing, if meaningful inferences are to be drawn regarding modulus of the layer being tested.

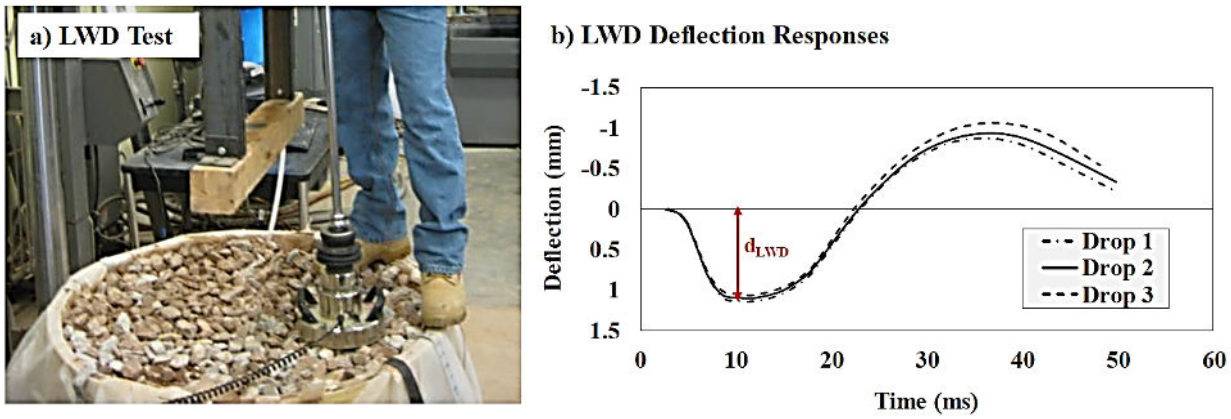

Figure 12. (a) Photograph showing LWD testing on top of the ballast layer in the lab; (b) Typical Deflection time history obtained during the LWD testing (Tamrakar and Nazarian 2019)

Another device that has been used to assess the in-place modulus of constructed ballast layers, is the PANDA, a Variable Energy Dynamic Penetrometer device designed and manufactured by SolSolution in France. Several researchers have reported that both the PANDA device as well as the LWD can be used to evaluate the quality of track-bed ballast layer (Benz 2009; Staatsministerium 2012; Shafiee et al. 2011; Tompai 2008 and Woodward et al. 2014). Lamas-Lopez (2016) conducted LWD tests on ballast layer to validate modulus estimated from PANDA tests and found that the modulus values reported by the two devices were correlated.

SUMMARY

This chapter presented findings from an extensive review of published literature focusing on modulus- or deflection-based compaction quality control methods for soil and aggregate layer using LWDs. First, the basic principles of LWD operation were discussed, followed by different material or site-related factors that affect LWD measurements significantly.

The most challenging task in front of modulus- or deflection-based compaction quality control specification development efforts was identified to be the establishment of a target modulus or deflection value. Establishing a target modulus or deflection value requires either extensive laboratory characterization of soils and aggregates under different moisture conditions and stress states, or the construction and testing of full-scale test sections. Implementing a modulus-based compaction protocol is particularly challenging because there is a significant difference between laboratory-measured resilient modulus values and modulus values measured in the field using LWDs.

A recently completed study at the University of Maryland attempted to establish the target modulus values for LWD measurements in the field by performing LWD tests on soil and aggregate samples inside Proctor molds. Through extensive laboratory and field testing, the researchers observed that target modulus values established through LWD testing in Proctor molds can be used as reference values for compaction control in the field with reasonable success. Test sections that satisfied density-based compaction thresholds values, also satisfied the modulus-based threshold values established through LWD testing on Proctor molds. Similarly, under-compacted sections failed to meet both the density- as well as modulus-based criteria.

Finally, this literature review summarized some of the state DOT specifications available on LWD use for compaction quality control of soils and aggregates. However, it should be noted that all such specifications are valid for fine-graded soils or dense-graded aggregate base/subbase courses only. No specifications are currently available governing the use of LWDs for compaction quality control of OGA aggregate bases such as the ones used underneath permeable pavements. There is a clear need for research in this area, and development of new modulus-or deflection-based compaction quality control approaches using LWDs will significantly improve the design and construction practices for these OGA base courses.

CHAPTER 3: MATERIAL SELECTION

To accomplish the tasks in this research study, two open-graded aggregate materials, conforming to ASTM #4 and ASTM #57 specifications, respectively, were selected. Two photographs of representative particles from these two aggregate materials are presented in Figure 13. Figure 14 shows their respective particle size distribution curves. The materials were directly collected from the onsite stockpile of ASTM #4 and ASTM #57 aggregates by following ASTM standard sampling guidelines. Table 5 shows the standard gradation ranges for ASTM #4 and ASTM #57 aggregates.

Figure 13: Photographs Showing Representative Particles from ASTM #4 and ASTM #57 Aggregate Materials

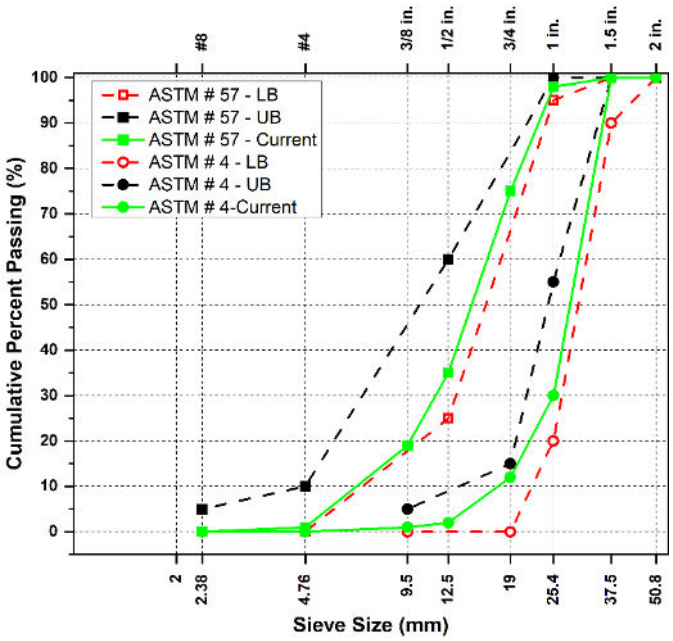

Figure 14: Particle Size Distribution (Gradation) Curves for the Selected Aggregate Materials (UB: Upper Bound of Gradation Specification; LB: Lower Bound of Gradation Specification)

Table 5: Gradation ranges for ASTM #4 and #57 Aggregates per ASTM D448.

Sieve Size		*Percent Passing*	
mm	*US (in.)*	*ASTM #4*	*ASTM #57*
63.0	*2.5*	*100*	
50.0	*2*	*100*	
37.5	*1.5*	*90-100*	*100*
25.0	*1*	*20-55*	*95-100*
19.0	*¾*	*0-15*	
12.5	*½*		*25-60*
9.5	*⅜*	*0-5*	
4.75	*#4*		*0-10*
2.36	*#8*		*0-5*

CHAPTER 4: RESEARCH HYPOTHESIS AND PLAN

RESEARCH HYPOTHESIS

Before going into details, it is important to explain the research hypothesis adopted for this study. Compaction control for any material involves checking a particular criterion based on some reference value. For example, the compaction control for dense-graded material in field is monitored by checking the achieved field density against the Maximum Dry Density (MDD) measured in the laboratory. The MDD values are usually measured using standard or modified compaction effort inside a mold. However, researchers found that the LWD-measured material modulus value inside conventional molds at various compaction stages are also related to the modulus value of the same material in the field (Schwartz et al., 2017). The reference value was first evaluated by LWD testing on soil (dense-graded aggregate), then this value was used as reference for field compaction. But OGA materials are usually large in particle size, having large voids in it. So, finding density or modulus of for this material inside conventional molds present certain challenges. For example, the size of the conventional mold might not be adequate for capturing the compaction behavior. Also, most of the agencies do not have the resources to perform resilient modulus testing on OGA materials. Accordingly, finding the reference value based on surface deflection measured from LWD testing, can be directly related to the pavement response. Therefore, the hypothesis for this study is that the deflection-based compaction control is related to degree of compaction after a given compaction effort. The research plan designed for the OGA materials is divided into four phases. In this case, recommendations made by previous researchers based on testing of dense-graded aggregate materials were carefully examined and modified to accommodate the testing of OGA materials.

RESEARCH PLAN

The research tasks undertaken in the current study to accomplish the overall objectives were divided into four phases. Each phase comprised distinct tasks and objectives aligned to enhance the overall understanding of OGA packing behavior. Completion of all four phases of the research would lead to the ultimate deliverable from this project: *"the development of a deflection-based compaction specification for OGA base/subbase courses such as the ones used underneath permeable pavements."* The following sections introduce the different phases of research undertaken in the current study.

Phase-1: Small Scale Laboratory Testing

In this phase, the packing characteristics of OGA materials were studied through small-scale laboratory testing. The main objective of Phase-1 was evaluating whether LWD tests in Proctor molds can be carried out to get a 'quick and easy' picture of the packing characteristics of OGA materials under different compaction efforts. Schwartz et al. (2017) developed and validated the LWD testing concept inside a Proctor mold. However, their testing effort included subgrade soils and dense-graded aggregate materials only. Whether a similar approach can be extended to OGA base courses was unknown. Theoretically speaking, if the same concept can be applied to OGA layers with large top-sizes, the only additional requirement should be to test in a larger mold to eliminate boundary (confinement) effects.

Accordingly, a scaled (enlarged) Proctor mold was manufactured by the research team for use in the laboratory test matrix. The custom-made Proctor mold has an inside-diameter of 12 in. (300 mm), and a total height of 11.5 in. (292 mm). The objective was to capture the variation in surface deflection (degree of compaction) of OGA materials inside the custom-made Proctor mold using LWDs. The variation in surface deflection under different modes of compaction was also studied in Phase-1. This included three different compaction modes in the laboratory: (1) impact compaction (LWD drop), (2) a combination of vibratory and impact compaction (using a jackhammer), and (3) constant vibratory compaction (using a vibratory shake table). These different compaction modes were tried to assess what mode best represents the compaction behavior of OGAs. This would also give a good picture of the constraints required to reach the maximum achievable packing condition in OGA materials. Under the scope of Phase-1, three types of molds, three types of compaction modes, and two types of aggregate were used for the laboratory testing. Details about the Phase-1 research tasks are provided later in this report.

Phase-2: Intermediate-Scale Laboratory Testing Phase

Understanding the behavior of the OGA as base/subbase material in Phase-2 involved testing with different configurations inside a wooden box. Unlike in Phase-1, in Phase-2, the materials were tested in a large box, free from the lateral boundary effects of a Proctor mold. This Phase acted as an intermediate testing stage between small-scale lab testing and full-scale field testing. Phase-2 was crucial to establishing the relationship between laboratory-measured surface deflection values in a Proctor mold, and field measured surface deflection values. In addition to this, several factors that could potentially affect the LWD evaluation were also studied in Phase-2. These included: (1) effect open-graded base layer thickness, (2) influence of LWD type and applied load levels on the surface deflections, and (3) stress level and patterns at different depths within the aggregate layers. Several pressure cells were installed at different depths within the aggregate layer to capture the stress distribution pattern inside the OGA layers.

Phase-3: Numerical Modeling Phase

In this Phase-3, the packing evolution in OGAs, and their corresponding effect on LWD-measured surface deflection were studied using a commercially available Discrete Element Modeling (DEM) software package. Due to the non-homogeneous nature of OGA, instead of the commonly used finite element method, DEM was used to capture the load-deflection behavior of OGAs under LWD loading. The commercially available software package, Particle Flow Code (PFC®) was used this purpose. The model was validated using results from Phase-1. Subsequently, the validated model was used to generate multiple OGA specimen representing different material properties and compaction conditions; simulated LWD tests were performed on these synthetic OGA specimens to study how the different factors interact to govern LWD-measured surface deflections. The primary objective of this phase was to identify different factors that have a potential to affect LWD-measured surface deflections in the lab as well as in the field.

Phase-4: Full-Scale Field Testing

Phase-4 was the most resource-intensive component of this research study and involved construction and testing of full-scale pavement sections. Findings from the other three phases of this research study were used to decide on the test section configurations as well as to decide on planned compaction protocols to

be implemented in the field. Different test cells were constructed comprising varying thicknesses of subbase and base layers, constructed using different lift thickness combinations. Each lift was compacted using a pre-determined number passes of a vibratory roller. LWD tests were conducted after each pass of the compactor, and the LWD-measured surface deflections were correlated with the compactive energy imparted to the layer.

Depending on the full-scale test results, final recommendations were made regarding deflection-based compaction control of OGA base/subbase layers. Figure 15 shows a flow chart of the overall research task structure in the current study.

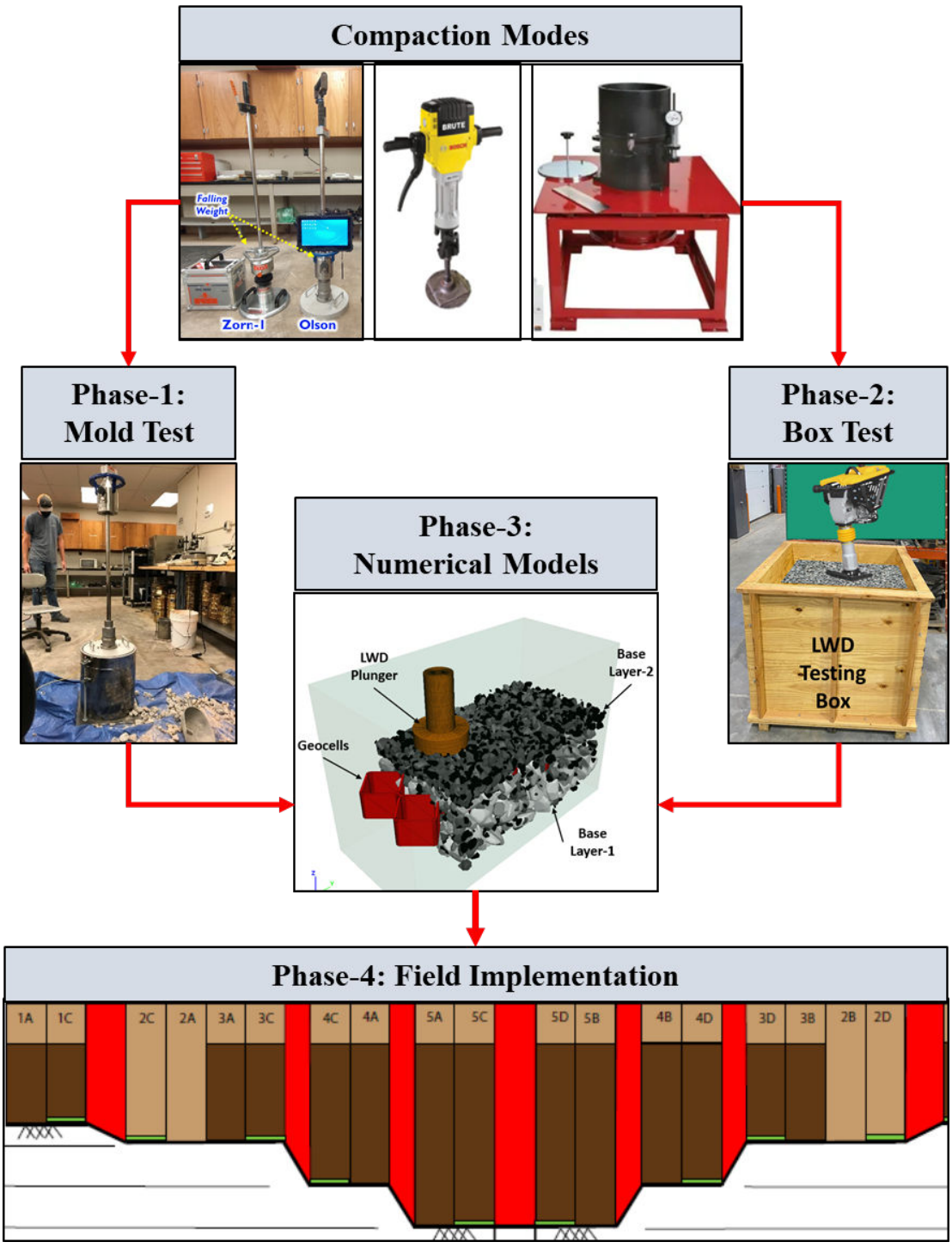

Figure 15: A Schematic Illustration of the Research Design in the Current Study

CHAPTER 5: TEST MATRIX

PHASE-1: SMALL SCALE LABORATORY EXPERIMENTS

In this section of the report, details regarding Phase-1 sample preparation and test setup are discussed.

Mold Selection

The small-scale laboratory testing phase (Phase-1) was primarily inspired from the LWD testing in Proctor molds, carried out by Schwartz et al. (2017). The traditional Proctor tests on soils/aggregates can be carried out using two different mold sizes (4-in. and 6-in. diameter molds, respectively). The difference in the mold size is governed by the particle size of the material being tested; soils/aggregates comprising larger particles should be tested using a larger-diameter mold. The primary objective behind this is to ensure the "confined" nature of the Proctor molds does not affect the material behavior under compaction. As already mentioned, the current study focused on testing two aggregate types: ASTM #57 and ASTM #4. The ASTM #57 material has a top-size of 37.5 mm (1.5 in.) whereas ASTM #4 material has a top size of 63 mm (2.5 in.). Therefore, testing such large aggregates inside conventional Proctor molds is not likely to lead to reasonable test results. This led the research team to develop a new "customized" mold with an inside-diameter of 304.8 mm. This mold facilitated LWD testing of the ASTM # 4 and ASTM # 57 materials.

In total, three configurations of LWD testing inside Proctor molds were studied in this testing effort. In the first scenario, the aggregate materials were tested inside a conventional 152.4-mm. diameter Proctor mold. As discussed later in this chapter, testing in this mold has been referred to as Mold Configuration # 1 or MC-1. In the second scenario, the custom mold (304.8-mm diameter) was used in such a way, that the height of the sample was kept at the same level as that in a conventional mold (116.5 mm). This was done to simulate a case where a thin layer is constructed using OGA materials and is tested using LWDs; this configuration has been referred to in this study as MC-2. In the third scenario, the custom-made mold (304.8-mm diameter x 292.1-mm tall) was filled with the aggregate materials and tested using LWDs (referred to as MC-3). Figure 16 shows the sample size inside the conventional and custom-made Proctor molds. Mold Types (or configurations) 1, 2, and 3 were used to represent scenarios 1, 2, and 3, respectively.

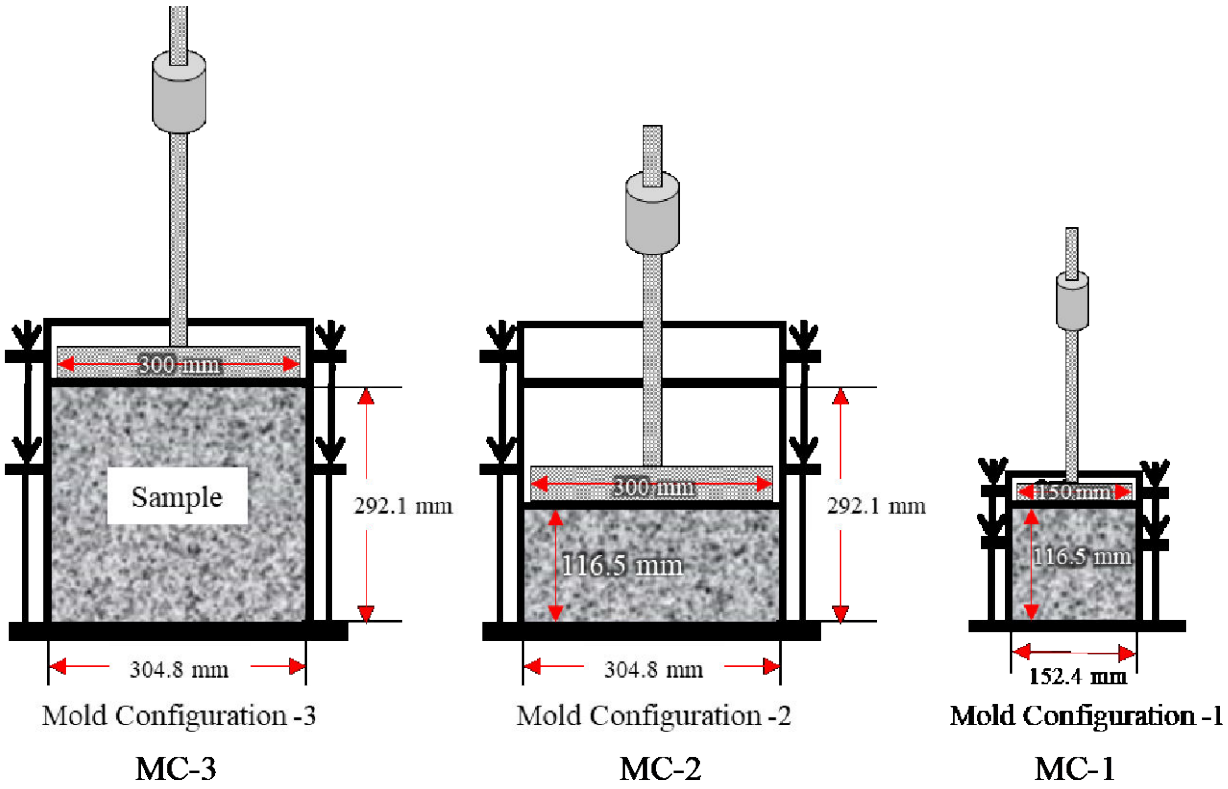

Figure 16: Different Configurations of Mold Size and Sample Height Considered in this Research Effort

LWD Device Selection

Several different types of LWDs are commercially available in the market. Under this research project's scope, two (2) LWD devices, commercially available in the US, were used. The first one was manufactured by Olson Engineering (Model: Olson-1), and the other was manufactured by Zorn Instruments (Model: ZFG-3000). As already mentioned, the Zorn device does not have a load cell to directly measure the applied load levels, but rather, uses a pre-established calibration relationship to "estimate" the load based on the drop height. On the other hand, the Olson LWD device uses a load cell to measure the applied loads from the dropped mass. The software package that comes with the Olson LWD has a provision to calculate modulus values inside Proctor molds as well by considering the lateral confinement conditions. The Zorn, on the other hand, is significantly less expensive, and is much more widely used by state DOTs in the US (low cost and simple interface drives popularity).
Figure 17 shows photographs of the two LWDs being used in the current study.

Figure 17: Photographs Showing the LWDs selected for Use in this Study: Zorn 3000 (Left), Olson (Right)

Compaction Strategy Selection

As already mentioned, three different compaction modes were selected to compact the aggregate materials in the Proctor molds during Phase-1 testing. Generally, for soils and aggregates, compaction energy has a proportional relationship with the level of compaction. Higher compaction effort ensures a higher degree of compaction. The three types of compaction efforts applied to the aggregate materials inside the Proctor molds were: (1) Impact/Drop hammer compaction applied through repeated dropping of the LWD mass; (2) A combination of vibratory and impact compaction applied using a Jackhammer, and (3) a constant vibratory compaction applied using a vibratory shake table. Further details about each of the compaction modes are presented below.

Impact compaction: Light Weight Deflectometer

A standard LWD drop weight can be used as an impact (or drop hammer) compaction energy source. When applying the compaction energy through drop hammer methods, the applied compaction energy can be primarily controlled in two ways. The first one involves changing the drop height for a given drop mass, and the other involves changing the drop mass for a given drop height. In the current study, all the options were explored. Two additional (supplementary) drop weights were manufactured to increase the amount of compaction energy imparted to the material. This customization was achieved in collaboration with Olson Engineering, as they served as industry partners in this research study. It is important to note that such customization may not be possible for all commercially available LWDs. Nevertheless, the primary objective of this research effort was to study the packing within OGA base/subbase courses under the application of different compaction efforts. Therefore, addition of the extra drop weights supported the research objectives. Figure 18 shows photographs of the two custom-made additional drop weights manufactured to be used in this research study.

Figure 18: LWD Impact Compaction additional weights

Vibratory Compaction: Jackhammer and Relative Compaction Table

Vibratory compaction is suitable for aggregate materials. Under this research project's scope, two types of vibratory compaction systems were used to compact the material inside the Proctor molds. In system-1, aggregate materials inside the Proctor molds were compacted using an electric-powered jackhammer. A custom-made rammer plate was used to apply the vibration on top of the samples inside the molds. Figure 19 (left) shows a photograph of the jackhammer with a custom-made top plate for compacting the aggregate inside the molds.

The second mode of vibratory compaction involves the use of a vibratory shake table (photograph presented in Figure 19, right). A vibratory shake table is an ASTM standard (D 4253) device used to measure the maximum relative density of cohesionless soils/aggregates. Under the scope of this research, it was decided to use the vibratory compaction table as a source of continuous compaction for the OGA materials. The objective was to correlate the relative compaction with aggregate packing (through surface deflection measurements with LWDs). In this research, the custom-made Proctor mold (Diameter = 305 mm) with sample aggregates was placed on top of the vibratory table with a static surcharge weight, and the table was vibrated at different frequencies for different periods of time to achieve different aggregate packing levels. LWD tests were then performed on the compacted aggregates inside the mold to study the effect of different degrees of compaction levels on the surface deflection.

Figure 19: Photographs Showing the Jackhammer and Vibratory (Relative Compaction) Shake Table Set-Ups used in the Current Study

The three compaction modes, i.e., drop-weight, jackhammer, and vibratory table, each have unique characteristics. For the drop-hammer approach, the compaction energy being applied can be closely controlled using the drop weight as well as the drop height. On the other hand, calculating the exact compaction energy applied by the jackhammer or the vibratory shake table can be challenging. The level of energy imparted by the jackhammer depends on the level of resistance offered by the material being compacted. Similarly, the energy imparted by the vibratory table depends on the frequency and duration of vibration. Nevertheless, the objective of this research effort wasn't to calculate the exact amount of compaction energy being applied to the aggregates. Rather, the primary objective was to determine the maximum (or likely optimum) level of packing achieved for the aggregate materials and how the mechanical behavior (characterized as LWD-measured surface deflections) of the aggregate layer changes with different levels of packing. In Chapter 6 of this report the summary of the findings from Phase-1 are discussed. Detailed discussions can be found in the 2nd Interim Report submitted to the Interlocking Concrete Pavement Institute Foundation.

PHASE-2: INTERMEDIATE-SCALE LABORATORY TESTING

This section presents details regarding the configuration and test set-up for the wooden box used in Phase-2 of this research project.

Box Configuration and Compaction

Due to the coarse nature of OGA materials, they are quite sensitive to boundary effects, and testing inside a confined mold could give significantly different results compared to those observed in the field. To establish some reference values to be targeted during field compaction, laboratory testing free from boundary effects was conducted. To establishes these values, a large wooden box 1.22 m x 1.22 m x 1.22 m (4 ft. x 4 ft. x 4 ft.) was constructed in the laboratory for testing the aggregates under different

compaction conditions. The bottom of the wooden box was continuously supported against the concrete floor to eliminate excessive deformations during testing.

The first stage of box testing used no subgrade layer and no reinforcement. The aggregates were directly poured into the box to construct layers of different thicknesses (152.4-mm, 304.8-mm, and 381-mm thick layers). These three layers were then tested using LWDs under different compaction conditions: uncompacted, as well as after different number of passes of a commercially available portable vibratory plate compactor. The compactor specifications are as follows: Plate Width: 13 in.; PLate Length: 17 in.; Compacting Force: 1950 lbs.; Weight: 110 lbs; Engine Power: 4.5 hp; Blows per Minute: 5900. Figure 20 shows photographs of the wooden box, the vibratory plate compactor, and a testing grid marked inside the box to compare the effect of testing position on LWD-measured surface deflections. In Figure 20(c), Grid 5 represents an ideal location that is free from boundary effects, and therefore, 'should' simulate a field-like condition.

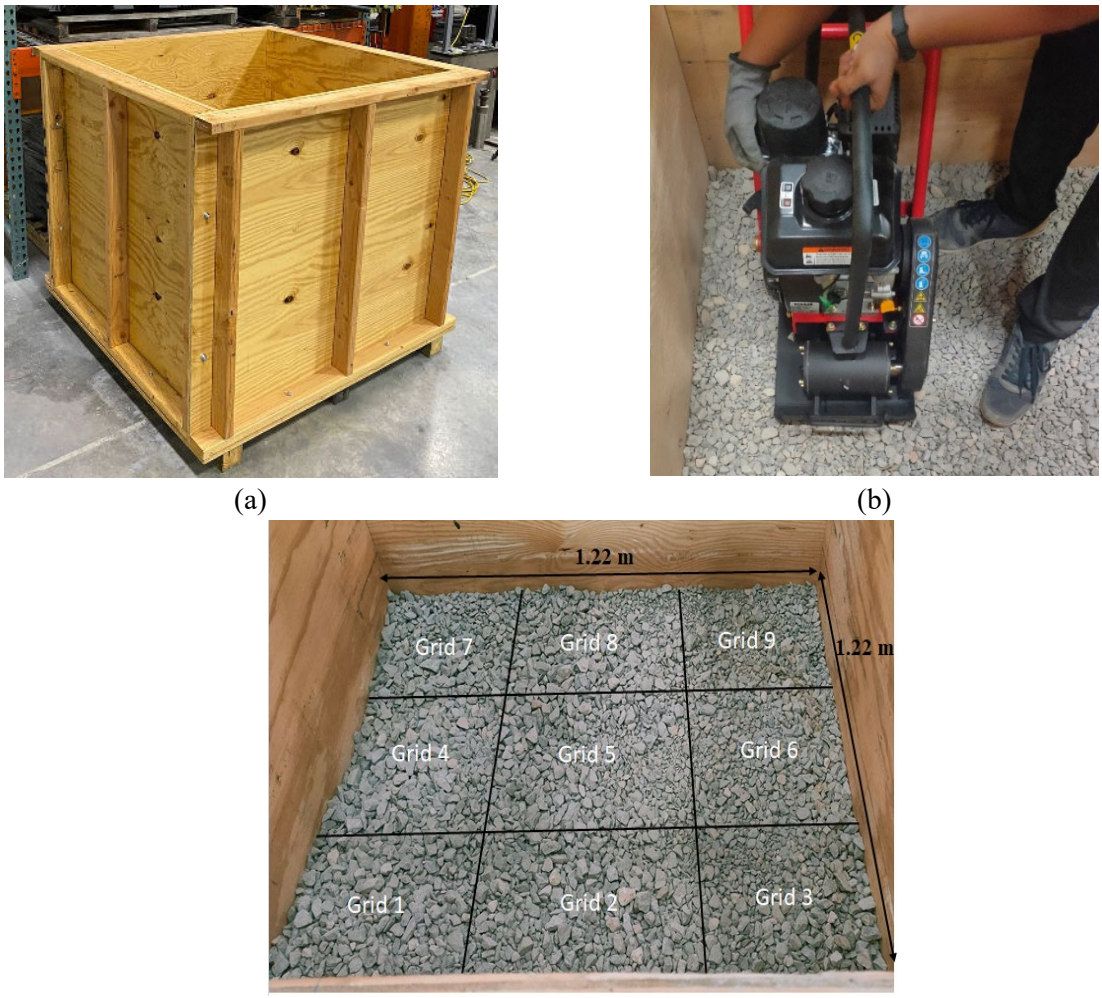

Figure 20: Photographs Showing the (a) Wooden box; (b) Vibratory Plate Compactor; and (c) Grid Orientation Inside the Box to Mark the LWD Testing Spots

In the second stage of testing, a subgrade was not used. Instead, a geocell reinforcement aggregate layer was built, and was used as the subbase layer. It is important to note that geocells are commonly used with OGA materials to provide lateral confinement, and impart additional 'stability' to the layers. In a parallel research effort, a commercial geocell manufacturer (Presto Geosystems), provided some geocells for use in this testing effort. Therefore, the geocell-reinforced aggregate layers were incorporated into the wooden box as well as during the full-scale field testing. Figure 21 shows a photograph of geocell-reinforced aggregate layer placed in the wooden box. At first, a 50.8-mm (2-in.) thick layer of aggregate (ASTM #4) was placed directly at the bottom of the box. Then, a 152.4-mm (6-in.) thick geocell-reinforced aggregate layer was constructed using ASTM #57 aggregates. Finally, 101.6-mm (4-in.) caping layer was constructed using the ASTM # 57 material. The capping layer was compacted using the commercially available vibratory plate compactor. The primary objective of this testing configuration was to assess how the stability of OGA layers can be improved through geocell reinforcement.

Figure 21: Photograph Showing a Geocell-Reinforced Aggregate Layer Constructed Inside the Wooden Box

Measurement of Pressure Dissipation Inside OGA Layers using Pressure Cells

In this study, earth pressure cells were installed to measure the stress distribution inside OGA layers. Due to limited resources, and because this component was not originally part of the project task plans, only four (4) earth pressure cells could be procured for use in the lab, and were placed inside the wooden box at strategically determined locations. Different positions of the pressure cells were used to study the pressure dissipation inside the unreinforced and geocell-reinforced aggregate layers. Figure 22 shows photographs of a pressure cell, and its placement on the OGA layer inside the wooden box.

(a) (b)

Figure 22: Photographs Showing: (a) An Earth Pressure Cell used in the Current Study; and (b) Placement of the Earth Pressure Cell during construction of the OGA Layer

Pressure Cell Placement in Unreinforced Samples

Depending on whether the aggregate layers were constructed in unreinforced or geocell-reinforced configurations, the position of pressure cells was varied to capture general trends in the pressure distribution patterns. For the unreinforced samples, pressure cells were placed at heights of 0, 75, 150 and 225 mm (0, 3, 6, and 9 in.) from the bottom of the box. Figure 23 shows the position of the pressure cells within the aggregate layers. The figure shows the cross section through Grids 2-8 so that the pressure cells seen in the figure are Grids 2, 5 and 8. Two pressure cells were placed in Grid 2 and 8 to observe the stress pattern while LWD drops were applied on top surface of the Grid 5.

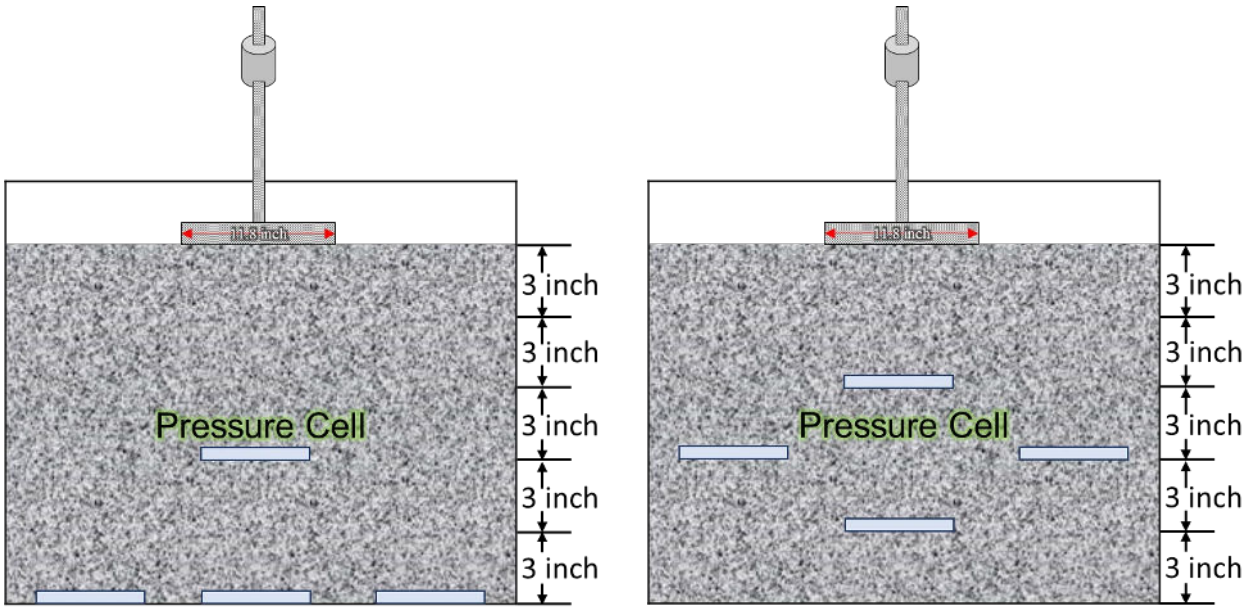

Pressure Configuration- 1 Pressure Configuration- 2

Figure 23: Position of Pressure Cells within the Unreinforced OGA Layers to Monitor the Stress Distribution Patterns

Pressure Cell Placement in Reinforced Sample

For the geocell-reinforced samples, the objective was to assess how the stress levels and stress distribution patterns are altered due to placement of the geocells. Figure 24 shows a schematic of the pressure cell placement corresponding to a geocell-reinforced layer. After the placement of the first 50 mm (2 in.) layer, three (3) pressure cells were placed in Grids 2, 5 and 8. This was followed by construction of the 6-in. thick geocell reinforced layer; the geocell pockets were manually stretched, and aggregate was poured into these pockets using shovels. Once the geocell pockets were fully packed with aggregates, a thin capping layer of ASTM # 57 material was spread. A pressure cell was place on top of it, and the final capping layer (4-in. thick) was constructed. Placement of pressure cells immediately above and below the geocell layer would facilitate direct quantification of how the pressure levels are altered due to placement of the geocell.

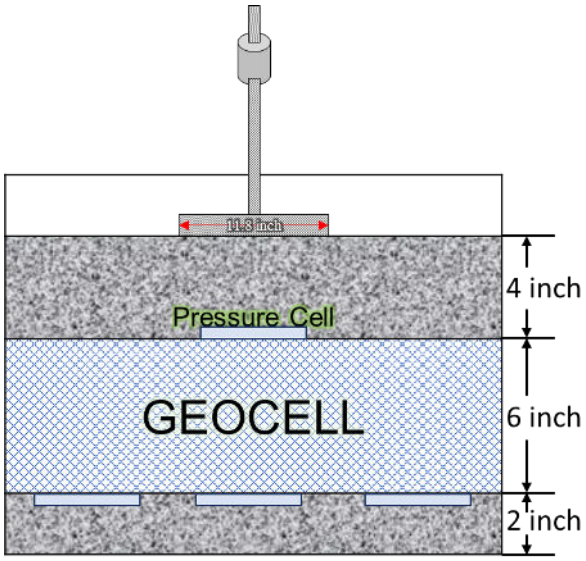

Figure 24: A Schematic Diagram Illustrating the Positioning of Pressure Cells Corresponding to a Geocell-Reinforced Aggregate Layer in the Wooden Box

PHASE-3: NUMERICAL MODELING

As already mentioned, details about the numerical modeling task in the current study was documented as a stand-alone research manuscript, which has been included in Appendix A of this report.

PHASE-4: CONSTRUCTION AND TESTING OF FULL-SCALE SECTIONS

This section provides details about the construction and testing of full-scale OGA pavement layers over varying subgrade conditions.

Test Section Location and Design

Test Section Location

The full-scale pavement test section was located on the north side of the OSU College of Engineering, Architecture, and Technology (CEAT) Construction Engineering Technology Laboratory. This section of land is adjacent to the OSU Asphalt Materials Laboratory and was not subjected to any vehicular traffic. The research team worked with the OSU Facilities and Management Department to designate this location for use during the field construction effort of this project. The test section location has been identified with a rectangular box in Figure 25.

Figure 25: Aerial view of the Test Section.

Test Section Design and Layout

The test section was designed targeting varying subgrade conditions (no-compaction vs. compaction), aggregate lift thickness, total aggregate thickness, and the presence or absence of geotextile at the subgrade-subbase interface. The overall objective was to study the surface deflections of OGA base/subbase layers constructed over different subgrade conditions, following different layer configurations, under different levels of compaction.

Figure 26 shows a longitudinal schematic of the test section layout followed in the current study. ASTM #57 was used in the base layer, whereas the ASTM #4 was used in the subbase layer. As marked on the figure, the west half of the test section was constructed over uncompacted (just smoothened) subgrade soil, whereas the east half was constructed by compacting the subgrade targeting 95% standard Proctor Maximum Dry Density. The aggregate materials were placed over uncompacted and compacted subgrade soil with different lift thicknesses. Different test sections were designated 1A, 1B, 1C, 1D, through 5A, 5B, 5C, and 5D. Four additional test cells, named 6A, 6B, 6C, and 6D, were constructed under the scope of a complementary research effort to study the effect of geocells on 'stability' of OGA layers. It should be noted that layer and construction lift thicknesses during the full-scale testing effort were planned to be representative of actual practice. Moreover, the construction sequence was planned so that some direct comparison can be drawn between the results from Phase-2 (intermediate-scale lab testing) and Phase-4 (Full-Scale Field Testing). Similar lift thicknesses were used in the field as well as during box testing in the lab to investigate whether the laboratory results can be extended to the field.

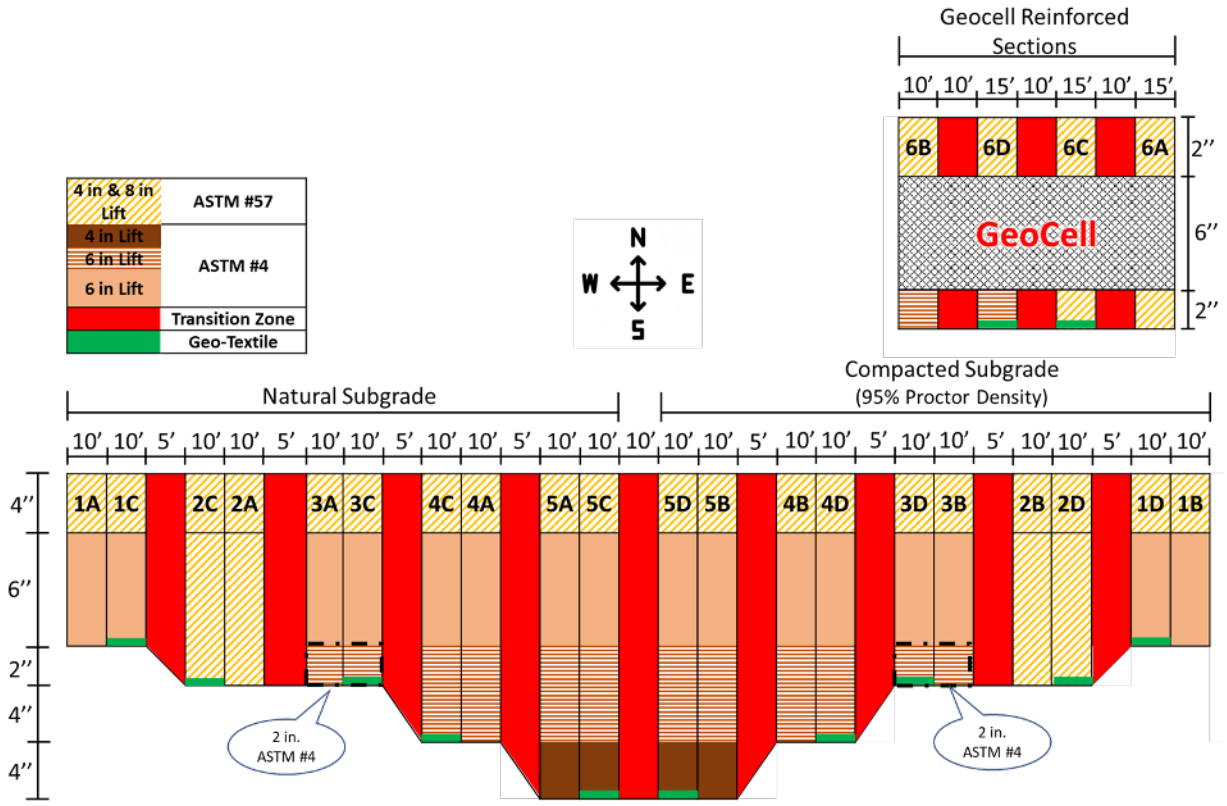

Figure 26: Schematic Diagram of Longitudinal Cross-Section of the Test Section

Test Section Construction

The test section was constructed between September 14, 2021, and September 17, 2021 by North Central Construction Ltd. The entire construction was overseen by Deb Mishra, the PI of this study. Every step of the construction and testing process was documented using detailed photographic and field notes. Additional photographs corresponding to different steps in the construction phase are presented in Appendix B of this report.

Excavation

The area identified for construction of the test section had an existing surface layer of approximately 6-in. thick crushed aggregates. This layer was removed to prepare the ground for construction of the test section. A backhoe was used for most of the excavation. Boundaries between different test sections, and the target excavation depths were measured using a rotating laser and marked with a string. Figure 27 shows photographs of the excavation and section depth establishing processes. The excavated soil was collected for detailed laboratory characterization (Atterberg's limits, moisture-density characterization, and shear strength testing). Results from these tests will help validation of full-scale models to be developed later as a part of subsequent research efforts.

(a) (b)

(c) (d)

Figure 27: Photographs Showing Different Stages of the Site Preparation Process: (a) Subgrade Excavation (b) Grading of the Subgrade Surface; (c) Rotating Laser used to Establish Target Elevations during the Construction; (d) Marking of Target Elevation using the Laser Target Rod

Subgrade Preparation

After excavating to target depths, the subgrade surface was smoothed with a blade attached to the backhoe. The subgrade for the test cells on the east end (Cells 1B, 1D, 2D, 2B, 3B, 3D, 4D, 4B, 5B, 5D) were compacted using two passes of the vibratory, smooth-drum roller. Dry and moist soil density tests on compacted areas were performed using a nuclear density gauge. Dynamic Cone Penetrometer (DCP) tests were carried out to establish the California Bearing Ratio (CBR) values for the compacted subgrade layer. The DCP testing was focused on the top 150 mm (6 in.) of the prepared subgrade layer to characterize the subgrade strength and to evaluate the uniformity of compacted subgrade. Figure 28 shows additional photographs of the subgrade preparation and testing process.

(a) (b)

(c) (d)

Figure 28: Photographs Showing Different Stages of Subgrade Preparation: (a) Surface Grading (b) Compaction using the Vibratory Smooth Drum Roller; (c) Dynamic Cone Penetrometer (DCP) Testing; and (d) Nuclear Density Gauge Testing

One of the objectives of this research study was to assess whether better compaction can be achieved for the OGA layers when a geotextile is placed at the subgrade-subbase interface. Therefore, half of the test cells were constructed by placing a nonwoven geotextile at the subgrade-subbase interface, whereas the other half comprised no geotextiles (refer to Figure 26). The geotextile may play an important role as a separation layer in case of subgrade layers that have high moisture contents, and are susceptible to pumping. If there is a possibility of significant rainfall, nonwoven geotextile is preferable as they provide good drainage properties; woven geotextile provides more strength, which was not of interest in this study. However, the field-tests in the current study did not span across significant rainfall events to realize potential benefits of the geotextile separation layer. Figure 29 shows a photograph of geotextile placement at the subgrade-subbase interface for selected tests cells.

Figure 29: Photograph Showing Geotextile Placement at the Subgrade-Subbase Interface

Material Placement and Compaction

After subgrade preparation, aggregates were placed into the test cells in four stages. The aggregate placement sequence was planned to optimize the layer compaction process. Accordingly, test cells where the finished subgrade was at the greatest depth, were filled with aggregate first. Following this protocol, a layer of ASTM #4 aggregate was first was placed in Cells 5A, 5B, 5C and 5D and compacted to a thickness of 100 mm (4 in.) using two passes of a single-drum smooth vibratory roller. It should be noted that all the thicknesses stated in this report refer to compacted thickness of the respective layers. LWD tests were conducted on this layer. Close inspection of Figure 26 indicates that LWD testing on these 100-mm (4-in.) thick layers of ASTM #4 material in Cells 5A, 5B, 5C, and 5D would facilitate the following comparisons:

1. Effect of geotextile placement on surface deflections by comparing Cells 5A vs. 5C or 5B vs. 5D);
2. Effect of subgrade compaction on surface deflections by comparing Cells 5A vs. 5B or 5C vs. 5D; and
3. Effect of subgrade compaction and geotextile placement vs. neither by comparing test results from Cells 5D vs. 5A.

Once testing on the first lift was complete, the second lift was placed using the ASTM #4 in Cells 3, 4, and 5, and ASTM # 57 in Cell 2. The objective of this stage of aggregate placement was to achieve the same final elevation with all the compacted aggregate layers. Therefore, aggregate placement during this stage involved the following:

1. A 150-mm (6-in.) thick layer of ASTM # 4 in Cells 4A, 4B, 4C, 4D, 5A, 5B, 5C, 5D;
2. A 50-mm (2-in.) thick layer of ASTM #4 in Cells 3A, 3B, 3C, and 3D; and
3. A 50-mm (2-in.) thick layer of ASTM #57 in Cells 2A, 2B, 2C, and 2D.

Only Sections 4 and 5 were compacted with two passes of the vibratory roller. LWD tests were conducted on Sections 4 and 5 to provide the following information: (i) surface deflections for a 150 mm (6 in.) lift thickness of ASTM #4 (Section 4); and (ii) surface deflections for a 250 mm (10 in.) thick layer of ASTM #4 constructed by placing and compacting a 100 mm (4 in.) lift followed by a 150 mm (6 in.) lift (Section 5).

After LWD testing on the second stage, the third stage involved placement of a 150 mm (6 in.) thick lift of ASTM #4 for Sections 1, 3, 4, and 5. A 150 mm (6 in.) thick lift of ASTM #57 was placed in Section 2. All the test sections were again compacted using two passes of the vibratory roller. LWD testing after this stage facilitated surface deflection measurements corresponding to the following scenarios:

i. A 200 mm (8 in.) thick lift of ASTM #4 (Section 3);
ii. A 200 mm (8-in.) thick lift of ASTM #57 (Section 2);
iii. A 150 mm (6 in.) thick lift of ASTM #4 placed directly on the subgrade (Section 1);
iv. A 150 mm (6 in.) thick lift of ASTM # 4 placed on previously compacted layers of ASTM #4 (Sections 4 and 5); and finally,
v. A 100 mm (4 in.) thick layer of ASTM #57 placed as the capping layer on all Sections. This layer was also compacted with two passes of the vibratory roller. LWD tests were conducted for all Sections.

Throughout the aggregate placement process, the thicknesses of the placed layers were constantly checked using the rotating laser. Cross-contamination of the aggregate materials between different sections was prevented by placing transition zones between adjacent cells where the material type or layer configuration changed. During construction, half of the transition zone was constructed using materials from the test cell to the east, whereas the other half was constructed using material from the test cell to the west. Figure 30 shows photographs of the material placement, leveling, elevation checking, and compaction for the aggregate layers.

(a)

(b)

(c)

(d)

Figure 30: Photographs Showing Different Stages of the Aggregate Layer Construction: (a) Material Placement; (b) Leveling; (c) Elevation Checking; and (d) Compaction

As already mentioned, one of the complementary objectives involved construction of test sections comprising geocell-reinforced subbase layers. Geocells impart enhanced 'stability' to unbound aggregate layers, through significant increase in lateral confinement. Therefore, this research study attempted to quantify the potential benefits of geocell reinforcement in OGA layers using LWD-measured surface deflection values. One additional test section (Section 6) was constructed near the north-east corner of the longer test strip.

Layer configurations used in Section 6 were significantly different from those used in the other test sections. Like the other sections, Section 6 was also divided into four cells. Layer configuration for Section 6 was also illustrated in Figure 26. Once the subgrade was prepared and the density levels were checked, a 50 mm (2 in.) thick layer of aggregate was placed on top of the prepared subgrade. ASTM #4 was used in Cells 6B and 6D where ASTM #57 was used in Cells 6A and 6C. Subsequently, one static pass of the compactor was applied on top of these layers to prepare a level surface for placement of the next layer. A geocell layer (6-in. thick) was placed on top of this aggregate layer, and aggregate material was poured into the geocell openings using a front-loader. The geocells received ASTM #4 in Cells 6B and 6D and #57 material in Cells 6A and 6C.

After initial pouring of the aggregate into the geocell pockets using a front-loader, the aggregate was spread manually using shovels and rakes to prepare a flat surface. This was followed by the placement of additional 50 mm (2 in.) of capping material (ASTM #57) and leveled using a grader, and then compacted using one static and one vibratory pass of the smooth-drum roller. This configuration of the test cells in Section 6 facilitated the comparison of LWD-measured surface deflections for similar sections constructed with and without geocells. Figure 31 shows photographs of different steps during the construction of the geocell-reinforced layers in Section 6.

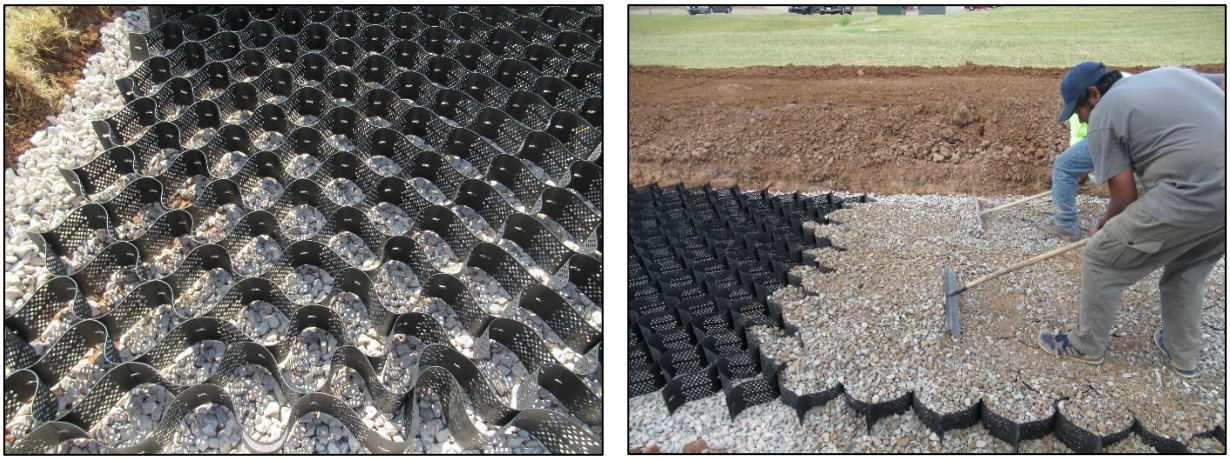

(a) (b)

(c)

Figure 31: Photographs Showing Different Steps during Construction of the Geocell-Reinforced Test Sections: (a) Placement and Stretching of the Geocell Over a 2-in. Thick Compacted Aggregate Layer; (b) Manual Spreading of the Aggregate Material Placed inside the Geocell Pockets using Rakes; (c) Geocell Layer Filled with Aggregates

Testing Protocol and Equipment Used

This section presents details about the different equipment used during this field-testing effort along with the testing protocol followed.

Instruments

Light Weight Deflectometer (LWD)

Two (2) LWD devices, one manufactured by (Olson LWD-1), and a Zorn ZFG-3000, were used throughout this field-testing effort. As previously mentioned, the ZFG-3000 does not measure the applied force directly, whereas a load cell in the Olson LWD-1 provides a direct measure of the applied load. Both devices provide surface deflection measurements by measuring the overall deflection of the loading plate. Both devices can be controlled using a laptop computer or a tablet. The Olson device has been designed to use ASTM E2583 standard test method, whereas the Zorn device uses ASTM E2835 standard

test method. Accordingly, the Olson has a precision buffer of ± 2µm whereas the Zorn has a precision buffer of ± 40 µm.

Dynamic Cone Penetrometer (DCP)

A Dynamic Cone Penetrometer (DCP) was used to assess the uniformity of the prepared subgrade layer. DCP testing was conducted over the top six inches of the prepared subgrade layer only. A pre-established correlation (Kleyn's correlation between CBR and penetration rate: Log (CBR) = 0.84-1.26 x Log (PR)) was used to estimate the in-situ California Bearing Ratio (CBR) values for the top six inches of the subgrade layer. Figure 32 shows a photograph of the DCP used in the current study. Figure 33a shows a photograph of the DCP testing in progress.

Figure 32: Photograph Showing the Dynamic Cone Penetrometer (DCP) with Accessories.

Nuclear Density Gauge

A nuclear density gauge (NDG) was used to measure the in-situ densities in the subgrade layer. The NDG testing also quantified in-situ moisture contents in the subgrade layer. The NDG testing followed ASTM D6938 test method. Figure 33b shows a photograph of the NDG testing in progress.

Testing Protocol for Subgrade

The testing protocol for the subgrade layer involved tests to confirm layer uniformity, compaction levels, and the in-situ stiffness (measured indirectly using surface deflection values). The compacted density and moisture contents for each cell were measured using an NDG. Once the subgrade surface was prepared to meet the required profile, DCP tests were conducted to assess the uniformity of compaction over the top 6 inches.

Surface deflection values for the subgrade were measured using the two LWD devices. Although the primary focus was on surface deflection values, the LWD-measured modulus values were also recorded for future analysis. One set of LWD tests was conducted for every two consecutive test cells with identical configurations. Close inspection of Figure 26 indicates that consecutive test cells in each section are identical in configuration, with the only difference being the placement of the non-woven geotextile at the subgrade-subbase interface. Obviously, LWD tests on the subgrade were carried out before geotextile placement. Therefore, it is logical to conduct only one test per consecutive test cells. In most cases,

testing at a given location was carried using both LWD devices to ensure the results were independent of the device type used. Each LWD test comprised data collection *under twelve drops*. No seating drops were applied before recording of the data. This approach was taken intentionally to study the significance of seating drops while testing on fine-grained subgrade layers. These results would then be compared against those for the two aggregate materials (ASTM #4 and ASTM #57), for which, seating drops played a significant role. Figure 33c and d, show photographs of the LWD testing on the prepared subgrade layer using the Zorn, and Olson devices, respectively.

(a) (b)

(c) (d)

Figure 33: Photographs Showing Different Tests Carried Out on the Prepared Subgrade Layer: (a) DCP Testing; (b) NDG Testing; (c) Zorn LWD Testing; and (d) Olson LWD Testing

Testing Protocol for Aggregate Layers in Unreinforced Sections

The unreinforced sections in Sections 1 through 5 were tested for surface deflection using LWDs at four (4) different stages during the aggregate placement and compaction. First, LWD testing was performed after placement of the first 4-in. thick aggregate layer in Section 5 (Cells 5A, 5B, 5C, and 5D). LWD

testing was conducted to measure the surface deflection under an uncompacted stage as well as 1, and 2 passes of the vibratory roller. The second set of LWD tests were carried out in Sections 4 (4A, 4B, 4C, 4D) and 5 (5A, 5B, 5C, and 5D) after the second stage of aggregate placement. This resulted in total aggregate thickness of 250 mm (10 in.) in Section 5, and 150 mm (6 in.) in Section 4. Once again, LWD tests were conducted on the uncompacted layer, as well as after one and two passes of the vibratory roller. A similar approach was followed for LWD testing in all test cells after different phases of aggregate placement. During LWD testing, surface deflection (as well as modulus) data were recorded under twelve (12) drops. This was based on findings reported earlier, wherein laboratory test results indicated that nine (9) seating drops were required to 'stabilize' the aggregate matrix during LWD testing. During the field-testing effort, although the first nine (9) drops could be interpreted as 'seating' drops, data was collected under all drops to facilitate the investigation of surface deflection evolution during LWD testing.

Aggregate placement in the test sections following the above-mentioned sequence facilitated surface deflection measurement using LWDs for different lift thicknesses (100, 150 and 200 mm) under different compaction levels (i.e., zero, one, and two passes of the vibratory roller). The subbase layers were primarily constructed using ASTM #4 aggregate, except for Section 2, which was constructed with ASTM #57 material throughout its entire depth. Construction of Sections 2 and 3 also facilitated LWD testing on single 200-mm (8-in.) thick lifts of ASTM #57 and ASTM #4, respectively. Figure 34 shows photographs of LWD testing on the aggregate layers. Chapter 6 of this report presents detailed analysis of all test results.

(a) (b)

Figure 34: Photographs Showing LWD Testing on the Aggregate Surface at Different Stages using the Two LWD Devices: (a) Olson LWD-1; and (b) Zorn ZFG-3000

Testing Protocol for Aggregate Layers in the Geocell-Reinforced Section

As mentioned, the subbase layer in Section 6 was constructed using a 150-mm (6-in.) tall geocell mat. Accordingly, the aggregate material placement in this test section followed a procedure that was completely different from those in the other test sections. LWD testing was carried out after placement of the first 50-mm (2-in.) thick aggregate layer over the prepared subgrade. Cells 6B and 6D contained ASTM #4 material in the subbase, whereas Sections 6A and 6C were constructed with ASTM #57 in the subbase as well as the capping layers. The second set of LWD tests were carried out in Section 6 after placement of the final 50 mm (2 in.) thick capping layer placed on top of the geocell-reinforced subbase layer. The capping layer comprised ASTM #57 material for all test cells. This capping layer was compacted through the application of one static and one vibratory pass of the roller. LWD testing was carried out for the uncompacted layer as well as after each pass of the roller. This construction and testing sequence enabled the investigation of the effect of compaction type on LWD-measured surface deflections for geocell-reinforced sections. Moreover, this layer configuration facilitated direct comparison of the test results between unreinforced and geocell-reinforced test sections. Finally, the selected layer configuration also enabled the research team to directly compare the effects of geocell reinforcement on the two aggregate materials (ASTM #4 and ASTM #57). Figure 35 shows LWD testing on the aggregate layers placed in the geocell-reinforced test cells. The next chapter presents results from the laboratory as well field-testing efforts carried out in this research study.

(a) (b)

Figure 35: Photographs Showing LWD Testing on Aggregate Layers Placed in the Geocell-Reinforced Test Section: (a) Olson LWD-1; (b) Zorn ZFG-300

CHAPTER 6: RESULTS AND DISCUSSION

This chapter presents results from all testing. First, results from the small-scale laboratory testing in Proctor molds have been presented. This is followed by results from the intermediate-scale laboratory testing, where the aggregate materials were tested in a wooden box. Finally, results from the field-testing effort are presented. Testing at three different scales gave a good picture of the effect of testing scale when using LWDs on OGAs.

RESULTS FROM PHASE-1: SMALL-SCALE LABORATORY TESTING

Phase-1 of this research effort comprised extensive small-scale laboratory testing to study the compaction behavior of OGA materials through LWD testing in Proctor molds.

Factors Affecting LWD-Measurements

Although the LWD has many advantages, LWD-measured deflection or modulus/stiffness values can be quite sensitive to slight variations in the testing procedure or conditions. Accordingly, the first task in this research study involved extensive testing to identify different factors that can affect the LWD-measured deflection or modulus/stiffness values when OGA materials are tested. The results are discussed below.

Impact of Floor Location

The laboratory floor stiffness could potentially influence the LWD test results. Therefore, a portion of the floor in OSU's geotechnical laboratory was divided into six individual grids. Figure 36 (left) shows the floor locations and test grids. After 30 LWD seating drops at location-1 (Loc.-1), the sample was tested for three consecutive drops on each location (Loc. 2 to Loc. 6) and the LWD-measured modulus values were recorded. It was observed that a change in the LWD test location significantly changed the measured modulus values. The variation in measured modulus values with the change testing location are shown in Figure 36 (Right).

It may seem that the change of test locations may be the only reason that influenced the LWD-measured modulus value. However, several additional reasons could affect the results as well. For example, the lab floor was not perfectly smooth to provide uniform support to the mold. Non-uniform contact between the lab floor and the bottom of the mold base plate may be another reason for the variation of results from Location-1 to Location-6. Moreover, the mold was moved from one location to another by sliding due to the heavy weight of the mold filled with aggregates. This sliding may have caused some disturbance in the aggregate matrix, and the packing within the matrix may have been loosened. In addition to this, during movement, the LWD contact plate may have moved slightly. That slight movement could also influence the results. LWD tests were also performed directly on the floor (on top of a thick rubber mat) at the six individual grid locations. The results showed non-uniform stiffness across the floor.

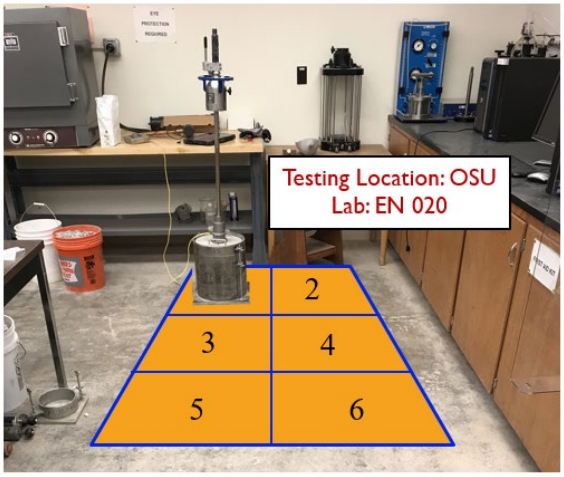

(a). OSU Lab Floors

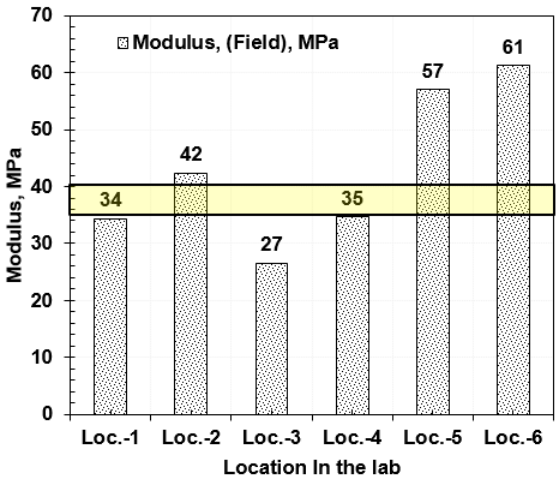

(b). Measured Modulus

Figure 36: Impact of Floor Location

Impact of LWD Device Type (Olson Vs. Zorn)

Despite its convenience and ease of operation, deflection or modulus measurements by LWDs can be significantly affected by slight variations in the testing procedure. For example, the results can vary noticeably if the user does not hold the device firmly against the surface of the layer being tested while dropping the weight. In the past, researchers found that LWD devices from different manufacturers provided somewhat varied results due to design and operational differences (Puppala, 2008; Ryden & Mooney, 2009; Vennapusa & White, 2009). In the current study, 30 drops using the Olson (standard 10 kg weight) LWD was applied on top of an uncompacted mass of ASTM #4 aggregate inside MC-3 followed by 30 standard drops of the Zorn LWD weight. This process was continued until 150 total drops were applied. The same process was repeated for the ASTM #57 aggregate. The measured surface deflection values from this test sequence are presented in Figure 37 and Figure 38. Figure 37 shows that after 30 drops the surface deflection values measured using the Olson and Zorn LWDs are quite similar for the ASTM #57 aggregate. At the same time, for ASTM #4 aggregate, the Zorn and Olson follow similar trends in calculating surface deflections up to 150 drops (Figure 38). Note that 30 LWD drops were applied to the ASTM #57 material to observe whether the measured result is device-agnostic. On the other hand, 150 LWD drops were applied to the ASTM #4 material to observe the impact of LWD drop on surface deflections, as well as to assess whether the results become device sensitive under an increased number of drops. Figure 38 also includes the bulk density levels achieved by the samples during different number of LWD drops.

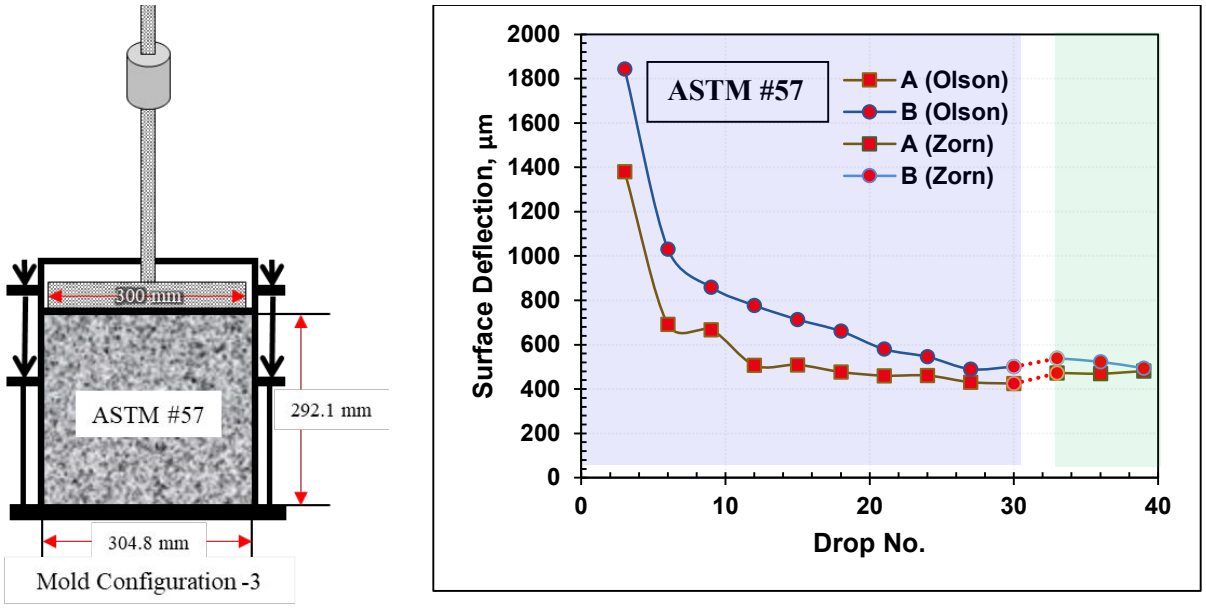

Figure 37 : Comparing the Results from Olson and Zorn LWDs for ASTM # 57 Aggregate

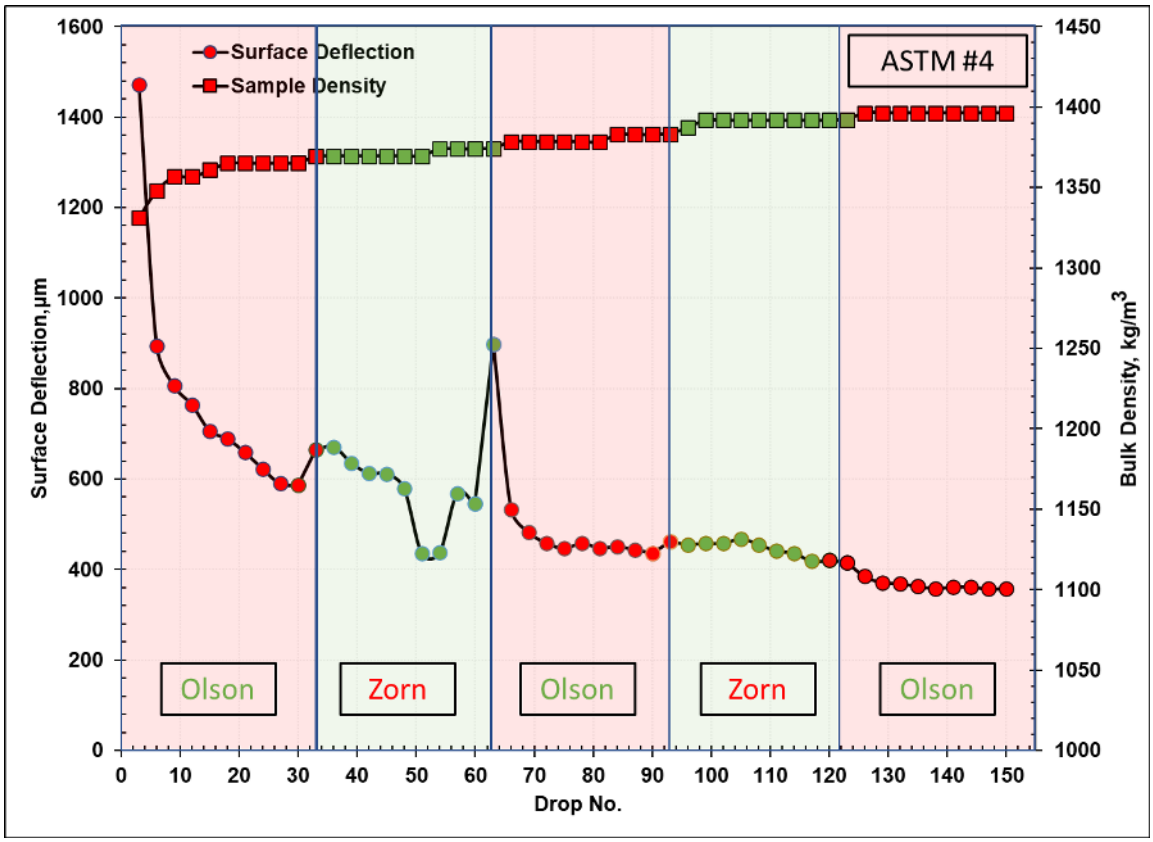

Figure 38 : Effect of Increasing Drop Numbers on the Surface Deflection and Density Values Measured for ASTM # 4 Aggregate Material using both Olson and Zorn LWDs

Figure 38 reveals that initially, surface deflection values change rapidly with increasing number of LWD drops, but the curve gradually flattens. This is a direct indication of change in packing condition of the aggregate matrix. Starting from an uncompacted stage, the surface deflection value decreases rapidly as the aggregate packing condition improves. This conclusion can also be confirmed by the initial rapid increase in density. However, the rate of change in packing condition decreases with increasing number of drops, therefore flattening the deflection reduction and density increment curve. Except for 2-3 instances of sudden 'jumps' in the surface deflection values observed at approximately 60 drops, variations in the surface deflection values were somewhat limited for both devices. *Based on these results, it can be concluded that the use of either Zorn or Olson LWD would result in similar surface deflection values for OGA materials when all other conditions such as level of compaction remain constant.*

Impact of Drop Number

The first task was to determine how many "seating" drops are required to ensure adequate contact between the LWD plate and the OGA layer surface. To study this aspect, both aggregate materials (ASTM #4 and #57) were compacted inside the standard and customized Proctor molds. The samples were tested with Olson LWD in uncompacted as well as compacted conditions. Five (5) samples were taken from the aggregate stockpile following standard sample collection protocols. In Figure 39, the LWD-measured surface deflection values and the surface stress levels are presented for the uncompacted ASTM #4 aggregate material inside MC-3. The surface deflection values have been plotted using solid lines, whereas dashed lines represent the surface stress levels. From this figure it can be observed that initially, the surface deflection value decreases rapidly with increasing number of drops. However, after 9 to 15 drops, the variation reduces, and approaches a "stable" state. Based on these results, the researchers selected nine (9) drops as a suitable number for seating drops during LWD testing. As the surface of the open graded aggregate layer is not smooth for uniform contact with the LWD plate, the energy from these "seating drops" can help ensure adequate contact between the LWD plate and the layer surface. Once this initial "seating" is achieved, subsequent measurements of surface deflection are representative of the entire aggregate matrix, rather than reflecting rearrangement of the surface particles. Figure 39 also reveals that the surface deflection values vary from sample to sample which indicates different packing characteristics owing to the angularity and surface texture of these non-homogenous materials.

Close inspection of the surface stress levels in Figure 39 also indicates no significant "jumps" as the samples undergo particle rearrangement. The only significant change in surface stress level was observed for Drop #15 in Sample C, which also led to a significantly lower surface deflection value. The authors are not sure what caused this significant jump for this point. No change in the stress level is observed with increasing number of drops. Nevertheless, the surface deflection decreases, indicating particle rearrangement into a 'denser' matrix.

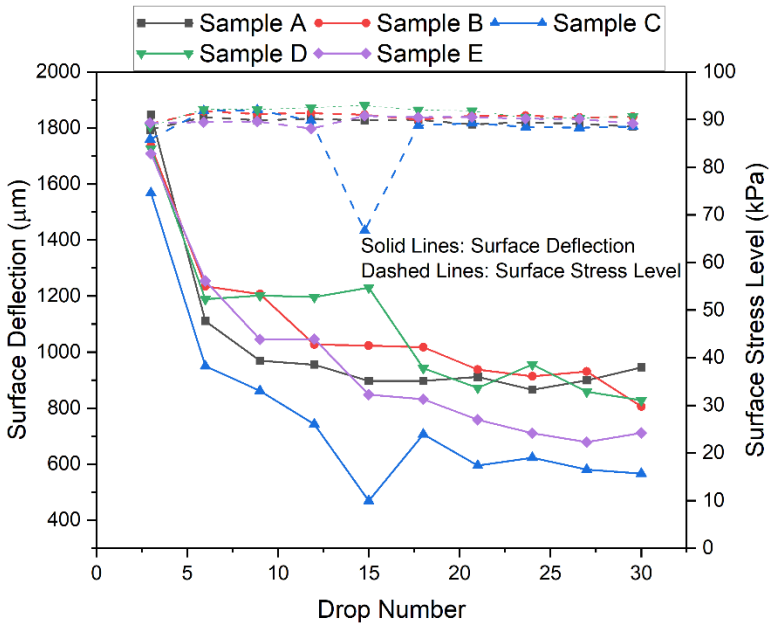

Figure 39: LWD Test Results for ASTM#4 Aggregate in MC-3.

Experimental Results: Vibratory and Impact Compaction using a Jackhammer

The compaction response of the OGAs to simultaneous vibratory and impact compaction (top-to-bottom compaction) has been studied in this section. This compaction force was applied by using an electric jackhammer on top of a 300-mm diameter plate. Although the vibration frequency in a jackhammer is not constant, use of the jackhammer and a top plate simulates the compaction procedure commonly applied by researchers for preparing unbound aggregate samples for laboratory testing. Assuming the vibration amplitude and frequency are consistent with time, the specimens were compacted with the jackhammer for different durations.

For example, the ASTM #4 aggregate in MC-3 was compacted by applying six (6) cycles of 5-second each, followed by two (2) cycles of 15-second each. LWD tests (9 consecutive drops) were performed after completion of each compaction cycle. The test results are presented in Figure 40. This figure also includes the density levels achieved by the sample under jackhammer vibration. Figure 40 illustrates that after completion of the first 5 seconds of compaction, the additional 55 seconds of compaction had minimal impact on surface deflection and density level achieved. It is important to note that even when significantly high 'jumps' in the surface deflection values are measured, the corresponding jump on the density value is not significant. The sample shows a relatively rapid increase in density under the very initial stages of compaction, and the density levels remain nearly constant thereafter. This again proves that the change in surface deflection is primarily due to 'stabilization' and 'destabilization' of the aggregate matrix, and not because of sudden changes in the sample density. After 5-10 seconds of jackhammer compaction, the sample achieves a bulk density value of approximately 1450 kg/m^3 (90 pcf), which is in the range of values typically expected for OGA materials. *This means five (5) seconds of jackhammer vibration is sufficient to reach maximum achievable compaction with this compaction method. Note that similar trends were observed for the LWD-measured modulus values.*

However, for the purpose of developing compaction control criteria using LWDs, using surface deflections is recommended. This is particularly important when using the Zorn LWD as it does not have the feature to directly measure the applied load levels. Therefore, modulus (or stiffness) calculations in the Zorn LWD are approximate in nature, based on prior calibration results. At this stage it is important to highlight that the Zorn LWD is commonly used by state DOTs because of its simplicity, and lower cost. *Moreover, most LWD-based compaction specifications currently implemented by state DOTs rely on surface deflections, and not modulus values.*

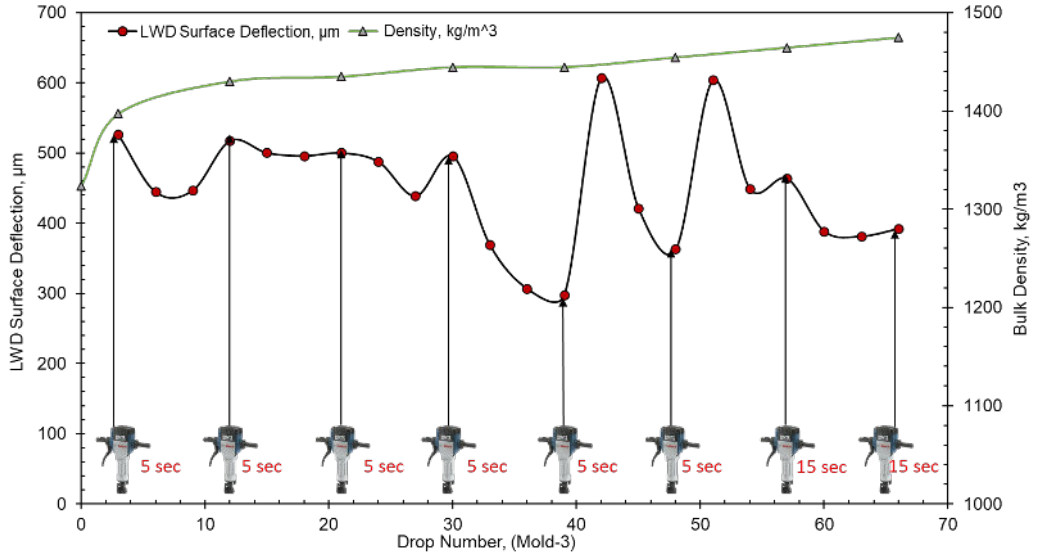

Figure 40: Effect of Jackhammer Compaction Time on the Surface Deflection and Density Values Measured for ASTM # 4 Aggregate

The results from extensive LWD tests after different levels (5, 10, and 15 second) of jackhammer compaction inside the three mold configurations for the two aggregate materials are presented in Figure 41 and Figure 42. Note that the reported surface deflection and density values are the averages from 5 samples after nine (9) seating drops. From Figure 41 it is observed that the deflection values for ASTM #4 and ASTM #57 are similar in MC-1. Beyond 5 seconds of jackhammer compaction, there is an increase in the surface deflection values.

This appears to be counter-intuitive, as increased compaction time should lead to improved packing of the aggregate matrix, which should in turn lead to lower surface deflections. However, compaction past 5 seconds appears to re-arrange the aggregates rather than consolidate them. From the achieved density levels, there is also a decrease in density after 10 seconds of vibration for the ASTM #4 material. For ASTM #57, on the other hand, no change in density was observed when the vibration time was increased from 5 seconds to 10 seconds. The primary reason for this is the size of the mold. In MC-1, the conventional 152.4-mm diameter Proctor mold is used. As this mold is too small for the aggregate materials being tested, the energy from the jackhammer compaction results in the destabilizing of the aggregate matrix, and with increased compaction time, the LWD-measured surface deflections increase. *Therefore, the use of MC-1 was discontinued in the test matrix after this stage.*

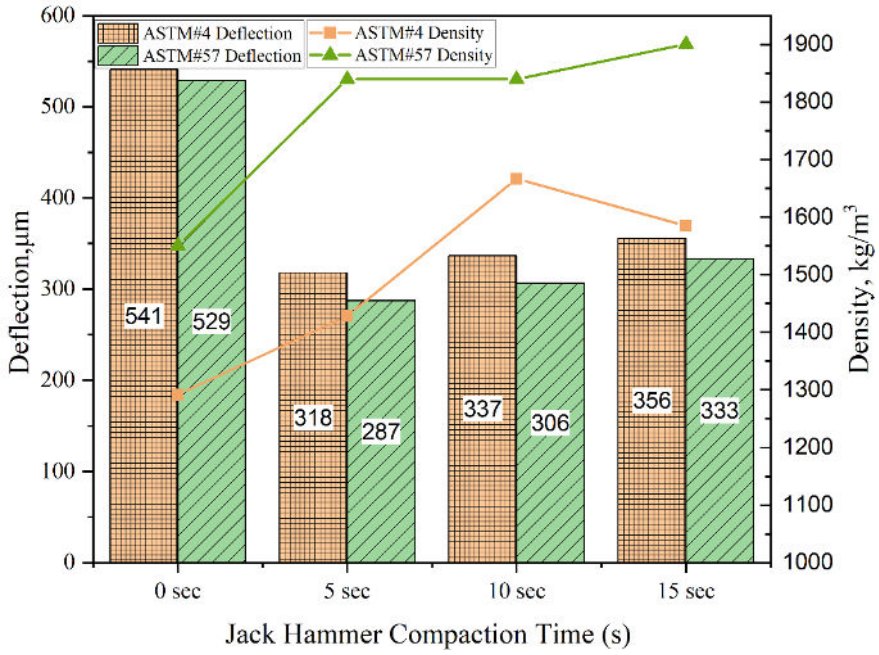

Figure 41: LWD Test Results in MC-1 under Varying Jackhammer Compaction Times

Figure 42 (a), presents similar results for MC-2 (mold diameter of 304.8 mm, but sample height of 116.5 mm). From the results, the surface deflections after compaction inside MC-2 for both ASTM #4 (300 to 332 µm) and ASTM #57 (258 to 282 µm) are close to the surface deflection values found inside MC-1. Also, no stabilization of the aggregate matrix was observed with increasing compaction time, just like in MC-1. This indicates that the 116.5 mm (4.6 in.) sample height is not sufficient for these larger particle-sized materials likely due to lack of particle interlock. When sample size is not sufficiently large compared to the particle size, larger materials can reorient under excessive compaction, destroying any ability to create packing. However, in case of MC-3 where the height of the sample is increased to 292.1 mm (11.5 in), the recorded average surface deflections (Figure 42 (b)) are 402 to 517 µm for compacted ASTM #4 and 320 to 412 µm for the compacted ASTM #57 material. The surface deflections measured in MC-3 are noticeably greater than those in MC-1 and MC-2. *It is important to note that some of the differences highlighted in Figure 42 (a) and (b) may be difficult to appreciate (or replicate) in the field with a device that has lower precision requirements e.g., devices meeting ASTM E2853 precision requirements but not ASTM E2583 precision requirements. Nevertheless, the current study used the Olson LWD for these tests, and with a precision level of ± 2 µm, these differences can be reliably detected.*

From Figure 41 and Figure 42 (a), it can be observed that testing in MC-1 and MC-2 provides an unusual density trend with increased compaction. For ASTM #4 and ASTM #57 after 10 and 5 sec of vibration, there is a decrease in density level indicating the destruction of packing in MC-1 and MC-2. This behavior can be attributed to the boundary effects imposed by the small mold sizes. As MC-1 and MC-2 represent significantly small boundaries for the particle sizes being used, after 5 seconds of jackhammer vibration the maximum packing is achieved. Additional compactive effort beyond 5 seconds does not contribute towards further densification of the matrix, rather leads to destabilization of the packing structure. This leads to a decrease in density and increase in measured surface deflections. Generally, with increasing compaction time effort (often indicated by increased density), surface deflections should decrease; this trend is observed for MC-3. It should also be noted that for the ASTM #4 material, 10

seconds of jackhammer compaction is required to stabilize the aggregate matrix, whereas the ASTM # 57 aggregate matrix stabilizes after only 5 seconds of jackhammer compaction. This indicates that the particle size has an influence on the compaction time required to stabilize the aggregate matrix when the vibration frequency is constant. *The reader is cautioned not to take these compaction times as absolute values, rather as a comparison between how the two aggregate matrices behave under similar compaction time.* In the field, the same two materials may require different compaction times under different roller vibration amplitude and frequencies. Nevertheless, the authors believe, the larger-sized ASTM #4 material will require slightly longer compaction time to achieve a stable matrix in field conditions, compared to the smaller-sized ASTM #57 material.

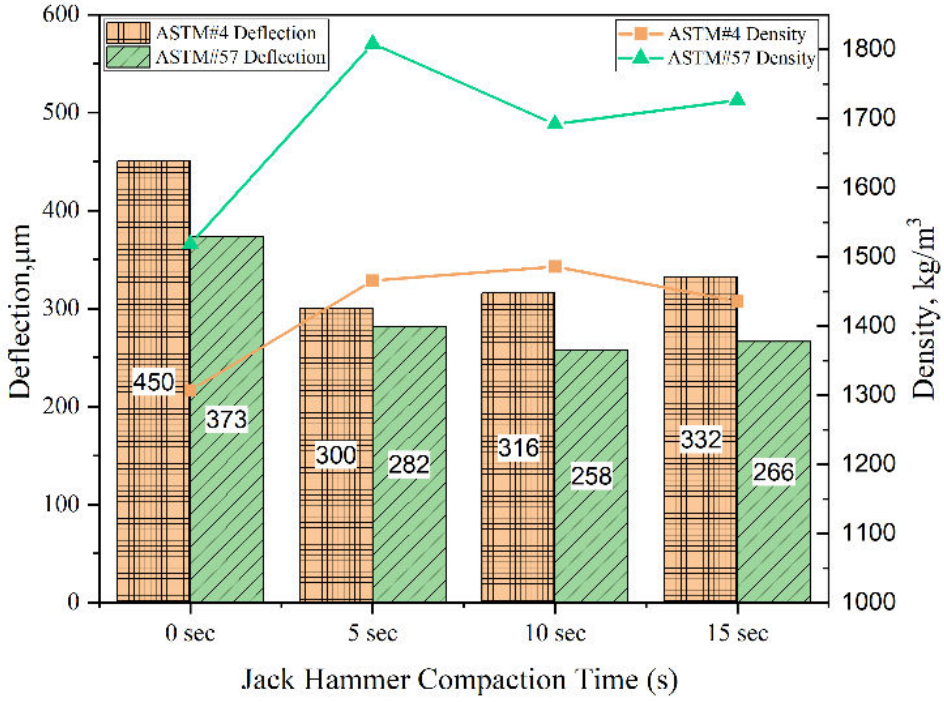

(a)

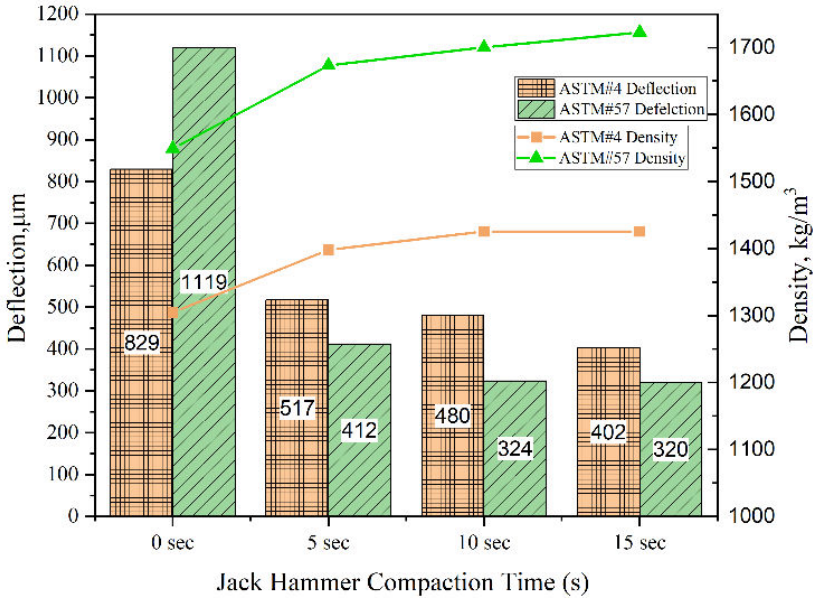

(b)

Figure 42: LWD Test Results under Varying Jackhammer Compaction Times in (a) MC-2 and (b) MC-3

Experimental Results: Constant Vibratory Compaction (using a Relative Compaction Table)

The third and final compaction method tried in this study was with a vibratory shake table. Testing in the vibratory shake table was carried out for MC-2 and MC-3 set-ups for both the aggregate materials. The results are presented in Figure 43. In this process, the mold with aggregate is placed on the vibratory table, and a heavy surcharge weight is placed on top of the top plate to ensure adequate compaction using a bottom-to-top mechanism. After different vibration times, the mold is removed from the table (without disturbing the aggregate), and LWD tests are conducted to measure the surface deflections. Three (3) sets of samples were collected from the two aggregate material stockpiles following standard sampling protocols.

Testing was carried out using the Olson LWD only, under both uncompacted conditions as well as after the sample was subjected to vibratory compaction for different durations. As usual, nine seating drops were applied, and the surface deflections were measured by taking averages of three subsequent drops. As seen from Figure 43(a), for the compacted ASTM #4 material in MC-2, the average recorded surface deflection ranged between 589 μm to 631 μm, whereas the same value for ASTM #57 was between 571 μm to 581 μm. A gradual decrease in the surface deflections was observed for the ASTM #4 material as the vibration time (VT) was increased from 0 to 10 seconds to 25 seconds. However, for the ASTM #57 material, no significant decrease in the surface deflections was observed when the VT was increased from 10 seconds to 25 seconds.

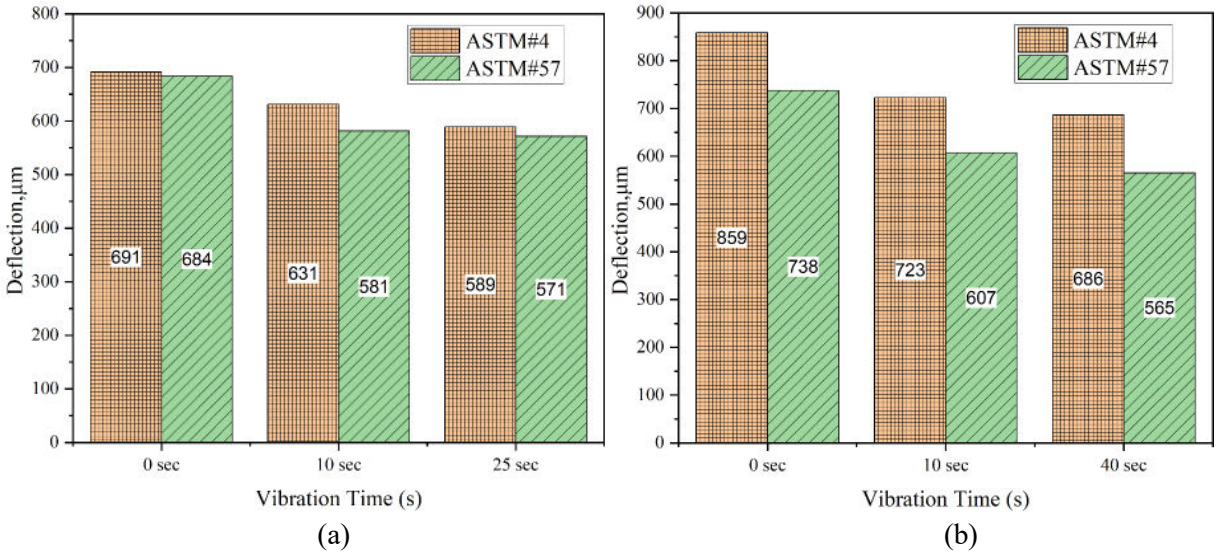

Figure 43: LWD Test Results under Varying Vibration Times with the Shake Table in (a) MC-2 and (b) in MC-3

In case of constant bottom-top vibration in MC-3, the average surface deflection was between 686 µm to 723 µm for compacted ASTM #4 and 565 µm to 607 µm for compacted ASTM #57 (Figure 43(b)) for different durations of vibratory compaction. For both the ASTM #4 and ASTM # 57 materials, their surface deflections decreased significantly with increasing time of vibratory compaction.

The results suggest that several factors could significantly influence the LWD-measured surface deflection (or modulus values) for OGA materials when tested inside the modified/custom Proctor molds. The major influential factors were LWD drop numbers and mold support condition. The results also showed no significant difference between the test results reported by the Olson and Zorn LWDs. Using vibratory compaction using a jackhammer, it was observed that the compaction of OGAs for more than 5 seconds does not improve the packing condition. These influential factors were taken under consideration during the remainder of the laboratory testing to ensure consistent results.

RESULTS FROM PHASE-2: INTERMEDIATE-SCALE LABORATORY TESTING

As mentioned earlier in Figure 20 (c), the box filled with aggregates (ASTM #57 and/or ASTM #4) was divided into nine (9) grids for the purpose of LWD testing. Grid-5 was located near the center of the box, away from the box boundaries. Accordingly, the researchers hypothesized that LWD testing on Grid-5 would not be affected by presence of the box boundaries, and the results should resemble those from field testing. With this hypothesis, LWD tests were carried out in the wooden box on the two OGA materials with three different layer compacted thicknesses (152.4 mm, 304.8 mm, and 381 mm). In each case, the aggregate layer was compacted by applying different passes of a vibratory plate compactor, specifically purchased for this study. First, a little larger than 152.4-mm thick uncompacted aggregate layer was placed and vibratory roller compaction was applied to make the 152.4mm thick compacted layer. LWD tests were conducted at three different stages of compaction: (1) No compaction; (2) One pass of the vibratory plate compactor, and (3) two passes of the vibratory plate compactor. Once LWD testing for

each compactive effort on the 152.4-mm thick layer was completed, the next layer of aggregate was placed to attain a total aggregate layer thickness of 304.8 mm (12 in.).

However, it should be noted that this aggregate layer should not be treated as a single lift, as the bottom 152 mm was compacted before placing and compacting the upper 152 mm. Once a total thickness of 304.8 mm was achieved, LWD tests were again conducted corresponding to 0, 1, 2, and 3 passes of the vibratory plate compactor. Finally, a third layer of aggregates was placed and LWD tests conducted corresponding to 0, 1, 2, and 3 passes of the vibratory plate compactor. In this case, only the upper 76.2 mm (3 in.) of aggregate received fresh compaction as the lower 152 + 152 mm layers had been compacted during the previous testing stages. Five (5) LWD tests were performed in each case.

Experimental Results: Aggregate Layers with No Reinforcement

Results from LWD testing in the wooden box are presented in Figure 44 (ASTM #57) and Figure 45 (ASTM #4). The surface deflections presented in Figure 44 & Figure 45 are the average values from six consecutive drops after six (6) seating drops were applied.

From Figure 44, surface deflection values decrease significantly after one (1) pass of the vibratory plate compactor. When the number of passes increases from 1 to 2, the surface deflection values decrease for the 152.4-mm thick layer. However, no noticeable reduction in surface deflection is observed between 1 to 2 passes for the 304.8-mm thick layer. In fact, for the 381-mm thick layer, the surface deflection increased moving from one to two passes of the vibratory plate compactor. In this case, a 'destabilization' of the compacted matrix was observed when more than one pass was applied. The surface deflection after three (3) passes was still higher than that after one (1) pass.

Based on the results presented in Figure 44, it is evident that the LWD-measured surface deflection values are significantly affected by the level of compaction of the underlying layers. Once the bottom 152.4-mm thick layer is compacted, the second 152.4-mm thick layer achieves optimum compaction even after a single pass of the vibratory plate compactor. When an additional 76.2 mm of aggregate is placed, that layer achieves optimum compaction after just one pass of the compactor. When additional compactive effort is applied, the aggregate matrix gets 'destabilized.'

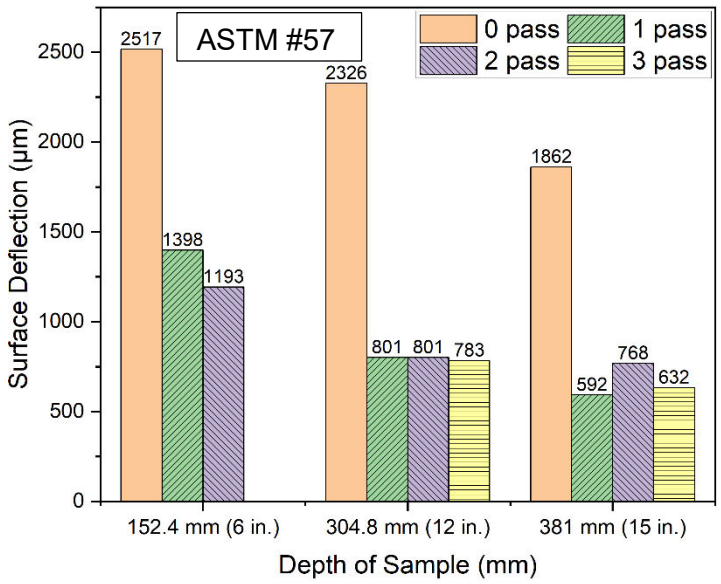

Figure 44: LWD Test Results in Wooden Box for ASTM #57 Aggregate Material (Vibratory Plate Compaction)

Similar results for the ASTM #4 materials are presented in Figure 45. The first thing to note from Figure 45 is that the overall surface deflection values in an uncompacted stage were less than those for the ASTM #57 material (see Figure 44). However, this difference decreased significantly with the application of compaction energy. Just like the ASTM #57 material, the ASTM #4 material also showed a sudden decrease in surface deflections while moving from an uncompacted stage to the application of one compactor pass. However, this reduction is significant only for the 152-mm (6-in.) and 304-mm (12-in.) thick layers. The reduction is not significant for the 381-mm (15-in.) thick layer, where the top-most layer was only 76-mm (3-in.) thick. *Therefore, the application of compaction energy did not lead to significant benefits as there was no space within the 3-in. thick surface layer for the aggregate materials to achieve a better packing.*

This clearly indicates that for the density benefits of compaction to be realized, the aggregate particles need enough space within the layer to rearrange and achieve a better packed stage. Interestingly, upon the application of the second and the third compaction passes on the 381 mm (15 in.) thick layer, the LWD-measured surface deflections decreased further. This was not the case with the 304 mm (12 in.) thick layer. Interestingly, the ultimate surface deflection value after 3 compactor passes on the 304 mm (12-in.) thick layer was 680 µm, and for the 381 mm or 15-in. thick layer was 518 µm. Even for the ASTM #57 material (see Figure 44), the lowest average surface deflection value recorded was 592 µm. *This suggests that for these open-graded materials in a compacted state, the LWD-measured surface deflection should be approximately 500 µm or 0.5 mm with a minimum thickness of approximately 300 mm or 12 in.* However, whether each layer can consistently achieve compacted state that would lead to surface deflection values less than 500 µm, remains to be seen. This will be further investigated using the field-test results.

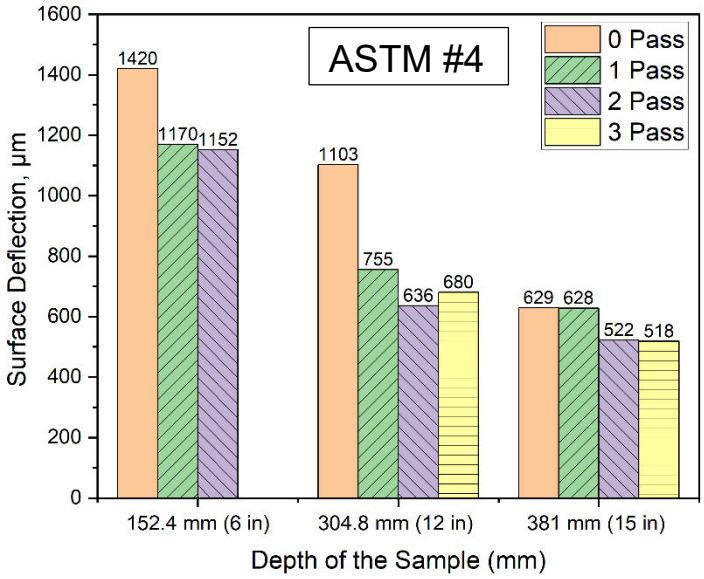

Figure 45: LWD Test Results in Wooden Box for ASTM #4 Aggregate Material (Vibratory Plate Compaction)

As already mentioned, one of the auxiliary tasks carried out in the current study involved measurement of pressure levels at different depths within the aggregate layer during LWD testing. The objective was to study how the pressure levels recorded by the earth pressure cells change with increasing compaction efforts applied to the aggregate layers. The level of pressure at different elevations was measured during the LWD testing. The results are presented in Figure 46 (ASTM #57) and Figure 47(ASTM #4). Pressure was recorded using 4 earth pressure cells using two configurations.

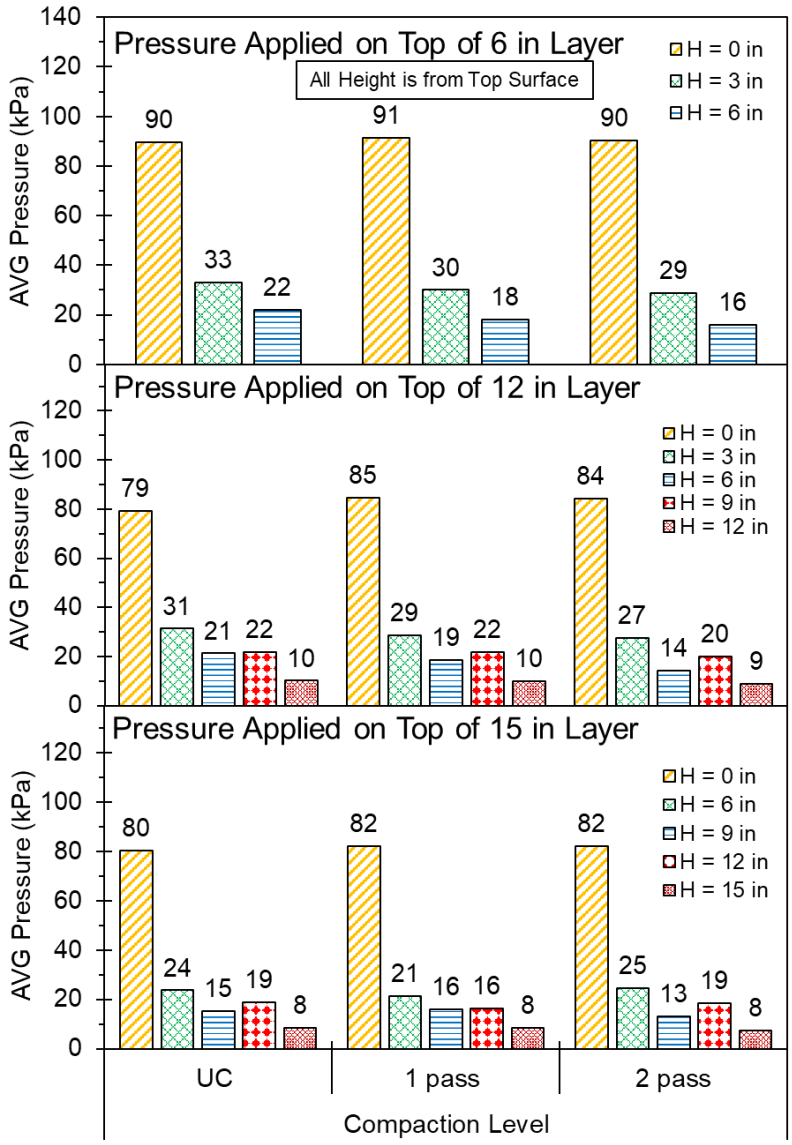

Figure 46: Pressure levels at Different Elevations under LWD Drops at Different Compaction Levels (ASTM #57).

From Figure 46 and Figure 47, following observations can be made:

- Most of the pressure appears to be dissipated within the top 76 mm or 3 in. layer irrespective of the type of the aggregate used. As seen for ASTM #57 after applying 79-91 kPa (11.4-13.2 psi) pressure on the top surface the pressure level becomes almost one-third at a 76 mm or 3 in. depth. Similar behavior is also seen for ASTM #4 material. As most of the stress is reduced in the top layer, the required base/subbase thickness using these materials should be low, from a subgrade protection point of view

- For the ASTM #57 aggregate material, when the LWD drops are applied on top of 381 mm (15 in.) and 304 mm (12 in.) layer, stress levels at the bottom remain constant with increasing compaction levels. For ASTM #4 the bottom stress level is seen to be very close at different compaction levels.

From this observation it can be concluded that for both aggregate types, the stress levels at different depths are not significantly affected by the number of vibratory-compactor passes.

- The stress dissipation within OGA layers does not follow a similar pattern to that commonly observed in dense-graded aggregate layers. Instead of distributing the pressure to a larger area with the depth increment, these materials absorb the pressure without spreading to a larger area. Therefore, the stress dissipation pattern can be thought of as being "cylindrical" rather than "conical" (the most-commonly observed pattern). This statement is justified by the negligible pressure levels recorded at Grid 2 and Grid 5 when LWD drops were applied on Grid 5. This clearly highlights a major difference between the behavior under loading for dense-graded and open-graded aggregate materials.

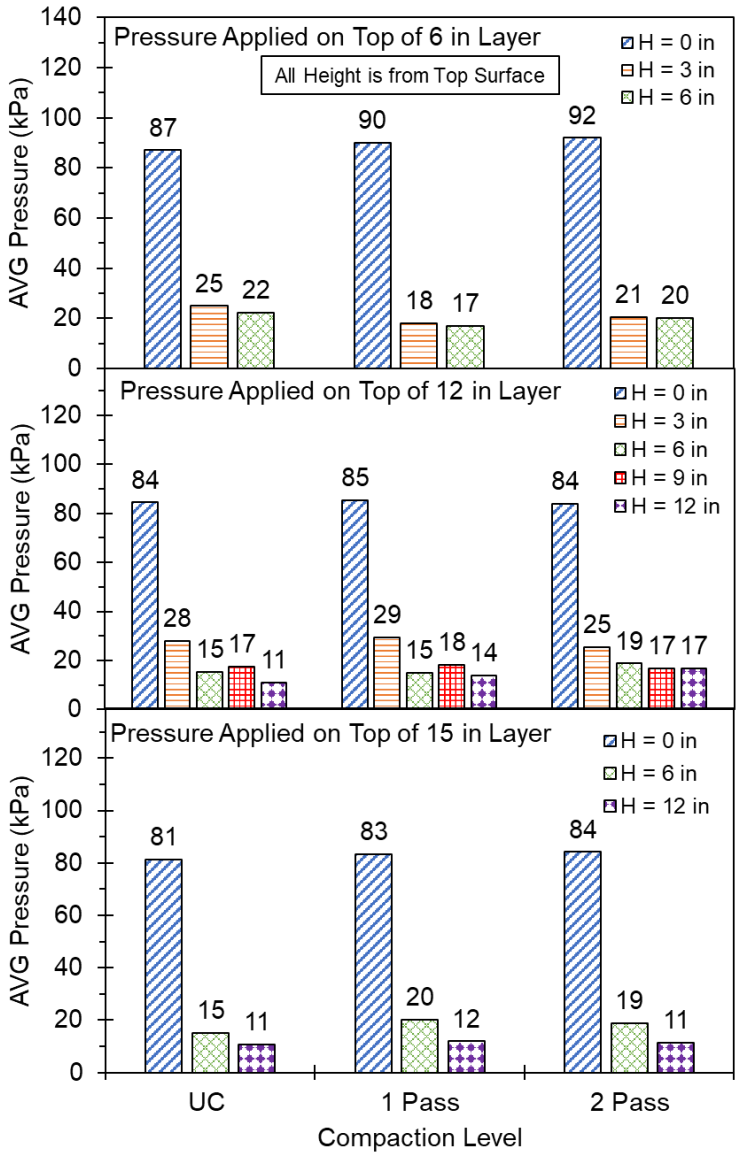

Figure 47: Pressure Levels at Different Elevations under LWD Drops at Different Compaction Levels (ASTM #4)

Experimental Results: Aggregate Layers with Geocell Reinforcement

This section presents findings from intermediate-scale box tests, where the OGA layer was reinforced using geocells. The surface deflection and stiffness values during LWD testing were recorded from the very first drop. The variation of LWD surface deflection is presented in Figure 48. In the figure, each point represents the average of 3 drops. It can be observed that initially, the surface deflection is high, and gradually decreases with increasing drop numbers; after 6 drops, the deflection values become 'stable'. As each line represents the surface deflection of the same location (Grid 5), this behavior indicates the necessity of "Seating Drops."

Open-graded material surface is not uniform in nature; this leads to difficulties in achieving a uniform contact between the LWD plate and aggregate surface. Therefore, initial drops are used to ensure maximum contact between the aggregate surface and the LWD plate. According to results from the current study, three seating drops were necessary before collecting the surface deflection and stiffness data inside the box. Note that the average surface deflection represents the average value after the seating drops.

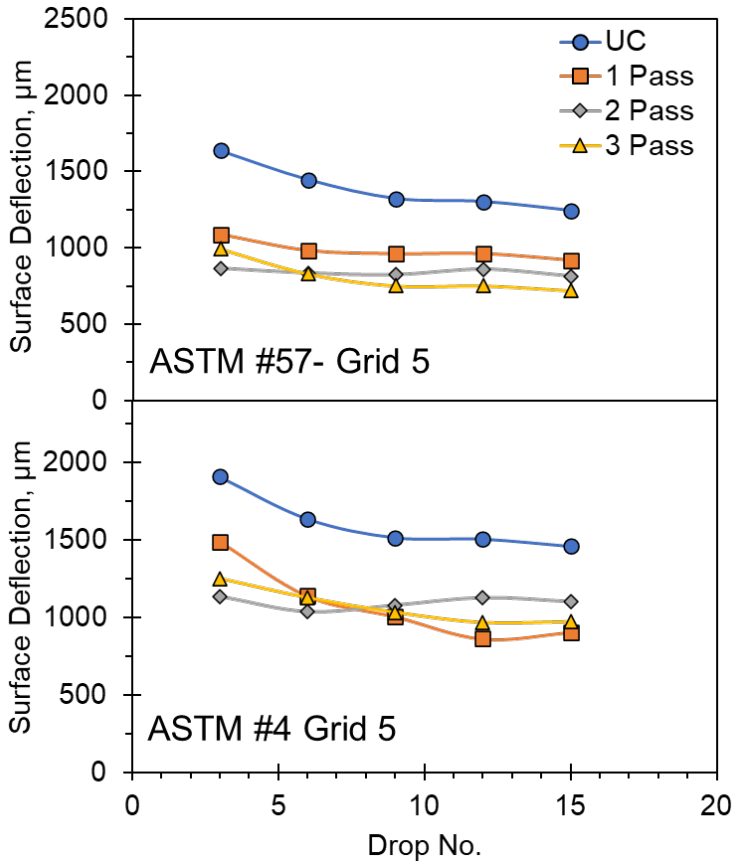

Figure 48: Surface Deflection Variation with Increasing LWD Drop Numbers for Geocell Reinforced Samples (UC: Uncompacted)

Figure 49 and Figure 50 show the average surface deflection values (Left Y- axis) and Stiffness (Right Y-axis) variation of ASTM #57 and ASTM # 4 materials, respectively, with varied compaction efforts. The

horizontal striped bars in the figure represent the average surface deflections after the seating drops without geocell reinforcement where the blue bars represent the average deflection for geocell-reinforced samples. The stiffness is showed using square (without geocell) and upper triangle (geocell) marked lines. The following observations can be made from the figure:

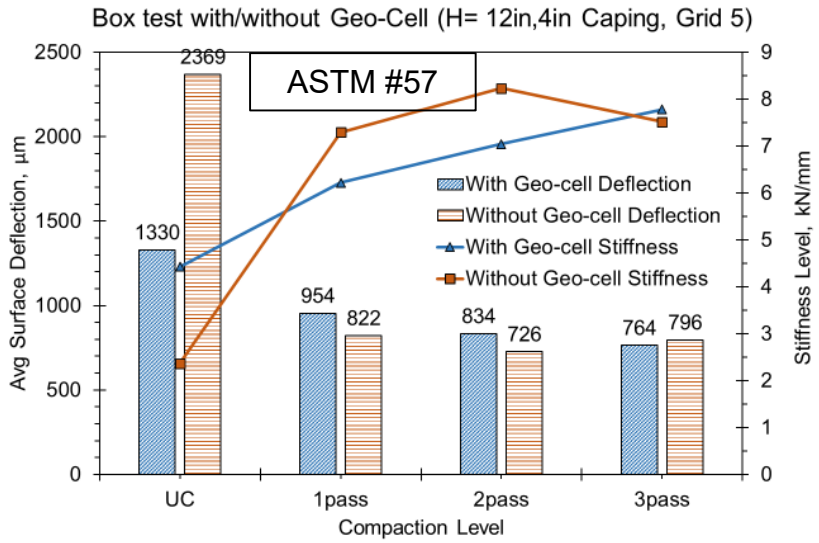

Figure 49: LWD Test Results Inside the Wooden Box (Material: ASTM #57)

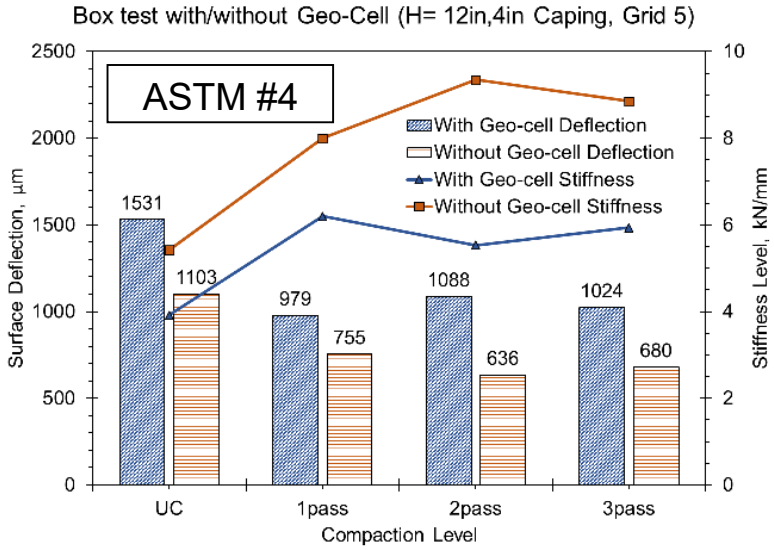

Figure 50: LWD Test Results Inside the Wooden Box (Material: ASTM #4)

- The surface deflection reduces with application of the additional compaction. However, for the ASTM # 57 material, the reduction is significant after the first pass of the vibratory compactor for the unreinforced sample.
- For the ASTM #57 aggregate material, the surface deflections after one pass of the vibratory compactor are close to each other for the unreinforced, and geocell-reinforced samples. No significant

improvement in the LWD-measured surface deflections were observed when the OGA material was reinforced using geocells. This is most likely because the LWD-induced stresses are not high enough to mobilize sufficient lateral movement of the aggregate particles. Therefore, effect of the geocell-reinforcement is not noticeable under such low stresses. Moreover, looking at the stiffness curves, interestingly, the stiffness values for the unreinforced specimen were greater than those for the geocell-reinforced specimen, particularly after 1 and 2 passes of the vibratory plate compactor. This may be because under such confined conditions of the wooden box, aggregate geocell-reinforced aggregate layer could not achieve adequate compaction.

- For the ASTM #4 material, the reduction in surface deflection with increasing compaction effort was not as noticeable as the ASTM #57 material. Specifically, the ASTM #57 material showed better compaction compared to the ASTM #4 material when the compaction energy is kept constant. This statement can also be confirmed by the stiffness value. For geocell reinforced samples, the achieved stiffness value for the ASTM #4 material (5.94 kN/mm) after the third pass of the vibratory compaction was lower than the stiffness achieved by ASTM #57 (7.5 kN/mm). Moreover, when the base/subbase layer was constructed with the coarser gradation material (ASTM #4), increased compaction effort makes the unreinforced layer stiffer than the geocell-reinforced layer.

Vertical stress levels were measured at different levels within the aggregate layer, even for the geocell-reinforced set-up. The locations were: top surface, 100 mm (4 in.) depth from the top (upper surface of the geocell), and 250 mm (10 in.) from the top (lower surface of the geo cell) using earth pressure cells. The recorded data is presented in Figure 51. Each bar represents the average of the stress levels from 15 LWD drops on Grid 5. From the figure, it is observed that most of the stress coming from the LWD drops dissipates in the upper 100 mm or 4 in. layer. The reduction of stress level in the 150 mm geocell layer is negligible compared to the upper 100 mm capping. However, in case of ASTM #4 the stress level is not reduced through the geocell layer as measured with an LWD.

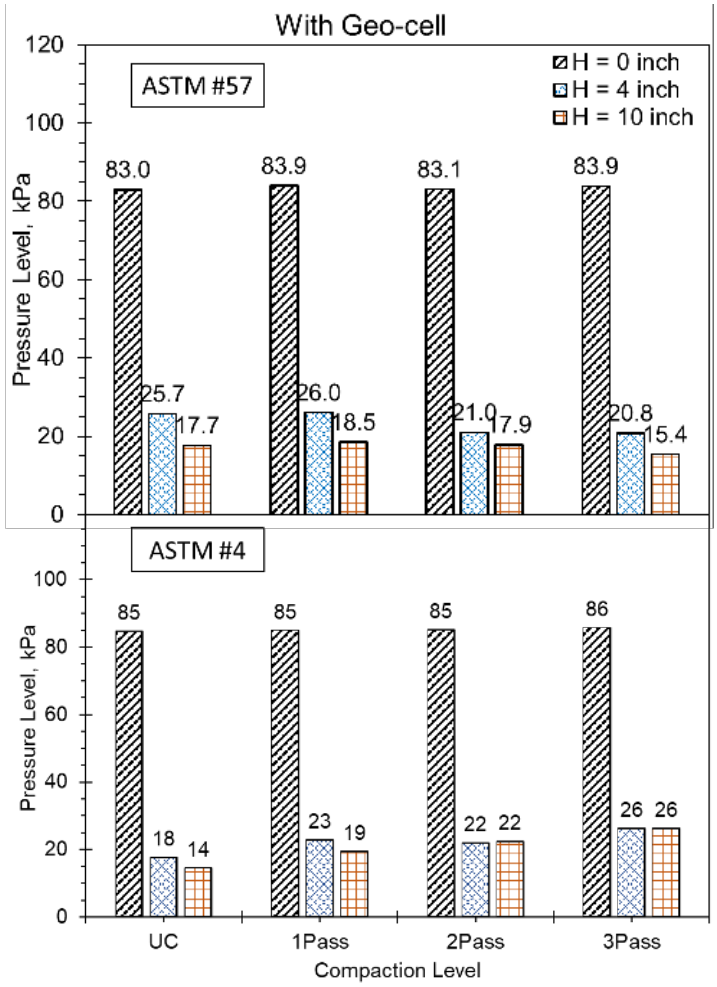

Figure 51: Stress Level at different Depth (from Surface) inside Box with Geocell Reinforcement (ASTM #57 and ASTM #4)

RESULTS FROM PHASE-4: CONSTRUCTION AND TESTING OF FULL-SCALE TEST SECTIONS

Subgrade Properties

Subgrade soil samples collected from the test strip were tested in the laboratory for basic characterization. Visual classification of soil samples collected from different test cells did not show significant variation. Therefore, all samples collected from different locations of the test strip were merged, and just one set of tests were conducted to represent the subgrade for the entire section. Atterberg's Limit tests were carried out following ASTM D4318 specifications. Based on the Atterberg limit values, and the overall particle size distribution, the USCS classification for the soil was CL (low-plasticity clay), whereas the AASHTO classification was A-7-6. Table 6 lists the relevant soil classification information.

Table 6: Subgrade Soil Classification

LL (Liquid Limit)	PL (Plastic Limit)	PI (Plasticity Index)	USCS Classification	AASHTO Classification
42	22	20	CL (Low-Plasticity Clay)	A-7-6 (Clayey Soil)

As already mentioned, one of the objectives during this field construction effort was to build half of the test sections without any subgrade compaction control, whereas the remainder of the sections were to be compacted to 95% of standard compaction dry density. The first step before subgrade compaction was to establish the moisture-density curve for this subgrade soil. *The maximum dry density was determined to be 103.0 pcf.* Table 7 shows results from the moisture-density checks in the field using a Nuclear Density Gauge. Cells B and D in Sections 1 through 5 were supposed to be compacted to 95% of maximum dry density established using the standard compaction effort. The rows corresponding to these cells have been highlighted in gray in Table 7. As seen from the table, several of the test cells did not achieve the target density even after roller compaction. The research team decided to stop compaction at that stage and continue with the testing as no growth in the compaction percentage was observed even after additional roller passes. This slight lower density compared to the target value of 95% is not likely to affect the study results as the test sections are not subjected to vehicular loading, and the LWD-imposed surface deflections are not likely to be affected by such small differences in the achieved layer density.

Besides checking the moisture-density values, Dynamic Cone Penetrometer (DCP) tests were also conducted on the subgrade layer to check the uniformity of compaction. The DCP test focused primarily on the top 150 mm (6 in.) of the prepared subgrade layer for the same reasons stated above (no vehicular loading applied to the test sections). The DCP penetration rates were used to calculate the in-situ CBR values for the compacted subgrade layer (6 in. only). The following equation, developed by Kleyne et al. (1982) was used to calculate the in-situ CBR values from DCP penetration rates.

Log (CBR) = 0.84-1.26 x Log (PR) ----------(6)

where CBR = California Bearing Ratio, PR = penetration rate (in./blow) of DCP.

Table 8 lists the moisture contents, LWD-measured surface deflections, LWD-measured surface modulus values, CBR values calculated from the first DCP drop, as well as the average CBR values calculated over the top six inches of the subgrade layer for each test cell. Once again, the highlighted rows in the table correspond to cells that are supposed to be compacted to at least 95% of standard compactive effort dry density. Figure 52 shows the variation in soil moisture content and the LWD-measured surface deflections for the prepared subgrade layer in each test section. As seen from the figure, the moisture content varied from 10.6% to 24.9 %, whereas the surface deflection varied from 0.45 mm to 1.78 mm.

Table 7: Results from Moisture-Density Checks on the Compacted Subgrade

Test Cell	Moisture Content (%)	Wet Density (pcf)	Dry Density (pcf)	Percent Compaction (%)
1A	16.6	110.2	94.5	91.8
1B	16.8	110.6	94.6	91.9
1C	15.2	98.1	85.2	82.8
1D	21.8	113.6	93.2	90.6
2A	12.7	91	80.8	78.5
2B	19.6	113.1	94.6	91.8
2C	10.6	94.5	85.4	83
2D	24.9	117.5	94.1	91.4
3A	13.8	81.2	74.4	69.3
3B	16.6	110.2	94.6	91.8
3C	12.8	97.7	86.6	84
3D	23.3	113.8	92.3	89.6
4A	15.9	99.1	85.6	83.1
4B	19.3	117.2	98.3	95.4
4C	15.8	103.9	89.7	87.1
4D	22.2	114.7	98	95.2
5A	17.4	116.2	99	96.2
5B	20	120.3	100.3	97.4
5C	16.6	114.2	97.9	95.1
5D	21.5	124.6	102.6	99.6
6A	16	110.7	95.5	92.7
6B	11.9	112.9	100.9	98
6C	12.1	109.4	97.6	94.8
6D	10.9	99.4	89.6	87

Table 8: Results from LWD and DCP Testing on the Subgrade

Test Cell	Moisture Content (%)	Surface Deflection (mm)	LWD Modulus (MPa)	1st drop CBR	Avg. CBR Value (Top 6 in.)
1A	16.6	0.57	35.20	5.22	11.23
1B	16.8	1.05	12.92	5.61	4.57
1C	15.2	0.57	35.20	3.94	9.14
1D	21.8	1.05	12.92	9.35	12.06
2A	12.7	0.56	21.38	6.12	7.70
2B	19.6	1.72	22.08	4.03	3.94
2C	10.6	0.56	21.38	3.90	6.48
2D	24.9	1.72	22.08	2.74	2.93
3A	13.8	0.63	36.41	5.17	4.80
3B	16.6	1.34	27.86	5.38	4.77
3C	12.8	0.63	36.41	3.27	3.42
3D	23.3	1.34	27.86	4.79	2.97
4A	15.9	1.22	14.47	4.98	4.28
4B	19.3	0.78	19.00	2.61	3.44
4C	15.8	1.22	14.47	3.67	4.72
4D	22.2	0.78	19.00	3.67	3.15
5A	17.4	0.99	33.83	4.31	3.49
5B	20	1.78	16.74	3.79	3.28
5C	16.6	0.99	33.83	2.81	2.55
5D	21.5	1.78	16.74	6.41	4.15
6A	16	0.59	35.01	13.4	22.57
6B	11.9	0.74	28.46	2.6	21.69
6C	12.1	0.45	46.16	3.9	15.92
6D	10.9	0.75	27.96	2.3	6.94

Looking at the 1st drop CBR values listed in Table 8, the variation was between 2.61 to 9.35 for the long test strip, and from 2.3 to 13.4 in the shorter strip (constructed for the geocell-reinforced sections). On the other hand, when the CBR values were averaged for the top 6 inches of the subgrade layer, the variation was from 2.97 to 22.57. Individual CBR values calculated at different depths during the DCP testing have been plotted in Figure 53. As seen from the figure, most of the data points correspond to CBR < 10. Cell 6A was found to have the highest subgrade CBR values.

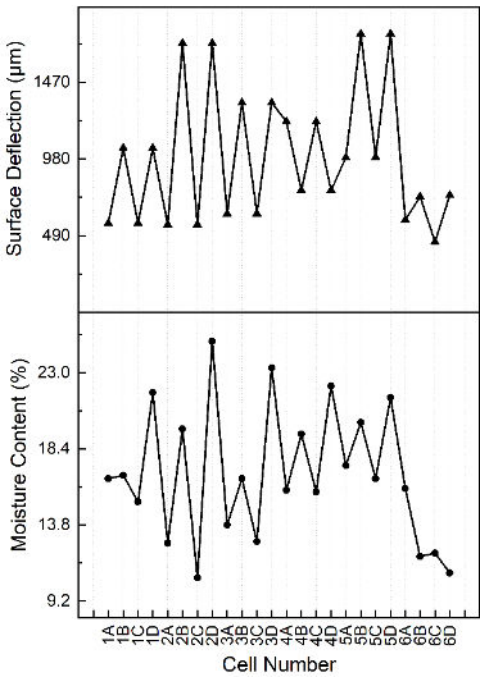

Figure 52: Variation in Soil Moisture Content and LWD-Measured Surface Deflections for the Subgrade Layer in Different Cells along the Test Strip

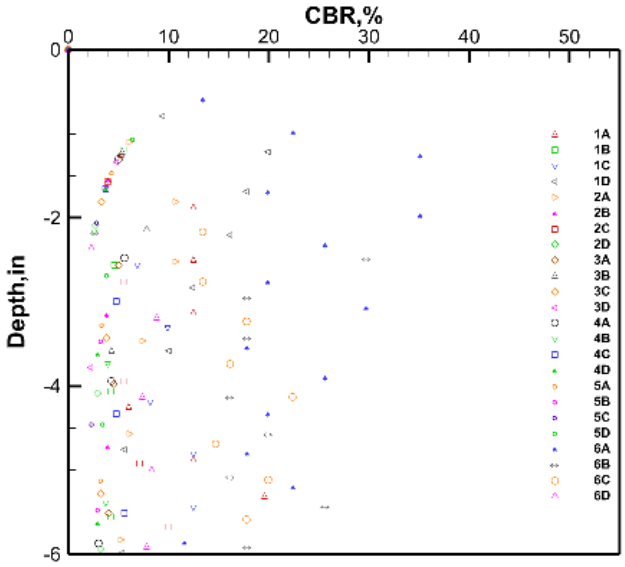

Figure 53: Subgrade CBR Variation with Depth

Figure 54 shows the average subgrade CBR values (top 6 in. of subgrade) for each of the test cells, plotted per their physical location along the test strip. Accordingly, Cell 1A is on the West end of the strip, whereas Cell 1B is on the East end. As seen from the average CBR values, subgrade layer was weaker as one moves from the West end to the East end of the long test strip. As an exception, Cell 1D, the second cell from the East end, showed a high average CBR value of 12.1. Except for five cells along the long strip, the average CBR values for the cells were lower than 5. It is important to note that the

current study did not include subgrade tilling and moisture control to achieve uniform CBR values for all cells. Therefore, this degree of variation in the average CBR values is expected. Cells 6B, 6D, 6C, and 6A, have been enclosed in a gray box in Figure 54 to indicate that Section 6 was constructed along a different strip, near the north-east corner of the longer test strip.

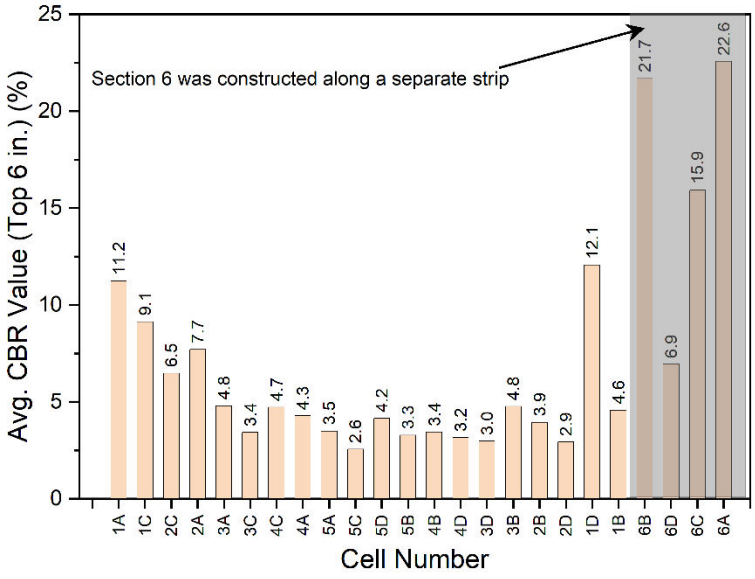

Figure 54: Average Subgrade CBR Value (Top 6 in.) for Different Cells

Figure 55 presents a scatter plot showing the variation of LWD-measured surface deflections on the subgrade surface with soil moisture contents. From the figure, as the subgrade moisture content increases there is a general increasing trend in the LWD-measured surface deflections. This is expected as increasing moisture content can reduce the soil shear strength, thereby increasing both the elastic as well as plastic deformations. Figure 56 shows a scatter plot of LWD-measured surface deflection with average CBR for the top 6 inches. For average CBR values less than 5, a large scatter in the LWD-measured surface deflection values is observed. However, as the subgrade CBR increases above 5, a rapid decrease in the LWD-measured surface deflection is observed. Except for a few outliers, the surface deflection values remain constant around 500 µm as the CBR value increases.

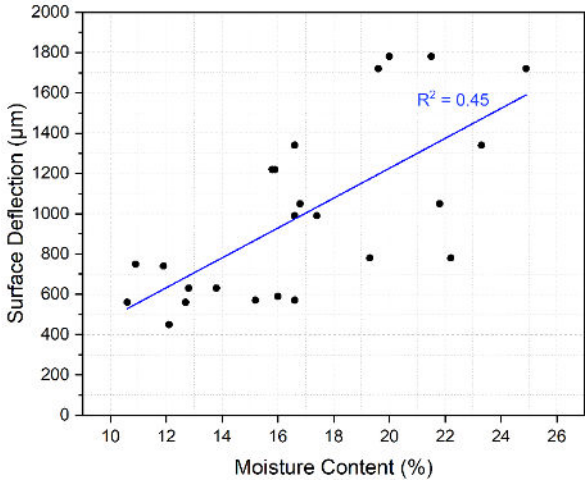

Figure 55: Scatter Plot Showing Variation in LWD-Measured Surface Deflection with Subgrade Moisture Content

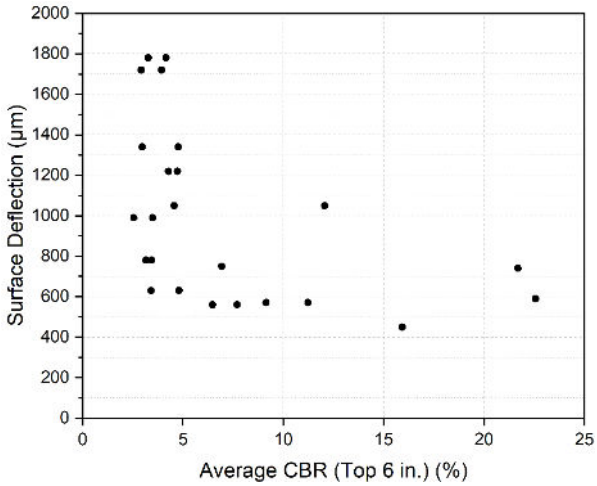

Figure 56: Scatter Plot Showing Variation in LWD-Measured Surface Deflection with Average Subgrade CBR (Top 6 in.)

Figure 57 shows the variation in LWD-measured surface deflections with increasing number of drops during testing on top of the finished subgrade layer. As seen from the figure, no significant change in the surface deflection was observed with increasing drop numbers except for Cells 2B/2D, and 5B/5D. No justification for this strange variation in Cells 2B/2D, and 5B/5D could be found. Nevertheless, this aspect will be further investigated later in this report. The negligible change in surface deflections with increasing drop number is expected when testing on a well-compacted subgrade layer. The layer has likely achieved a dense packing state under the rollers; accordingly, no significant change in the packing occurs with increasing number of drops during LWD testing. *This also indicates that no seating drops are needed during LWD testing when testing on top of a compacted fine-grained subgrade layer.*

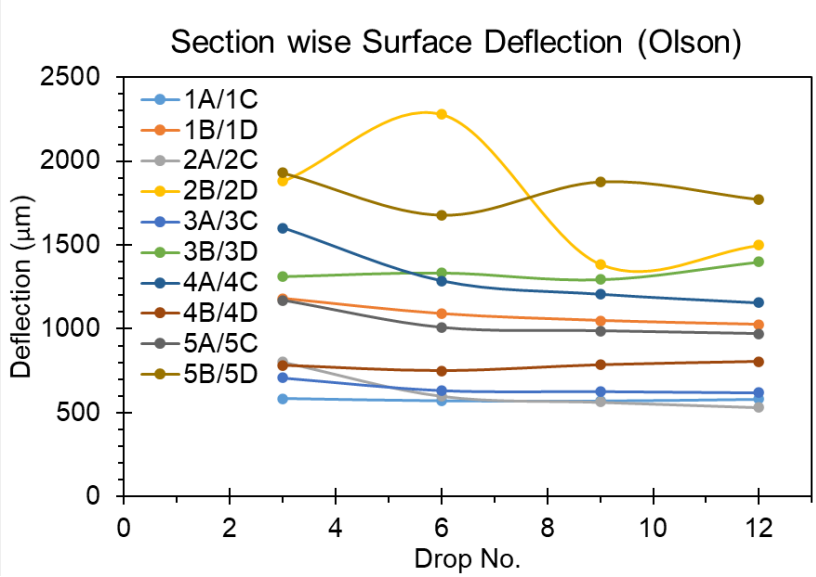

Figure 57: Subgrade Surface Deflection with LWD Drop Number for the Different Test Cells

LWD testing on the compacted subgrade layer was conducted using both LWD devices. Figure 58 compares the surface deflections measured on each subgrade test cell using the two devices. From the figure it is apparent that for some test cells (2B/2D, 4B/4D) the Zorn LWD resulted in higher surface deflection values compared to the Olson device. For the remainder of the test cells, both devices resulted in similar surface deflections. Here it should be re-emphasized that the Zorn device, confirming to ASTM E2853 specifications has a precision tolerance of ± 40 µm, whereas the Olson device, confirming to ASTM E2583 specifications has a precision tolerance of ±2 µm. This difference in the tolernace values should be kept in mind when comparing resutls from the two devices. Nevertheless, results from the subgrade tests clearly indicate that either device can be reliably used during field compaction control activities.

LWD Testing on Aggregate Layers – Unreinforced Sections

Seating Drops

Surface deflection values were recorded after every drop of the LWD mass. Results from the third stage of aggregate placement (6 in. thick aggregate layer) are presented in Figure 59 . From the figure, it can be observed that beyond the application of 6 drops, no significant reduction in the measured surface deflections is observed. *This indicates that while testing on this ASTM #4 material, at least six drops are necessary as 'seating' drops to ensure adequate/uniform contact between the aggregate surface and the LWD plate.* It should be noted that the data in Figure 59 corresponds to the case where two vibratory passes of the smooth-drum roller were already applied to the aggregate layer. Due to the open-graded nature of this layer, even two passes of the vibratory roller does not completely stabilize the aggregate matrix.

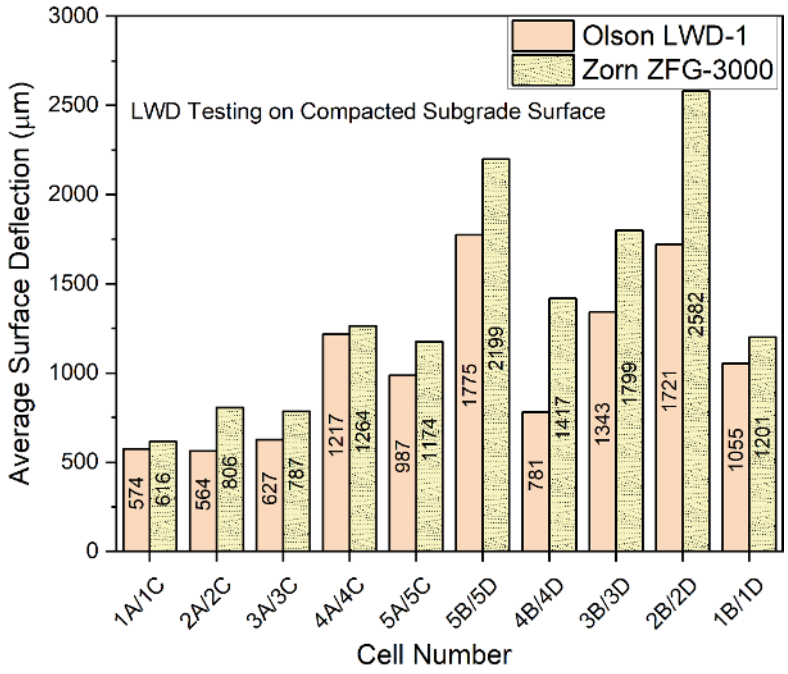

Figure 58: Comparison of Subgrade Surface Deflection Measured by the Two LWD Devices

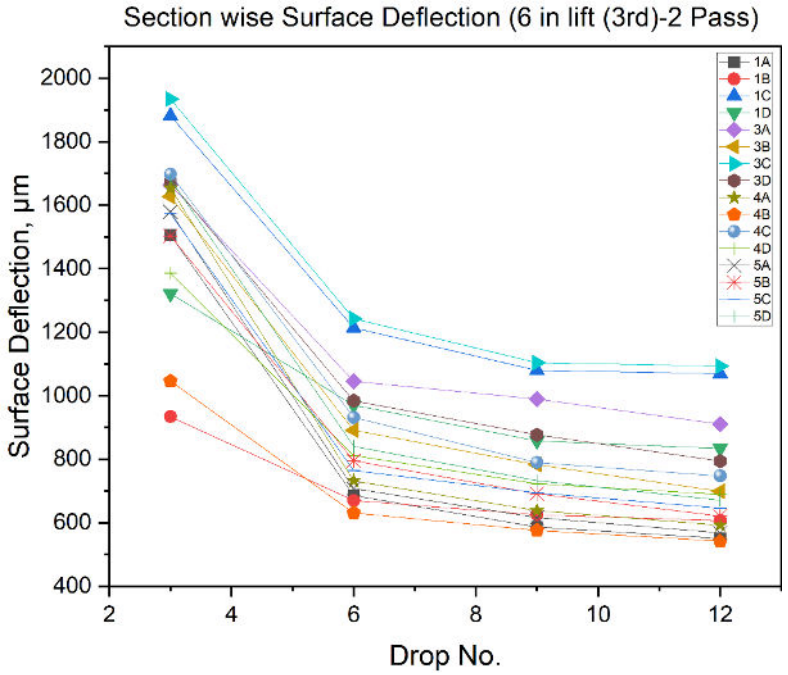

Figure 59: LWD Test Results after 3rd Lift (6-in. thick) and Compaction using Two Passes of the Vibratory Roller (Material: ASTM # 4)

Effect of Aggregate type

The type of aggregate material, in terms of gradation, used for construction might be an important factor governing the surface deflection measurement (an indicator of degree of compaction). To investigate this effect Figure 60 compares the LWD-measured surface deflection values for the two aggregate materials

(ASTM #4 and ASTM #57) at different layer thicknesses. The columns with green horizontal stripes represent the measured surface deflection values after one pass of the vibratory roller, whereas the columns with the red inclined stripes represents the deflection values after two passes. Overall, as the cumulative layer thickness increases from 200, to 250 to 300 mm or 8 to 10 to 12 in., there is a decreasing trend in the measured surface deflection values. From the figure, when the total layer thickness equals 12 inches, there is no significant difference in the surface deflection values irrespective of whether the layer is constructed using ASTM #4, ASTM #57, or by placing a layer of ASTM #57 over a layer of ASTM #4. On the other hand, for the ASTM #4 material, when the total layer thickness was increased from 200 mm (8 in.) to 300 mm (12 in.), the average surface deflection value decreased from 0.95 mm to 0.70 mm after 2 passes of the vibratory roller. A similar reduction in surface deflection was also observed for the ASTM #57 material, i.e., from 0.82 mm to 0.69 mm (after two roller passes) when the layer height was increased from 200 to 300 mm. *From these results it can be concluded that the compaction level achieved within a particular layer does not vary significantly between ASTM #4 and ASTM #57 materials.*

On the other hand, the degree of compaction after a certain number of roller passes is directly governed by the cumulative layer thickness, and degree of compaction of the layer(s) underneath the surface layer being compacted. The compaction behavior of these OGAs is largely governed by particle shape and angularity, and not as much by the grain size distribution. However, it is important to note that the compaction behavior will most likely be significantly different from what would be observed for dense-graded aggregate layers. *Finally, the results presented in Figure 60 indicate that for none of the material-thickness combinations, the surface deflection values were less than 0.5 mm (500 µm), which is the current criteria used by the ICPI to ensure adequate compaction of a minimum thickness of 300 mm (12 in.) of base/subbase layers.* At this stage, it appears a threshold value of 0.5 mm (500 µm) for this minimum thickness may be too stringent as values lower than 0.5 mm have been achieved on layers thicker than 300 mm.

Effect of Layer Thickness

LWD-measured surface deflections from different test cells at different stages of aggregate placement are sorted and compared in Figure 61. This figure shows results from LWD testing on Direct Lift (DL) as well as Staged-Lift (SL) constructions. A SL construction corresponds to the case where multiple layers are compacted on top of each other to achieve a cumulative layer thickness whereas Direct Lift (DL) corresponds to the case where a single layer of aggregate is placed and compacted to achieve the desired compacted layer thickness. The figure also includes data for section with and without placement of the non-woven geotextile at the subgrade-subbase interface. The following primary observations can be made from close inspection of Figure 61:

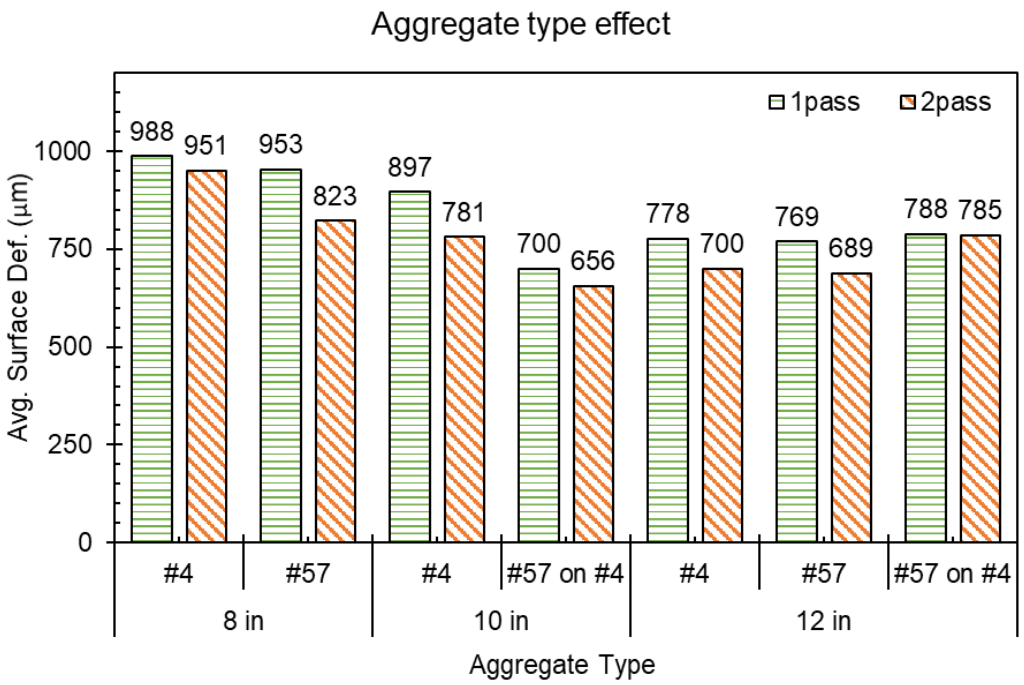

Figure 60: Comparing the LWD-Measured Surface Deflection Values for Different Material-Layer Thickness Combinations

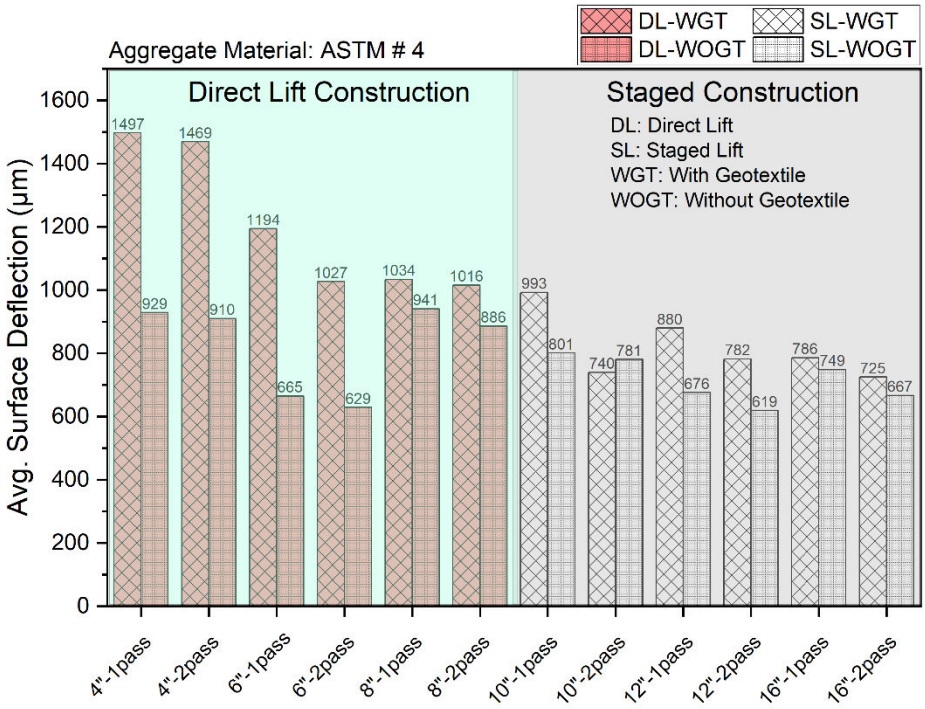

Figure 61: Effect of Layer Thickness on Measured Surface Deflection.

a) Overall, comparing the surface deflection values for the sections with and without geotextile at the subgrade-subbase interface, it is seen that the cells with geotextile results in higher surface deflection

values compared to those without. This difference is greater for the thinner aggregate layers, and gradually diminishes as the cumulative layer thickness increases. *This interesting observation can be attributed to the fact that placement of the geotextile at the subgrade-subbase interface creates an artificial plane of slippage (or failure plane). This prevents penetration of the aggregates into the subgrade surface for better packing.*

For thinner layers, when the geotextile is within the depth of influence of the LWD stress pulse, detrimental effect of this artificial plane of slippage is reflected through higher recorded surface deflections. However, as the layer thickness increases, the geotextile gets farther and farther away from the LWD, and its detrimental effects is not as clearly noticeable. At this point it is important to discuss the role that a geotextile is intended to play in actual pavement sections. When the pavement section is subjected to water intrusion, and subgrade pumping and migration of fines into the subbase/base layer is likely to be an issue, the geotextile plays an important role as a 'separator'. Presence of the geotextile greatly benefits the pavement section in the long term, and integrity of the layers is preserved. In the current study, the subgrade was dry, and migration of fines into the subbase layer was not an issue. Moreover, the constructed test sections were not subjected to any vehicular traffic that would present a possibility of fines migration or pumping. Therefore, the geotextile did not serve any beneficial purpose, rather presented a 'weak' plane for aggregate slippage, thus leading to greater surface deflection. *This trend should not be construed as an indicator of geotextiles being detrimental to pavement performance.*

b) The surface deflection values reduce with increasing of direct lift thickness. Also, there is a reduction in surface deflection with the application of additional vibratory passes except for the 100 (4 in.) direct lift case. This indicates that the energy coming from a single pass of the vibratory compactor is sufficient to induce maximum interlocking between the aggregate particles. Additional compaction does lead to improved packing (densification), rather can lead to 'destabilization' of the aggregate matrix. *Therefore, in the field, the number of compactor passes should be changed depending on thickness of the layer being compacted. Excessive compaction of thin aggregate layers is likely to 'destabilize' the packing structure*.

c) As the cumulative layer thickness increases, compaction of the underlying (intermediate) layers leads to lower surface deflection measurements in the surface layer. *This is the reason, the surface deflections for staged lift construction were lower than those for thick single lift constructed layers*.

LWD Testing on Aggregate Layers: Geocell-reinforced section

The reinforcement (150 mm or 6 in. thick) was introduced at the subbase layer using geocell filled with different aggregates. The surface deflection was first measured after the placement and static compaction of a 50 mm (2 in.) aggregate layer. Test cell 6B and 6D used ASTM #4 material where 6C and 6A used ASTM#57 aggregate. After placement of the 2 in. caping layer, the next surface deflection was measured after 1 static and 1vibratory pass of the vibratory compactor. The deflection values involve recording data using 12 drops of standard LWD weight. The results are presented in Figure 62. From the figure, the requirement of 3 drops for getting stable deflection data is also observed. Another observation is that the deflection variation between the test cells gets reduced when the layer thickness is increased. Also, the

deflection does not significantly vary with the type of material used as all the test cells provide close deflection value after 1 static and 1 vibratory pass of the smooth-drum roller.

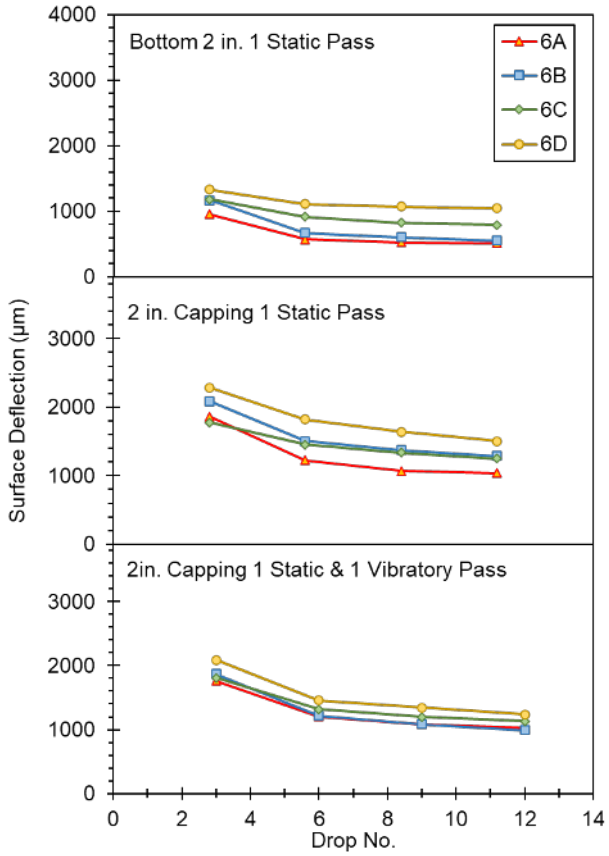

Figure 62: Surface Deflection Variation with LWD Drops in Geocell-Reinforced Sections

Figure 63 presents the average deflections for different test cells at different layer and compaction efforts. The average surface deflection values were recorded after 3 seating drops. From the Figure 63 it is seen that-

a) Vibratory compaction is suitable for OGA materials, as indicated by the reduction of surface deflection after vibratory compaction. However, the ASTM #57 material shows better compaction over ASTM #4 when then compaction energy is kept constant. This is indicated by higher reduction in surface deflection values of vibratory pass of the roller as compared to a static pass for a fixed layer thickness. This may be because of better packing of the ASTM # 57 materials inside the geocell openings compared to the coarser-grained ASTM # 4 materials.
b) The use of geocell reinforcement is somehow increasing the surface deflection indicating poor compaction. For example, with 250 mm or 10 in. thick unreinforced layer, the surface deflection after 2 vibratory passes is 0.74 mm whereas with reinforcement the value is 1.22 mm. From this data, it can be concluded that when for layers with geocell reinforcement either additional vibratory compaction may be needed to adequately pack the aggregates inside the geocell openings or multiple layered compactions should have been applied. Moreover, as already mentioned, the stress levels imposed by the LWDs are not large enough to mobilize the beneficial effects of the geocells.

c) Just like the results from the longer test strip, test cells with a geotextile placed at the subgrade-subbase interface exhibit higher surface deflection values compared to those without any geotextile. This is most likely because the geotextile presents an artificial 'slippage plane' at the subbase-subgrade interface.

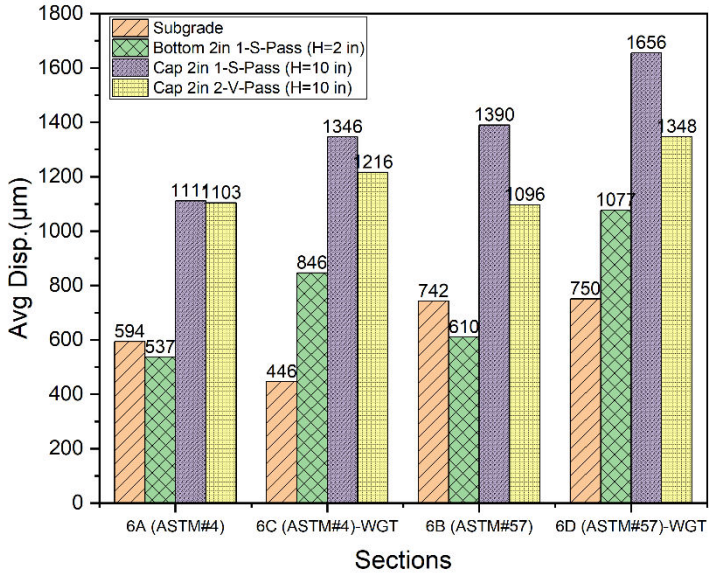

Figure 63: LWD Test Results from Geocell-Reinforced Section.

CHAPTER 7: SUMMARY AND CONCLUSION

This report summarized findings from a recently completed research study at the Oklahoma State University focusing on the development of a deflection-based compaction control specification for OGA base/subbase courses commonly used in permeable pavements. For this purpose, Portable Impulse Plate Load Testing Devices, also known as Light Weight deflectometers (LWDs) were used to measure the surface deflections on the aggregate layers under different compaction levels. Although the LWD device has several advantages (Portable, Nondestructive, Easy to use, Quick assessment, and Commercial availability), due to the non-homogeneous nature of OGA types, getting consistent results from the LWD test was challenging. Apart from that, currently, there is no established protocol for LWD testing on these materials (e.g., the required number of "seating" and "measurement" drops). Therefore, the study adopted an integrated approach involving laboratory testing, numerical modeling, and field testing to develop a compaction control protocol for the OGA materials.

This study comprised laboratory and field testing on two types of OGA materials, following gradation specifications for ASTM #4 and ASTM #57, respectively. Two commercially available LWD devices, manufactured by Olson and Zorn respectively, were used in this research to study the influence of LWD types on the measured surface deflection. The research was divided into four phases. In Phases-I, and II, extensive LWD tests were conducted on top of the selected aggregate materials inside a custom-made large cylindrical mold, and wooden box, respectively. As mentioned earlier, the ASTM standard vibratory shake table and a typical jackhammer were used to impart vibratory compactive energy to the samples inside the mold, whereas the aggregate sample placed inside the box were compacted using a commercially available vibratory plate compactor. Both the mold and box configurations were used to test aggregate OGA samples corresponding to various thickness and compaction efforts. Finally, a full-scale test section was constructed in the field to correlate the box and mold test samples with the field test section results. The significant findings from the laboratory and field-testing effort are as follows:

1. There was no significant difference between the results produced by the Olson and Zorn LWDs under the same compaction and testing conditions. Even considering the measurement precision difference between the LWD types, Olson & Zorn provided similar deflection both in laboratory (refer to Figure 37 & Figure 38) and field (refer to Figure 58).

2. Several external factors influenced the LWD measurement inside the custom/modified Proctor mold (e.g., mold support condition and contact between mold and the floor surface). Moreover, the LWD operator's testing style can also influence the test results. Accordingly, good contact between the LWD loading plate and aggregate samples is crucial for accurate measurement of LWD surface deflection.

3. For the OGA materials inside the customized mold, nine (9) "seating" drops were found to be adequate to ensure good contact between the LWD loading plate and aggregate surface. However, while testing in the wooden box or in the field, six (6) "seating" drops were sufficient to establish adequate contact between the loading plate and the aggregate layer surface.

4. As compaction effort was increased, the relatively smaller ASTM #57 aggregate achieved better packing compared to the coarser ASTM #4 aggregate. This is expected as the ASTM #4 matrix has a significantly low number of smaller particles that can provide a “stabilizing” effect to the aggregate matrix. Unless very high confining pressures are applied, coarse-grained particles rarely achieve “tight” packing. This clearly explains the variability in the LWD test results.

5. Excessive compaction did not improve the packing conditions in either aggregate material. In fact, the aggregate matrix for the coarser ASTM #4 was ‘destabilized’ under excessive compaction. In fact, there are some compactors used in construction practice that have indicator lights to avoid over-compaction in the field. From the box, the surface deflection value significantly decreased after one pass of the vibratory compactor; however, the reduction was not significant when additional vibratory compaction effort was applied. The value slightly increased with the third pass, indicating the aggregate matrix's destabilization due to excessive compaction.

6. For the ASTM #57 and ASTM #4 aggregate materials, 5 seconds of jackhammer pre-compaction inside Proctor molds (both conventional as well as customized) was sufficient to achieve maximum packing. Based on results on the custom-made larger mold, it was observed that compaction in layers (application of vibratory compaction on 100 mm or 4-in. compaction lifts) resulted in more consistent deflection trends compared to the case where the mold was completely filled before the vibratory compaction was applied. This may have some implications on the maximum lift thickness in the field before compaction can be applied. Similarly, in the field, it was observed that staged construction reduced the surface deflection significantly.

7. Underlying layer stiffness plays a vital role to the achieved compaction level of any layer if the compaction energy is kept constant.

8. From the pressure cell data in the box, the pressure level at a particular elevation did not change significantly after different number of passes of the vibratory plate compactor. A major portion of the stress levels applied to the top of the aggregate layer (through the LWD drop) was dissipated within the top 3 to 6 in. of the layer. The reduction of pressure level with the depth was not significant beyond this. The pressure dissipation within the OGA layer formed a “cylindrical” pattern unlike the “conical” pressure dissipation pattern observed in dense-graded aggregate layers. Even when the aggregate layer was reinforced using geocells, the pressure dissipation pattern did not change significantly.

9. For the subgrade layer in the field, seating drops were not needed before LWD testing. Adequate contact between the loading plate and the subgrade layer could be established from the beginning, ensuring consistent measurements with each drop.

10. For unreinforced base/subbase layers constructed with OGA materials, the LWD-measured surface deflections were not significantly affected by the type of aggregate material; rather, the surface deflections were significantly affected by layer thickness.

11. When geotextiles were used at the subgrade-subbase interface, the LWD-measured surface deflections reduced with increasing layer thickness. When no geotextiles were used at the subgrade-

subbase interface, an exception to this trend observed due to penetration of aggregate particles into the subgrade layer. The difference between the measured surface deflection with or without geotextile reduced significantly with increasing layer thickness, especially when the layer thickness was increased beyond 10 in. (254 mm), and construction was carried out in lifts.

12. For the geocell-reinforced base/subbase layer, additional vibratory compaction was necessary for the OGA materials to achieve better compaction and stability within the geocell openings. The beneficial effects of geocell reinforcement could not be tracked using LWDs (due to the low applied stress levels).

Observations from each phase of this research project are crucial for the development of logical, evidence-based construction and compaction control guidelines. Therefore, as the final task in this study, the results from different phases were compared to identify similarities and differences. The ultimate objective was to assess whether any of the laboratory testing approaches can be used to realistically simulate the compaction behavior of OGA materials in the field. Once such a method has been identified, it would be possible to establish compaction targets for implementation in the field. These targets can be based on LWD-measured surface deflections. Figure 64 presents such comparisons from the different phases of this project. The bar plots in Figure 64 present the average value of surface deflection measured using LWD on top of 12-in. (304.8-mm) thick ASTM #4 and ASTM #57 aggregate layers. Here it is essential to mention that aggregate specimens inside the Proctor mold were compacted in a single compaction lift of 304.8 mm (12 in.). In contrast, identical thick aggregate layers inside the box and field were constructed using two equal compaction lifts (6 in. each).

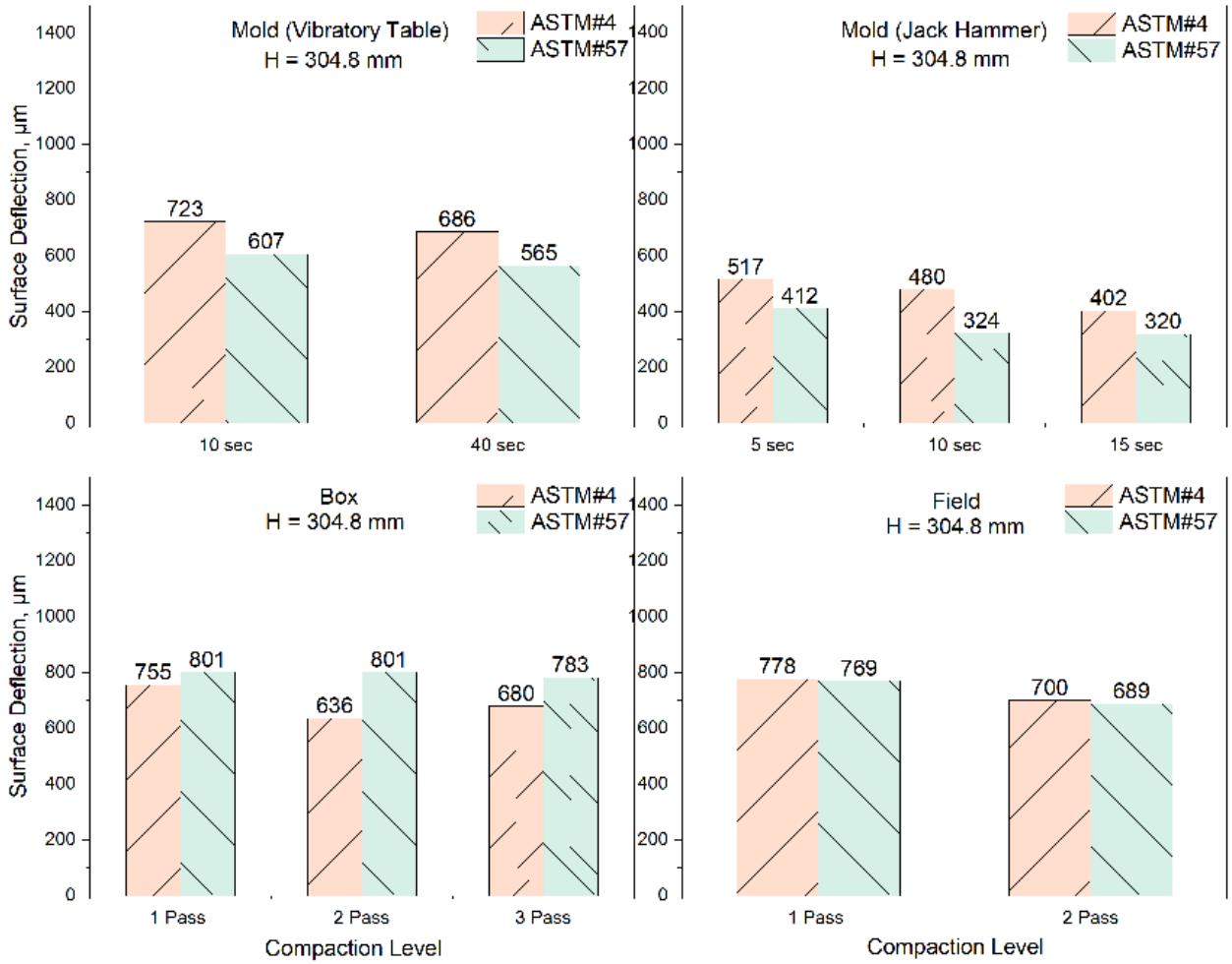

Figure 64: Comparing the Surface Deflection Values for 12-in. Thick Aggregate Layer from Different Phases of the Research Study

Figure 64 shows that the LWD-measured surface deflection values on top of an aggregate specimen in the custom-made Proctor mold, compacted using the vibratory shake table, closely matched the surface deflections measured on the same aggregate material in the wooden box as well as the field. As seen from the figure, the surface deflections for a sample compacted in the lab for 10 seconds (on the vibratory shake table) closely matched the results for samples subjected to one pass of the vibratory plate compactor in the wooden box as well as one pass of the vibratory smooth-drum roller in the field. Similarly, 40 seconds of vibratory compaction using the vibratory shake table corresponded to two (2) passes of the vibratory plate compactor (in the wooden box) or two (2) passes of the vibratory smooth-drum roller (in the field).

From the field data, the surface deflections after 1-pass of the vibratory roller is 778 µm for the ASTM #4 material, and 769 µm for the ASTM # 57 material. Similarly, after 2-passes of the vibratory roller, the corresponding surface deflections are 700 µm (ASTM #4) and 689 µm (ASTM #57). The corresponding surface deflection values in the mold were 686 µm for ASTM #4 (40 sec) with 2% error, 565 µm for ASTM #57 (40 sec) with 18% error. Similarly, the corresponding surface deflection in the box were - 636 µm for ASTM #4 (2 pass) with 9% error, 801 µm for ASTM #57 (2 pass) with 16% error. On the other

hand, samples compacted using the jackhammer resulted in significantly lower surface deflection values compared to those in the wooden box or the field. This indicates that the jackhammer compaction is not representative of field compaction condition. Even 5 seconds of jackhammer compaction resulted in significantly lower surface deflections compared to those in the wooden box or the field.

Figure 65 shows the Coefficients of Variation (CoVs) of the measured surface deflection values among different aggregate samples for 304.8 mm (12 in.) thick layer of ASTM#4 & ASTM#57. From this figure, the variability is less than 10% for compaction using the vibratory shake table. On the other hand, the variability in surface deflection for samples compacted using a jackhammer was greater than 10%. This indicates that the jackhammer compaction not only imparts significantly higher compaction levels to the sample, it also leads to inconsistent surface deflection measurements. Therefore, the jackhammer compaction approach should not be considered as a suitable replication of field compaction efforts. The variabilities in the field-measured surface deflections were found to be between 12% to 21%, which is greater than the variation observed in the lab using the vibratory shake table. This is expected as response of the OGA layer in the field is affected by several other factors such as subgrade properties, relative position of the compactor with respect to the testing position, etc. Therefore, CoV values less than 20% are considered to be acceptable.

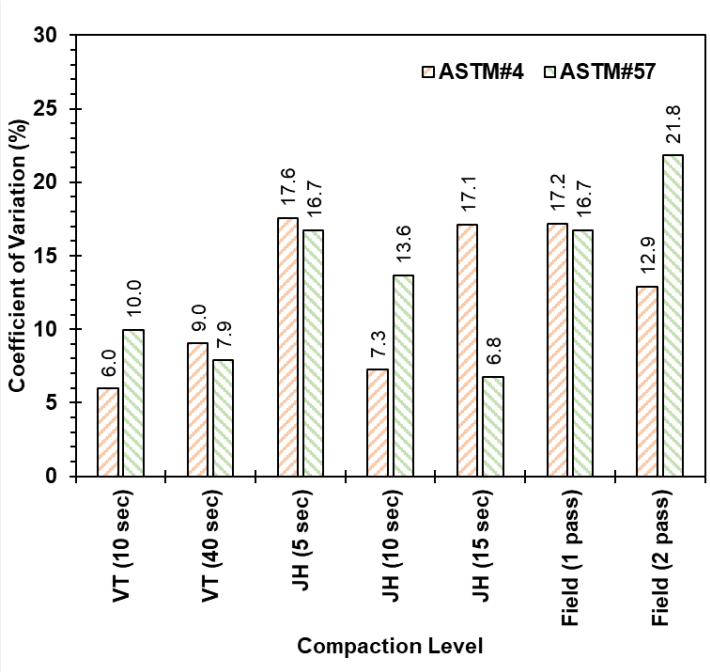

Figure 65: Coefficient of Variation Among Surface Deflection Measurements from Different Phases of the Research Study

CHAPTER 8: RECOMMENDATIONS FOR IMPLEMENTATION

This chapter provides overall recommendations concerning the implementation of research findings from the current study. These recommendations can guide subsequent development of a deflection-based compaction control protocol for OGA base/subbase layers, particularly, the ones used underneath permeable block pavements.

1. *Device Agnostic:* As the surface deflection measurements from the two LWD types used in the current study were consistently close to each other, it is safe to assume that LWD-based surface deflection measurements on OGA layers is device-agnostic. Therefore, any deflection-based compaction control protocol to be developed for such layers can allow the use of any commercially available LWD device. However, it is important to note that due to irregularities in the OGA layer surface, it is important for the LWD to measure the deflection of the plate as a whole. The deflection measurement should not be point-based (for example, using a sensor protruding through the center of the loading plate). OGA layer surfaces are non-uniform, and point-based measurements can lead to significant errors due to movement/reorientation of individual particles.

2. *Laboratory Testing Mold Size:* From the laboratory testing in Proctor molds, it was concluded that the conventional Proctor mold (6-in. diameter) is not adequate for testing of such coarse-grained materials. The custom-made Proctor mold (D = 12in. & H = 11.5 in.) yielded results similar to the field, especially when a vibratory shake table was used to compact the samples. Agencies can use such a set-up in the laboratory to get a close picture of the overall compaction behavior of different OGA materials. However, the authors acknowledge that the availability of a custom-made mold or a vibratory shake table may not be a trivial matter for all agencies.

3. *Application of "Seating" Drop:* Due to the uneven nature of OGA layer surface, seating drops become extremely critical before consistent surface deflection measurements can be accomplished using LWDs. While testing in the custom-made mold at least nine (9) seating drops were required. This was because of the confined nature of the mold, and 'reflection' of the stress pulses from the mold boundaries. However, in the in the field, it was observed that six (6) seating drops were sufficient to ensure adequate contact between the LWD loading plate and the OGA layer surface. It is recommended that after the six (6) seating drops, six (6) measurement drops should be used, and the average surface deflection values from the six measurement drops should be reported. It is also important to track the CoV for the six measurement drops. For a well-compacted layer, the CoV should be less than 20%.

4. *Compaction Method and Time (in Laboratory):* If an agency is to use a custom-made mold to perform preliminary testing to establish target deflection values, it is recommended that a vibratory shake table be used. As reported earlier, 10 seconds vibratory shake table compaction (at 80 Hz) replicated one pass of a vibratory smooth-drum roller, whereas 40 seconds of compaction replicated two passes of the roller. The authors acknowledge that these values are not universal and can change significantly on the type or roller being used in the field as well as the layer depths. Nevertheless, some idea could be obtained about the expected LWD-measured surface deflection values for well-compacted OGA layers.

5. *Geotextile Effect:* For OGA layers less than 10-in. in thickness, placement of a geotextile at the subgrade-subbase interface resulted in higher surface deflections during LWD testing. Therefore, it is hypothesized that the use of a geotextile at the subgrade-aggregate interface may negatively affect the compaction behavior of OGA layers less than 10-in. in thickness. For layers thicker than 10 in. (254 mm), no significant difference was observed for layers with or without the geotextile separation layer. It is also important to note that geotextile placement may be required due to reasons beyond the scope of this research study. Therefore, in cases where geotextiles are used, ICPI may want to consider allowing greater surface deflection values.

6. *Staged vs Direct Lift Construction:* Staged construction provided better compaction to the OGA layers compared to direct-lift construction, as observed from the lower surface deflection measurements. Therefore, it is recommended that OGA layers thicker than 8 in. (203 mm) should be constructed using a staged approach, rather than using a direct lift.

7. *Geocell Reinforcement:* Reinforcement using geocell in OGA layers requires vibratory compaction effort to ensure adequate packing of the aggregate particles within the geocell pockets. Static roller pass was not sufficient to achieve this. Due to limited data available, detailed recommendations regarding geocell-reinforced OGA layers cannot be developed through the current study.

8. *Recommended Deflection-Based Compaction Control Protocol*

   For the ASTM #4 aggregate material, for a 12-in. thick aggregate layer, the minimum surface deflection achieved after 2 passes of vibratory roller compaction was 0.689 mm. It is possible that the surface deflection will further reduce upon application of a third roller pass. However, based on results from the current study, it is not likely that the surface deflection will reduce below 0.50 mm or 500 μm, which is the current standard used by the Interlocking Concrete Pavement Institute (ICPI). For the ASTM#57 material, for a 12-in. thick layer, the minimum surface deflection achieved after 2 passes of vibratory roller compaction, is 0.735 mm. Once again, this value may be further reduced upon a third pass of the vibratory roller.

   Nevertheless, based on results from the current study, it is recommended that the target surface deflection should be changed to less than or equal to 0.6 mm (600 μm). From extensive laboratory and field testing, the research team strongly believes that an OGA layer with LWD-measured surface deflections less than or equal to 0.6 mm (600 μm) represents an adequate packing condition.

REFERENCES

AASHTO T307, (1999). Standard Method of Test for Determining the Resilient Modulus of Soils and Aggregate Materials. AASHTO'S Standard Specification for Transportation Material and Methods of Sample and Testing.

ASTM E2835-11, (2011). Standard Test Method for Measuring Deflections Using a Portable Impulse Plate Load Test Device. Annual Book of ASTM Standards, Vol. 04.03, ASTM International, West Conshohocken, PA.

ASTM E2583-7, (2007). Standard Test Method for Measuring Deflections with a Light Weight Deflectometer (LWD). Annual Book of ASTM Standards, Vol. 04.03, ASTM International, West Conshohocken, PA

BS 1924-2, (2018). Hydraulically bound and stabilized materials for civil engineering purposes: Sample preparation and testing of materials during and after treatment. BSI Standards Publication.

Benz, M.,2009. Mesures Dynamiques Lors du Battage du Pénétromètre Panda 2 (Doctor of Philosophy Dissertation). University Blaise, France.

Cary, C. E., and Zapata, C. E. (2010). Enhanced model for resilient response of soils resulting from seasonal changes as implemented in mechanistic–empirical pavement design guide. *Transportation research record*, *2170*(1), 36-44.

Cary, C. E., and Zapata, C. E. (2011). Resilient modulus for unsaturated unbound materials. *Road Materials and Pavement Design*, *12*(3), 615-638.

CDF Rogers, AJ Brown, and PR Fleming. Elastic stiffness measurement of pavement foundation layers. In Proc. of the 4th Int. Symp. Unbound Aggregates in Roads (UNBAR4), pages 271{280, 1995.

Cho, Y., Kim, Y., Kabassi, K., Zhuang, Z., Im, H., Wang, C., and Bode, T. (2011). *Non-nuclear method for density measurements* (No. SPR1 (10) P335). Lincoln, NE: Nebraska Department of Roads, Report SPR1 (10).

Design Guidance for Road Pavement Foundations (Draft HD25). Interim Advice Note 73/09 Revision 1, Design Manual for Roads and Bridges, UK Department of Transport, 2009.

D.J. White, P.K.R. Vennapusa, and M.J. Thompson. (2007). Field Validation of Intelligent Compaction Monitoring Technology for Unbound Materials. Technical report, Center for Transportation Research and Education, Iowa State University.

Eisenberg, B.E.; Lindow, K.C.; Smith, D. R. Permeable Pavements, 1st ed.; American Society of Civil Engineers: Reston, VA, USA, 2015; ISBN 978-0-7844-7867-7.

Frost, M. W., Fleming, P. R., Gordon, M., and Edwards, J. P. (2010, August). Pavement foundation stiffness testing–a new regime. In *Proceedings of the Institution of Civil Engineers-Transport* (Vol. 163, No. 3, pp. 119-125). Thomas Telford Ltd.

Gupta, S., Ranaivoson, A., Edil, T., Benson, C., and Sawangsuriya, A. (2007). Pavement design using unsaturated soil technology.

Indiana Department of Transportation ITM No. 514-15T, (2015). Test sections for aggregates and Recycled Materials. Office of Material Management.

Indiana Department of Transportation (2018). Standard Specifications. (https://www.in.gov/dot/div/contracts/standards/book/sep17/2018Master.pdf)

Kleyne, E., J. Maree, and P. Savage (1982). The Application of a Portable Pavement Dynamic Cone Penetrometer to Determine in Situ Bearing Properties of Road Pavement Layers and Subgrades in

South Africa. In Proceedings of the 2nd European Symposium on Penetration Testing, Amsterdam, volume 1, pages 272–282. National Institute for Transport and Road Research, 1982.

KP George, (2006), Mississippi. Dept. of Transportation. Research Division, University of Mississippi. Dept. of Civil Engineering, and Portland Cement Association. Portable FWD (Prima 100) for In-situ Subgrade Evaluation. University of Mississippi,.

Lamas-Lopez, F., Cui, Y. J., and Calon, N. (2016). Geotechnical auscultation of a French conventional railway track-bed for maintenance purposes. *Soils and Foundations*, *56*(2), 240-250.

Lekarp, F., Isacsson, U., and Dawson, A. (2000). State of the art. I: Resilient response of unbound aggregates. *Journal of transportation engineering*, *126*(1), 66-75.

Li, H., Jones, D. Wu, R., and Harvey J, 2014, *Development and HVS Validation of Design Tables for Permeable Interlocking Concrete Pavement: Final Report*, University of California Pavement Research Center, UCPRC-PP-2011-01

M.A. Mooney and P.K. Miller. (2009) Analysis of Lightweight Deflectometer Test Based on In Situ Stress and Strain Response. Journal of Geotechnical and Geoenvironmental Engineering, 135:199,.

Mazari, M., Navarro, E., Abdallah, I., and Nazarian, S. (2014). Comparison of numerical and experimental responses of pavement systems using various resilient modulus models. *Soils and Foundations*, *54*(1), 36-44.

Mishra, D. Aggregate Characteristics Affecting Response and Performance of Unsurfaced Pavements on Weak Subgrades. Ph.D. Dissertation, University of Illinois at Urbana-Champaign. 2012.

Nazarian, S., Yuan, D., and Williams, R. R. (2003a), "A Simple Method for Determining Modulus of Base and Subgrade Materials," ASTM STP No. 1437, ASTM, pp. 152-164.

Nazarian, S., Yuan, D., Tandon, V., and Arellano, M. (2003b), "Quality Management of Flexible Pavement Layers with Seismic Methods," Research Report 1735-3F, Center for Highway Materials Research, The University of Texas at El Paso, El Paso, TX.

Nazarian, S., Mazari, M., Abdallah, I., Puppala, A. J., Mohammad, L. N., and Abu-Farsakh, M. Y. (2014). Modulus-Based Construction Specification for Compaction of Earthwork and Unbound Aggregate. NCHRP Project 10-84.

Nazarian, S., Mazari, M., Abdallah, I. N., Puppala, A. J., Mohammad, L. N., and Abu-Farsakh, M. Y. (2015). Modulus-based construction specification for compaction of earthwork and unbound aggregate. Washington, DC: Transportation Research Board.

Nebraska Department of Transportation Standard Test Method T 2835, (2014). Deflection Measurement of Soils Using a Light Weight Deflectometer (LWD). Modified ASTM Designation: E2835.

P. R. Flemming and M. W. Frost and C. D. F. Rogers. A Comparison of Devices for Measuring Stiffness in-Situ. In Unbound Aggregates in Road Construction, pages 193{200. A. A. Balkema, Rotterdam, Netherlands, 2000.

Puppala, A. (2008). Estimating stiffness of subgrade and unbound materials for pavement design. NCHRP Synthesis 382. Washington, DC: Transportation Research Board.

Richart Jr., F. E., Woods, R. D., Hall Jr., J. R., (1970). Vibrations of Soils and Foundations, Prentice-Hall, Inc., Englewood Cliffs, New Jersey.

Richter, C. A. (2006). *Seasonal variations in the moduli of unbound pavement layers* (No. FHWA-HRT-04-079). United States. Federal Highway Administration.

Rowshanzamir, M. A. (1995). “Resilient Cross Anisotropic Behavior of Granular Base Materials Under Repetitive Loading”. Ph.D. Dissertation. University of New South Wales, Australia.

Ryden, N., and Mooney, M. (2009). Analysis of surface waves from the light weight deflectometer Soil Dynamics and Earthquake Engineering, 29, 1134–1142.

Schwartz, C. W., Z. Afsharikia, and S. Khosravifar (2017). “Standardizing Lightweight Deflectometer Modulus Measurements for Compaction Quality Assurance”. Report No. MD-17-SHA/UM/3-20, Maryland Department of Transportation State Highway Administration.

Shafiee, M., Nassiri, S., Khan, R.H., Bayat, A., (2011). Evaluation of New Technologies for Quality Control/Quality Assurance of Subgrade and Unbound Pavement Layer Moduli.

Smith, D. R., R. Bowers, and G. Aicken (2018). “The Lightweight Deflectometer (LWD) as an Acceptance Tool for Compacted OGAs in Permeable Pavements”. Proceedings of the 12th International Conference on Concrete Block Pavement; Oct. 16-19, 2018, Seoul, Korea.

Smith, D.R. (2017). Permeable Interlocking Concrete Pavements, 5e. Interlocking Concrete Pavement Institute (ICPI).

Staatsministerium, Bayerischen, (2012). Dynamic Plate-Load Testing with the Aid of the Light Drop-Weight Tester. TP BF-StB Part B 8.3.

Tamrakar, P., and Nazarian, S., (2019). Permanent Deformation and Stiffness of Fouled Ballast Based on Static and Impact Load Tests. GAP 2019 Proceedings, Colorado Springs, CO.

Terzaghi, K., Peck, R. B., and Mesri, G. (1996). Soil mechanics in engineering practice. John Wiley and Sons.

Titi, H. H. (2012). *Base Compaction Specification Feasibility Analysis*. Wisconsin Highway Research Program.

Tompai, Z.,2008. Conversion between static and dynamic load bearing capacity moduli and introduction of dynamic target values. Period. Polytech. – Civil Eng.52,97–102.

Tutumluer, E., and U. Seyhan, U. (1998). “Neural Network Modeling of Anisotropic Aggregate Behavior from Repeated Load Triaxial Tests”. In Transportation Research Record: Journal of the Transportation Research Board, No. 1615, Transportation Research Board of the National Academies, Washington, D.C., pp. 86-93.

Tutumluer, E. Practices for Unbound Aggregate Pavement Layers. NCHRP Synthesis No. 445, NCHRP Project 20-05, Topic 43-03, 2013.

Vennapusa, P., and White, D. (2009). Comparison of light weight deflectometer measurements for pavement foundation materials. Geotechnical Testing Journal, 32(3), 1–13.

W. Kudla, R. Floss, and C. Trautmann. Dynamic Plate Compression Test-Rapid Testing Method for Quality Assurance of Unbound Course. Autobahn, 42(2), 1991.

Woodward, P.K., Kennedy, J., Laghrouche, O., Connolly, D.P., Medero, G., (2014). Study of railway track stiffness modification by polyurethane reinforcement of the ballast. Transp. Geotech. 1,214–224 Elsevier Ltd.

Zhao, G., Yao, Y., Li, S., and Jiang, Y. (2018). Maximum Allowable Deflection by Light Weight Deflectometer and Its Calibration and Verification.

Zorn, (2011). User Manual for the light drop weight tester ZFG 3000 GPS ZFG 3000 ECO, Zorn Instruments, Stendal, Germany.

APPENDIX-A: NUMERICAL MODELING REPORT (PHASE-3)

Discrete Element Modeling of Light Weight Deflectometer Testing on Open-Graded Aggregate Materials

Numerical Modeling Report Submitted to

Interlocking Pavement Institute

By

Debakanta (Deb) Mishra, Ph.D., P.E.
Associate Professor, Email: deb.mishra@okstate.edu
School of Civil and Environmental Engineering

Research Team Members:

Md. Fazle Rabbi, M.S.
Graduate Research Assistant; Email: mrabbi@okstate.edu
School of Civil and Environmental Engineering, Oklahoma State University

Mahsa Gharizadevarnosefaderani, M.S.
Graduate Research Assistant; Email: mghariz@okstate.edu
School of Civil and Environmental Engineering, Oklahoma State University

Ratul Mondal, B.S.
Graduate Research Assistant; Email: rmondal@okstate.edu
School of Civil and Environmental Engineering, Oklahoma State University

September 2022

Abstract

Open-Graded (OG) aggregate layers underneath permeable pavements present significant challenges for construction quality control. Traditional density-based compaction control is not feasible for these layers as density measurement devices become ineffective in the presence of large void structures. In such a case, surface deflections measured on top of a compacted aggregate layer could indicate the nature of packing in the aggregate matrix. This manuscript presents findings from an ongoing research study focusing on developing deflection-based compaction control protocols for OG aggregate layers. Extensive laboratory testing was carried out to study the packing evolution within OG aggregate layers under different compactive efforts. The OG aggregates were compacted inside a custom-made cylindrical mold using a vibratory shake table. Surface deflections at different compaction stages were measured using a Light Weight Deflectometer (LWD). To further study the packing characteristics, the Discrete Element Method (DEM) was used to simulate the laboratory tests. A parametric analysis was carried out using DEM to study the effects of different model parameters on packing evolution and LWD-measured surface deflections. The results clearly demonstrated that LWD-measured surface deflection is directly related to the applied compaction effort on the materials. In addition, the numerical analysis showed that inter-particle friction coefficient and stiffness of individual aggregate particles greatly influence LWD-measured surface deflection magnitudes. Finally, DEM results for an aggregate material conforming to ASTM # 4 gradation established that approximately 0.5 mm surface deflection under conventional LWD testing load can be used as a threshold value for determining optimum compaction levels.

Keywords: Open-Graded Aggregates, Light-Weight Deflectometer, Discrete Element Method, Compaction Control

Introduction

Pavement base and subbase layers are conventionally constructed using open/dense-graded aggregates and serve as one of the primary load-carrying layers in flexible pavement systems. From a pavement engineering perspective, Open-Graded (OG) aggregate materials can outperform dense-graded materials in certain conditions, particularly in the presence of water. OG materials have less than 2% fines (material finer than 0.075 mm, or passing the No. 200 sieve), thus giving them desirable drainage characteristics, and making them significantly less susceptible to moisture-induced and freeze-thaw-related damage. In addition, pavement layers constructed with OG aggregates demonstrate higher shear strengths, particularly under high stress states.

Despite the advantages of the pavement layers constructed with OG aggregates, significant research is required to ensure their adequate performance. Conventionally, the stability of unbound layers is directly controlled by the degree of compaction. Accordingly, construction quality control processes have traditionally been based on density-based threshold values. The most common method used to study the compaction characteristics of soils and dense-graded aggregates, is the drop-hammer based method like the one originally developed by Proctor. In this method, the Maximum achievable Dry Density (MDD) for a soil/aggregate is established under a standard compactive effort. Subsequently, this MDD values is used as a reference during field compaction, and the degree of compaction in the layer is established relative to the MDD. Field density measurement methods such as Nuclear Density Gauge (NDG) method, Sand Cone Method, Rubber Balloon Method, among others, can be adopted to determine the density of the compacted layer in the field.

Establishing the degree of compaction in OG aggregates, on the other hand, can be quite challenging. The large voice contents in OG aggregate layers make conventional density check methods such as the NDG impractical. Moreover, density is not a direct measure of an aggregate layer's mechanical property. Although higher densities often lead to improved mechanical properties, there is no consensus regarding the relationship between density and Resilient Modulus (MR). which is the primary indicator of layer behavior in a Mechanistic-Empirical (M-E) Pavement Design framework. Accordingly, it is desirable to develop compaction quality control methods that are based on mechanistic response parameters, that can be directly linked to the layers' performance under loading. For years, several studies have focused on developing modulus-based compaction control approaches for soils and aggregates. One such approach involves the use of Portable Impulse Plate Load Test Devices (PIPLTDs) such as the Light Weight Deflectometer (LWD). An LWD, as defined in ASTM E2583, must have a load cell to measure the load levels applied by each impact. A PIPLTD, on the other hand and does not have a requirement regarding load cells (refer to ASTM E2835). The current research study involved devices falling into both categories. Therefore, although the devices technically fall under the PIPLTD category, *they have been commonly referred to as LWDs in the current manuscript, adhering to common engineering practices.*

LWDs can be used to measure/estimate the in-situ modulus values for compacted unbound layers. Depending on the device type, the modulus is either directly calculated using load and deflection measurements or is estimated by using the load levels pre-established for certain drop heights during the calibration process. Although numerous research studies have been performed focusing

on LWD testing of fine-grained soils, studies involving LWD testing of aggregate materials are relatively limited in number. Recently, Jibon et al. (2021), Nazarian et al. (2003a, b, 2014, 1015) discussed how LWD-measured modulus values can be correlated with MR values established through laboratory triaxial tests. However, it should be noted that most of these studies focused on fine-grained soils and/or dense-graded aggregates. No studies were found focusing on OG aggregate materials, primarily owing to difficulties associated with laboratory testing (for both triaxial testing as well as testing with LWDs). Moreover, researchers (refer to the NCHRP 10-84 report by Nazarian et al.) have highlighted several challenges associated with the development and adoption of modulus-based compaction protocols. Under these circumstances, LWD-measured surface deflections can serve as a practical surrogate for a mechanistic-based degree of compaction measure.

Increasing degree of compaction in an unbound aggregate matrix leads to reduction in load-induced surface deflections. In this regard, LWD-measured surface deflections on top of an OG aggregate layer can indicate the level of packing within the aggregate matrix. Recently, Smith et al. (2017) concluded that the stiffness values of compacted OG aggregate base layers could be quickly assessed using LWDs. Likewise, The Interlocking Concrete Pavement Institute (ICPI; Smith 2017) and the American Society of Civil Engineers (Eisenberg et al. 2015) have also highlighted advantages associated with the use of LWD-measured surface deflections for construction quality control of OG aggregate layers. However, no specifications are available regarding the LWD test procedure to obtain a representative picture of the layer compaction level. In this regard, a correlation study between the degree of compaction of OG aggregate layers and LWD-measured surface deflections could help in the development of a deflection-based compaction control specification. An ongoing research study at Oklahoma State University has been focusing on the development of such a specification. The current manuscript presents partial findings from laboratory testing and numerical modeling tasks carried out under the scope of this research study.

Objectives and Scope of Work

The current research study can be divided into two phases: (1) Laboratory/Field Testing; and (2) Numerical Modeling. The experimental phase was aimed at assessing the degree of compaction of OG aggregate materials through LWD-measured surface deflections and was performed at three scales: (a) Small-Scale, (b) Intermediate-Scale, and (c) Field-Scale. For the small-scale component, LWD tests were performed on OG aggregates inside a cylindrical steel mold with a diameter of 304 mm and a height of 192 mm; this mold was a scaled-up version of commercially available Proctor molds. Open-graded aggregate materials were placed in the mold, and the mold was placed on a vibratory shake table with a heavy surcharge weight. The degree of compaction of aggregates inside the mold was controlled by varying the frequency and time of the vibratory shake table.

For the intermediate scale testing, OG aggregate materials were placed inside a 1.2 m x 1.2 m x 1.2 m wooden box and were compacted by different number of passes of a vibratory plate compactor. LWD tests were conducted after different number of passes of the plate compactor to track the change in the LWD-measured surface deflections with increasing compaction effort. For the field testing, several full-scale pavement base/subbase sections of varying OG layer thicknesses were constructed and compacted under different number of passes of a vibratory roller. Details

regarding the intermediate- and full-scale testing efforts will be presented elsewhere (Mondal et al., 2022) As the final task, small-scale laboratory tests were numerically modeled using the Discrete Element Modeling (DEM) technique. The primary objective of the numerical modeling phase was to microscopically study the evolution of packing within the aggregate matrix, and the corresponding effect on LWD-measured surface deflections.

First, LWD testing was performed on OG aggregate samples inside the scaled-up Proctor mold to get a study the effect of compaction effort on surface deflections. Next, a numerical model was prepared using the commercially available DEM package, PFC Suite The Pavement Design Package (PdPkg) addon for PFC was used for this purpose (Potyondy, 2018). Abbreviated details about the PdPkg are presented in the next section with appropriate citations directing the reader to relevant references. Details of the modeling approach are presented, along with the calibration procedure to match model-generated results to those generated in the laboratory. Upon calibration, different model parameters were systematically altered to generate varying aggregate packing scenarios. The PdPkg enables users to simulate LWD tests on synthetic aggregate specimens. Surface deflections from the simulated LWD tests were used as direct indicators of the aggregate matrix's response to loading. The following section presents a brief overview of the LWD testing procedure, and how LWD testing can be carried out in a steel mold to assess the overall compaction conditions.

LWD Testing Inside Molds: Theory and Background

The LWD performs as a dynamic plate load testing device that can be used to determine the surface deflections and corresponding moduli of unbound pavement layers. As shown in Figure 1, once the LWD comprises a drop weight, which when released, falls along a rod and strikes a bearing plate which is in direct contact with the surface of the layer being tested. Therefore, a pulse load is generated and transferred to the underlying material. The speed or acceleration of movement of the underlying layer is recorded using velocity sensors or accelerometers attached to the plate, and the deflection time history is calculated by double- or single-integration of the measured acceleration or velocity, respectively. A load cell is included in some devices to measure the magnitude of the impact load of the falling weight.

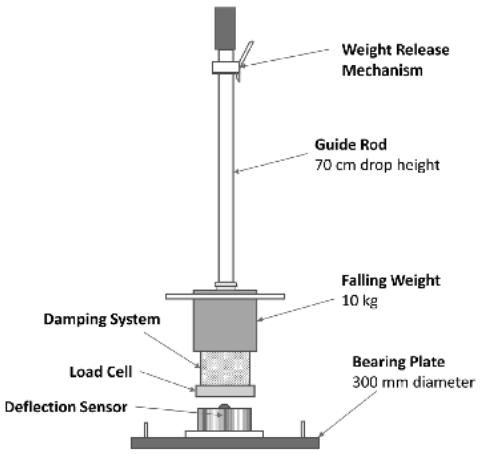

Figure 1. Schematic Showing a Typical Light Weight Deflectometer (LWD) Device (Schwartz et al. 2017)

In the testing procedure, several drops are usually performed, among which the first several drops are taken as "seating" drops as the energy from those drops goes into ensuring adequate contact between the loading plate and the underlying layer. Once adequate contact is established, data from subsequent drops can be taken to represent the load-deflection behavior of the underlying layer. The peak recorded surface deflection and the peak loading magnitude can be used to calculate the layer stiffness; the layer modulus can be calculated using Boussinesq's theory assuming that the layer is isotropic, linearly elastic, and represents a homogenous semi-infinite continuum.

Recently, Schwartz et al. (2017) performed LWD testing inside Proctor molds. They proposed the following equation to estimate the modulus of the material being tested inside the mold. The equation is based on the theory of elasticity for the elastic material, and can easily developed by constraining the lateral deflections (lateral deflections equal zero inside a steel mold):

$$E = \left(1 - \frac{2 \times \nu^2}{1 - \nu}\right) \times \frac{4H}{\pi D^2} \times k \quad \text{----------(Eq. 1)}$$

In the above equation, ν is the Poisson's ratio, H is the mold's height, D is the plate or mold diameter, and k is soil stiffness (ratio of peak force to peak deflection). Given the equation, the LWD-measured surface deflection is directly correlated with the material modulus. For results presented in the current manuscript, the mold dimensions were kept constant. Accordingly, variations in measured surface deflections can be primarily attributed to changes in the material modulus. To maintain simplicity, surface deflections were directly used in this study as an indicator of the compaction level of the aggregate matrix. This is particularly important because some of the devices used in the current study did not comprise a load cell to directly measure the applied load levels by each drop. Under such circumstances, the modulus estimates may not be as accurate.

Material Selection

Results presented in this manuscript correspond to a limestone aggregate conforming to ASTM #4 specifications. Although the study also included another aggregate material conforming to ASTM #57 gradations, only results for the ASTM #4 material have been presented in the current manuscript for the sake of brevity. Moreover, the modeling efforts primarily focused on the ASTM #4 material from computational resource considerations; the greater amount fine particles in an ASTM # 57 matrix would lead to impractical computational resource requirements for the DEM simulations. The aggregate material was directly collected from stockpiles based on sampling instructions provided by ASTM. Figure 2a shows the GSD of the selected material, along with upper and lower specification limits for the ASTM #4 gradation. From the GSD plot, the material is uniformly graded ($C_u = 1.66 < 4$, $C_c = 1.28$), and the grain sizes mostly lie between 19 mm to 40 mm (90% mass Fraction).

Sample Preparation and Laboratory Compaction

Figure 2b (Left) shows a schematic of the cylindrical mold used for the LWD test. The mold was filled with aggregates, and LWD testing was carried out under 'compacted' and 'uncompacted' conditions of the aggregate material. The uncompacted sample did not experience any external compaction, whereas the 'compacted' samples were prepared by placing the mold with aggregate on a vibratory shake table (along with a surcharge load; see Figure 2b, Right). For both samples, the sample surface was leveled by hand before LWD testing. Leveling of the top surface is a critical step in this method as a level surface would ensure uniform contact between the LWD plate and the aggregate layer. For the 'compacted' samples, the degree of compaction was controlled by adjusting the vibration time and frequency of the shake table. Three replicates each, of 'compacted' and 'uncompacted' samples, referred to as Samples A, B, and C, were prepared for LWD testing.

LWD test results for both sample types are presented in the form of bar charts in Figure 3. The diameter of the LWD loading plate was ~304 mm. A 10 kg weight was dropped six times per sample from a height of 60 cm. Results from the first three drops (Drop Numbers 1, 2, and 3) were isolated, and were taken as the seating drops. The subsequent three drops (Drops 4, 5, and 6) were taken as the 'measurement' drops. Each drop applied approximately 6.22 kN force on top of the sample. For the data presented in Figure 3, the compacted sample was subjected to forty (40) seconds of vibratory compaction (Compaction Time, or C.T. = 40 sec) at a vibration frequency of 80 Hz. The figure clearly shows that the uncompacted samples (C.T = 0.0 sec) yield higher surface deflections compared to the compacted samples for both the seating as well as measurement drops. The average surface deflection value for the seating drops decreased from 1.65 mm to 0.91 mm when the samples were subjected to vibratory compaction. On the other hand, for the measurement drops, the average value reduced from 1.11 mm (for uncompacted samples) to 0.75 mm (for compacted samples). These average values will be used later in this manuscript during the numerical model calibration stage.

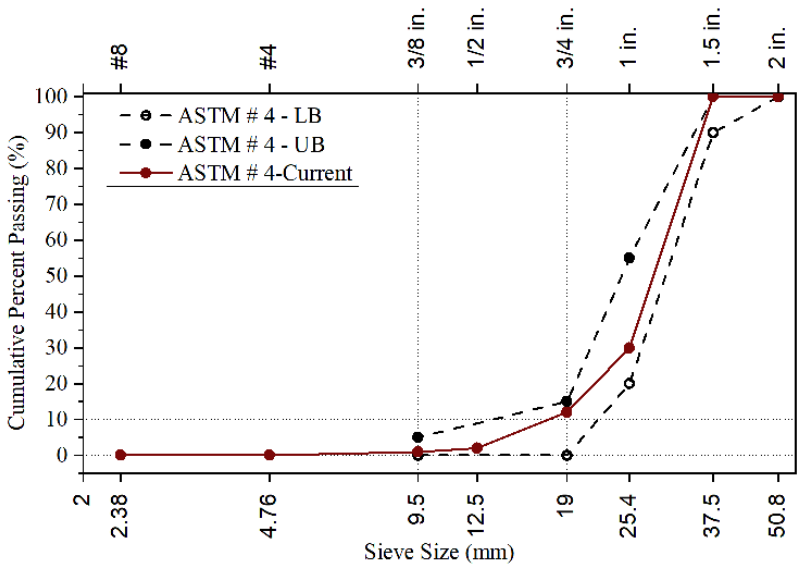

(a)

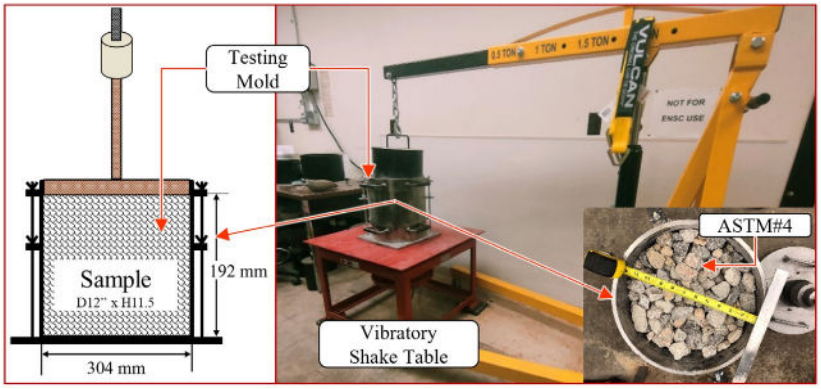

(b)

Figure 2: (a). ASTM#4 OG Aggregate Gradation; (b). Vibratory shake table setup: Apply vibratory compaction in the sample inside the custom cylindrical mold.

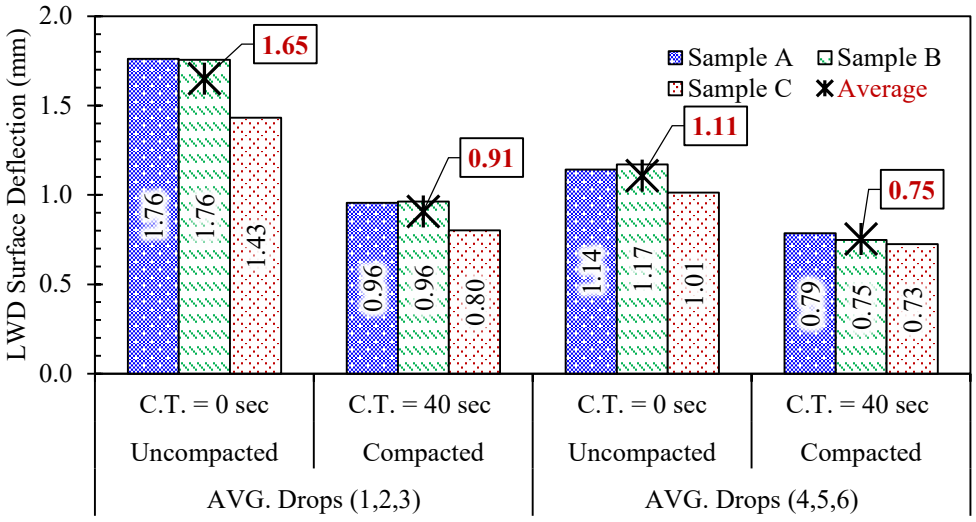

Figure 3: LWD Test Results for Compacted and Uncompacted Samples in a Mold

Discrete Element Modeling of LWD Tests on Open-Graded Aggregate Materials

Understanding of packing behavior within an OG aggregate matrix can be improved through micro-scale investigation of the system. This is possible through Discrete Element Modeling (DEM). Due to its ability to consider the interaction between individual aggregate particles, the DEM is well-suited for studying the packing behavior within aggregate matrices. A calibrated numerical model can facilitate parametric studies to isolate different factors likely to govern the compaction characteristics of OG aggregate matrices. Researchers have numerically simulated the LWD tests with different modeling approaches. In numerical modelling of LWD tests using DEM, in addition to the granular material and contact modeling, the simulation of the packing process and preparation of the test specimen are key steps; initial packing and sample preparation approach (in the model) can significantly affect the (simulated) LWD test results. This section presents a brief review of past studies focusing on numerical simulation of LWD tests, and also discusses the modeling approach used in the current study.

Tan et al. (2014) reported that physical properties of the aggregate materials have significant effects on their mechanical properties and the DE approach is a powerful method to simulate and investigate the mechanical response. They studied the behavior of unsaturated coarse-grained materials considering the effect of moisture content and fine particles using the DEM; the models were calibrated using field LWD test results. In their DEM modeling, first they took a gravitational approach to randomly deposit the particles in a cylinder, and subsequently applied a drop-hammer compaction by modeling four impact loads from a small drop height. This was followed by simulation of a falling weight to represent the actual LWD tests. After several successive drops, the average of the peak deflections was employed to calculate the bulk modulus of the underlying material. The results showed that the DE model could adequately predict the increasing peak deflections at higher moisture and fine particle contents compared to the experimental ones. They also compared the lowest and highest values of the simulated deflections with the corresponding LWD-measured deflections (Δ_{exp}) and developed a transformation relationship between these two sets of values. They observed that the laboratory-measured surface deflection values were approximately 2.1 times those predicted using the DEM simulations. (i.e., $\Delta_{exp} \approx 2.1\ \Delta_{DEM}$).

Wang et al. (2019) remarked that the LWD test is a promising tool for modulus-based compaction quality control, if there is a fundamental understanding of its experimental configuration and results interpretation. They modeled LWD in a DEM-based program and calibrated the model with corresponding field test results to evaluate the effect of moisture and fine particle content of unbound granular materials on the LWD-measured modulus. They used the Hertz contact model to simulate the inter-granular attractive forces due to suction (negative pore-water pressure). Different ranges of fine particles were introduced in the model by assigning smaller inter-particle friction coefficients. The loading steel plate was also modeled, and the peak stress was only applied on the plate. They followed the boundary contraction procedure to generate and compact the specimen. They used the DEM results to develop a linear relationship between LWD-measured surface deflections and the model parameters (i.e., interparticle friction, and suction), and then compared it with the developed relationship for actual test results. This comparison demonstrated that the measured peak deflection (Δ_{exp}) was about 5.2 times the value predicted in numerical analysis (Δ_{DEM}). They used this information during subsequent calibration of their model.

Numerical Modelling Approach in the Current Study

As already mentioned, a commercially available Distinct Element Modeling (DEM) program, Particle Flow Code or PFC, was used in the current study. Potyondy (2018) developed a module for PFC that can simulate LWD testing synthetic granular assemblies; the current study created a 3-dimensional synthetic granular assembly using this add-in feature incorporated into the Pavement Design Package (PdPkg). The DEM simulations were targeted to simulate the small-scale laboratory testing approach involving LWD testing inside the scaled-up Proctor mold. The following two sub-sections present details about the numerical model approach adopted in this study. First, details about the initial sample preparation are presented, followed by description of the procedure to simulate the LWD tests.

Initial Sample Preparation

In this sample step, first, the Grain Size Distribution (GSD) and contact properties were introduced into the model. This was followed by the selection and implementation of an appropriate packing

protocol to simulate the aggregate assembly inside a scaled-up Proctor mold. The following paragraphs present relevant details.

Grain Size Information: In PFC, a synthetic granular assembly is generated using a pre-determined number of bins and specifying the volume fraction of aggregate particles corresponding to each bin. In this study, all particles are assumed to have the same specific gravity. Therefore, the terms 'volume fraction' and 'mass fraction' can be used interchangeably in the current context. Although PFC (since Version 6.0) can simulate polyhedral particles, all models created in the current study focused on spherical particles only. The model run time can increase significantly with increased number of particles. Moreover, the simulation times and computational resource requirements are significantly affected by differences between the largest and smallest particles included in the model. To ensure adequate representation of the ASTM # 4 aggregate gradation while at the same time keeping the computational resource requirements within reasonable values, the current modeling effort considered only two 'bins' for the GSD, with volume fractions set to 70% and 30%, respectively. Table 1a lists the GSD bins used the current study.

Contact Modeling: One of the most important aspects of DE modeling involves simulation of inter-particle contact behavior. PFC is equipped with several different contact models to simulate the interaction between individual particles. In this modeling effort, the Hill-contact model (Tan et al., 2014) was used for grain-grain contact. Relevant parameters to define this contact model are: (1) local radii of contacting grains, (2) Young's modulus, (3) Poison's ratio, (4) the density of the grains, (5) friction coefficients, (6) damping constant, (7) suction, and (8) moisture gap. This contact model accommodates 'wet' or 'dry' conditions by assigning a suction value between individual grains. In DEM, the presence of fines can either be directly modeled by generating small-diameter particles, or indirectly modeled by altering the friction coefficient between the larger-sized particles. This latter approach reduces the number of particles and, consequently, the computational expense. The contacting grains are like elastic spheres with an infinitesimal interface behaving nonlinear elastic and frictional. The interface carries only compressive forces (no tension and moment) and is the sum of surface interaction and moisture forces. Table 1. b presents the material contact properties. It is necessary to mention that in this modeling effort, the material condition is set to 'dry'. Initial values for the different model parameters were determined from past studies on similar materials (Tan et al. 2014, Wang et al. 2019; Lu and McDowel 2008, 2010; Dahal and Mishra 2020). Reviewing past studies, the elastic modulus was between 0.833 GPa and 29 GPa, the Poison's ratio was in the ranges of 0.15 and 0.2, and the interparticle friction coefficient varied between 0.2 and 0.6 to represent increasing amounts of fine particles.

Packing Process: This phase produces the material specimen consisting of connected grain assembly with non-zero contact pressure (Potyondy, 2019b). Two main packing processes can be used within the PdPkg to generate synthetic material assemblies with specific gradations: (1) Grain Scaling; and (2) Boundary Contraction. In both processes, a cloud of overlapping grains is generated in the material vessel and rearranged until the net unbalanced force reaches a user-defined threshold level (the net unbalanced force is captured using a parameter known as 'Aratio'; a threshold value of ARatio = 1e4 was used in the current study). The 'Boundary Contraction' procedure uses the servomechanism to move the vessel walls and apply confining pressure to the sample. On the other hand, in the 'Grain Scaling' approach the grain sizes are iteratively scaled to achieve the desired contact stress level. The 'Boundary Contraction' procedure is generally used

to generate both dense- and loosely packed materials, whereas 'Grain Scaling' only produces densely packed assemblies. The 'Boundary Contraction' procedure was used in the current study. The steps followed are outlined below:

1. First, a cloud of grains was generated with an initial cloud-porosity (n_c) of 0.25. This low value of initial porosity causes a large number of grains to be packed in the material vessel, and there will be significant grain-grain overlaps. The grains are placed inside a cylindrical-shaped material vessel, with an initial size different from the mold size. Table 1b also presents information on the initial and final dimensions of the material vessel. The inter-particle friction coefficient is set to ZERO at this stage.
2. Rearrange the grains inside the cylindrical mold to obtain a zero mean-stress (indicating static equilibrium).
3. The friction coefficient (μ_{CA}) is then set to the desired value, and the material is confined by moving the vessel walls using servocontrol as long as the wall pressure (P_m) is within the target value, and static equilibrium is maintained. A small value of friction coefficient leads to lower resistance during the packing process, and a denser packing is obtained (lower value of final porosity).
4. In this study, two types of synthetic granular assemblies were prepared: (1) Uncompacted and (2) Compacted. The initial friction coefficient value (μ_{CA}) has a significant impact on the degree of packing inside the sample. This can be thought of as a surrogate of the laboratory compaction effort applied using the vibratory shake table. Figure 5a shows a screenshot of the generated material specimen in a cylindrical vessel (simulating the scaled-up Proctor mold). Table 1b lists the material vessel properties and the values of relevant packing parameters.

Numerical LWD Test Procedure

The process to model LWD tests using the PdPkg in PFC Suite has been exhaustively described by Potyondy (2018). Simulation of the LWD test using the PdPkg comprises three phases once the specimen preparation has been simulated using the procedure described above. Different phases to simulate LWD testing include: (1) Setup Phase, (2) Placement Phase, and (3) Hammer-Drop Phase (Potyondy, 2018). Parameters used for simulating the LWD test have been listed in Table 1c. The following paragraphs provide details about different phases of the LWD simulation procedure.

Setup Phase: In this phase, the model boundary conditions are established, gravity is activated, and static equilibrium is established. A schematic of the test set-up has been presented in Figure 4, along with forces being applied on each of the specimen walls. As seen from the figure, the forces on the top wall as well as the sidewalls can be changed based on the type of test being simulated. In the current study, the lateral as well as top walls are fixed during LWD testing to simulate the situation inside a scaled-up Proctor mold.

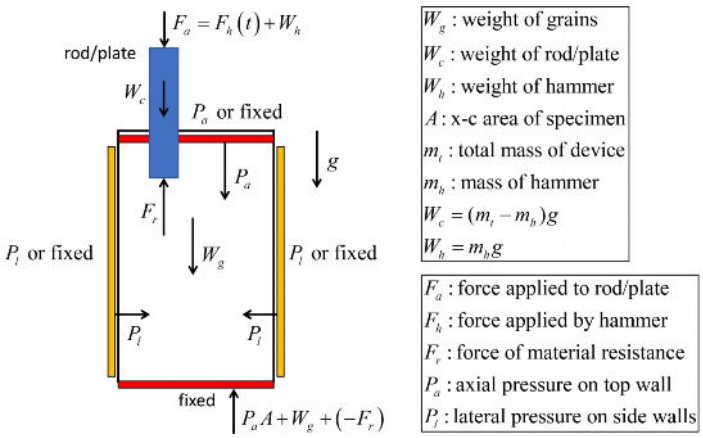

Figure 4: Schematic Representation of the Forces Acting on the Specimen Wall during LWD Test Simulation in the PdPkg (Potyondy, 2018)

Placement Phase: In this phase, the LWD plate is placed on top of the sample. The LWD loading plate is modeled as a clump of overlapping pebbles of the same diameter. As listed in Table 1c, the plate diameter is 302 mm, and it consists of 6 pebbles in the diametrical direction (see Figure 5b). The plate's rotation and lateral movement is constrained; it is only allowed to move in the vertical direction (axial direction of the sample).

Hammer-Drop Phase: In this phase, first the weight of the LWD (~ 34 kg) is assigned to the plate simulated using the clump. The impact force due to dropping of the weight is simulated by applying an additional force in the axial direction to the centroid of the loading plate. The load pulse applied by the drop has a magnitude of 6227 KN, and a pulse width of 40 ms. A symmetric load pulse is modeled. In other words, the peak load is applied at half-way into the load pulse (t = 20 ms). The time interval between each drop is approximately 0.46 seconds.

Due to the dynamic nature of hammers drops during the LWD test, the loading plate accelerates downward, and penetrates into the underlying material resulting in significant overlap between the spheres constituting the loading plate and those representing the aggregate particles. This overlap results in high magnitudes of unbalanced forces in the model. Therefore, the model is cycled at this stage to let the balls "rebound" from the overlapped position, and for the model to reach a state of static equilibrium. In this model, the local damping factor and the Hill damping constants were set to 0.02 and 0.07, respectively. To have an adequate representation of the load application and system response during testing, the model run time should be kept within acceptable limits. The drop process includes the time required for the pulsed load application, and the additional time required for the system response (i.e., the resisting force) to return to a value equal the LWD weight (static loading condition). The run time is primarily controlled by the timestep selected to model the load response of the system.

Interpretation of LWD Tests Data

An LWD device directly measures the applied load magnitude (for models equipped with a Load Cell), and the corresponding induced surface deflections. The surface deflection is either directly measured using a Linear Variable Differential Transducer (LVDT) or is calculated from velocity/acceleration measurements using a geophone or accelerometer, respectively. Physically

speaking, the surface deflection is a representation of the amount by which the LWD plate penetrates into the surface of the material being tested, with respect to its original position. As expected, every drop of the LWD mass results in elastic + plastic deformation in the material being tested. Figure 5c presents example data from the current modeling effort, where the displacement of the LWD plate is plotted against time. As shown in the figure, each drop of the LWD mass results in a deflection pulse, which comprises both elastic and plastic components. The plastic or permanent deformation component can be isolated by comparing the initial and final position of the load plate, after the system has come to equilibrium, post dropping of the LWD mass. The next section discusses results from this numerical modeling effort.

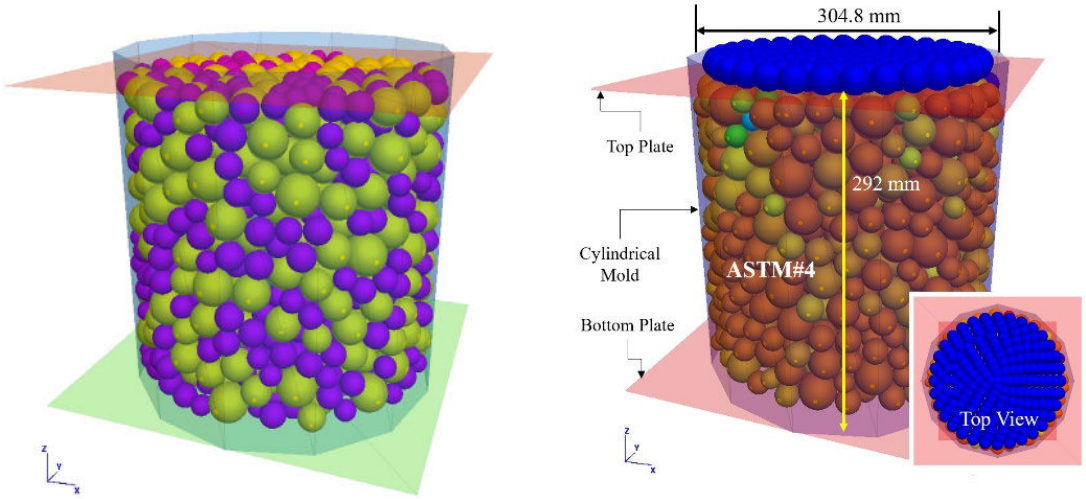

(a). **(b).**

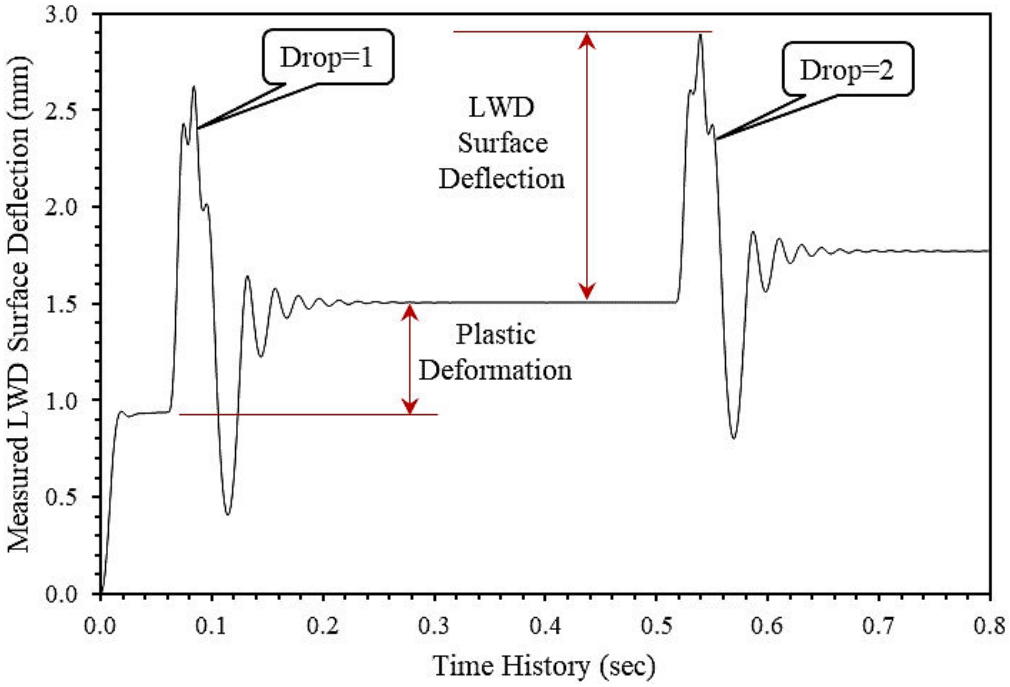

(c).

Figure 5: (a). Initial Sample Preparation Phase; **(b).** LWD Testing Phase; **(c).** Calculation of Elastic and Plastic Deformation of the Sample Under LWD hammer drop

Table 1: Parameters of The Numerical Modelling

(a) Adjusted Gradation of ASTM#4 Aggregate in PFC	
ASTM#4 Aggregate	
Aggregate Grain Shape	Spherical Balls
Bin-1: Minimum Diameter of Balls	2.50E-02 mm
Bin-1: Maximum Diameter of Balls	3.75E-02 mm
Bin-1: Volume Fraction	70 %
Bin-2: Minimum Diameter of Balls	1.90E-02 mm
Bin-2: Maximum Diameter of Balls	2.50E-02 mm
Bin-2: Volume Fraction	30 %
(b) Contact and Packing parameters	
Initial Material Parameters (Hill material contact model)	
Contact-Model Name	Hill
Young Modulus (E_g)	5 GPa
Poisson Ratio (ν_g)	0.15
Friction Coefficient (μ or μ_f)	0.2, 0.4, 0.6, 0.8
Damping Factor (α_h)	0.60

Local Damping Factor (α)	0.70	
Aggregate Materials Density (ρ_g)	1500 kg/m^3	
Packing Parameters		
Packing procedure (C_p)	Boundary Contraction	
Grain Cloud Porosity (n_c)	0.25	
Confining Pressure (P_m)	5 kPa	
Friction Coefficient during confinement (μ_{CA} *or* μ_i)	var. (0, 0.2, 0.4, 0.5, 0.7)	
Material Dimension Inside the Mold		
For Compacted Material (Initial Friction Coefficient μ_{CA}=0)		
Name	Initial (m)	Final (m)
Height	0.2730	0.2929
Diameters	0.2835	0.3029
For Uncompacted Material (Initial Friction Coefficient μ_{CA}=0.5)		
Name	Initial (m)	Final (m)
Height	0.2750	0.2946
Diameters	0.2835	0.3047
(c) LWD Testing Phase Materials Properties		
LWD Probe Parameters:		
Plate Diameter	~302 mm	
Number of touching balls in radial direction of the LWD plate (n_r)	6	
Total Mass of the LWD	34 kg	
Mass of the LWD Dropping Hammer	10 kg	
Surface Stiffness of the LWD plate (E_s)	1 GPa	
Gravity (g)	9.81 m/s^2	
Peak force applied by the hammer (F_h)	6227 N	
Duration of the hammer's impulsive force (t_h)	40 ms	

Numerical Results

Impact of Initial Friction Coefficient (μ_{CA} *or* μ_i) and Model Dimension

This section discusses the effects of the initial friction coefficient on the LWD-measured surface deflections. As already discussed, during the packing process, the 'Boundary Contraction' approach was used to create the synthetic aggregate assembly inside of a cylindrical material vessel. The sample size is not fixed, and rather varies based on the target mean stress to be achieved within the aggregate assembly as well as the initial cloud porosity value used during material genesis (the initial cloud porosity directly controls the number of particles being generated in the system). Therefore, an iterative approach was adopted in this effort to ensure the final dimensions of the material vessel closely matched the scaled-up Proctor mold dimensions used during laboratory testing. This iterative approach has been referred to as '*dimensional optimization*' in the current manuscript. Table 1b lists the initial and final dimensions of the aggregate sample inside the material vessel for 'compacted' and 'uncompacted' sample cases corresponding to the initial friction coefficient values of 0.0 and 0.5, respectively. In both cases, the final dimensions of the aggregate sample are close to the dimension of the laboratory sample inside the mold. A second

'compacted' sample compacted was simulated with the initial sample dimension identical to that of the 'uncompacted' sample. As expected, the final dimensions for this second 'compacted' sample were slightly different from the other 'compacted' sample as no dimensional optimization was performed. Figure 6a shows the influence of dimensional optimization of the material vessel on the response of the system to the simulated LWD drops. As indicated in this figure, for $\mu_i = 0.0$ (compacted sample), the surface deflections remain almost the same irrespective of whether dimensional adjustment was performed during the material genesis, or not. Therefore, to minimize computational effort, dimensional optimization was eliminated from all subsequent models.

Figure 6b shows the influence of the initial friction coefficient (μ_i) on the LWD-measured surface deflections. As already mentioned, the μ_i value controls initial packing of the synthetic granular assembly. If the μ_i is set to ZERO, there would be no inter-particle friction, and the particles being generated, can easily slide past each other to attain a densely packed state. On the other hand, if μ_i is set to a high value, inter-particle friction would resist the packing process, and the resulting aggregate assembly would have higher porosities. The results (see Figure 6b) indicate that the behavior of samples with lower μ_i values is similar to those for a compacted sample. Consequently, for samples with low μ_i values, the LWD-measured surface deflection and porosity values are lower. Figure 6c shows changes in the final porosity value for the sample as the μ_i changes between 0.0 to 0.7. Figures 6b and 6c both illustrate that the μ_i value in the numerical modeling process is well-correlated with the actual compaction energy applied to the sample. The effects are similar on both porosity as well as the LWD-measured surface deflection values.

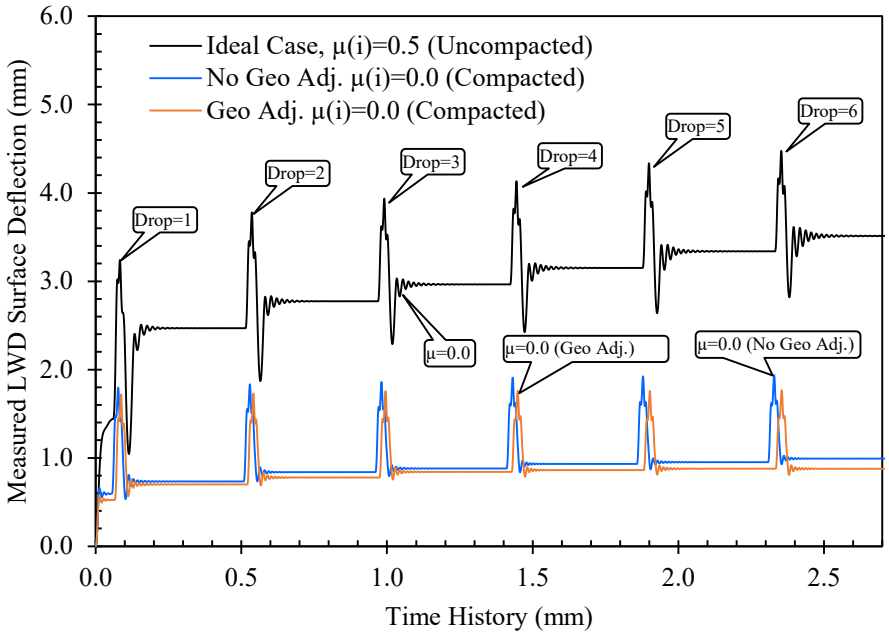

(a).

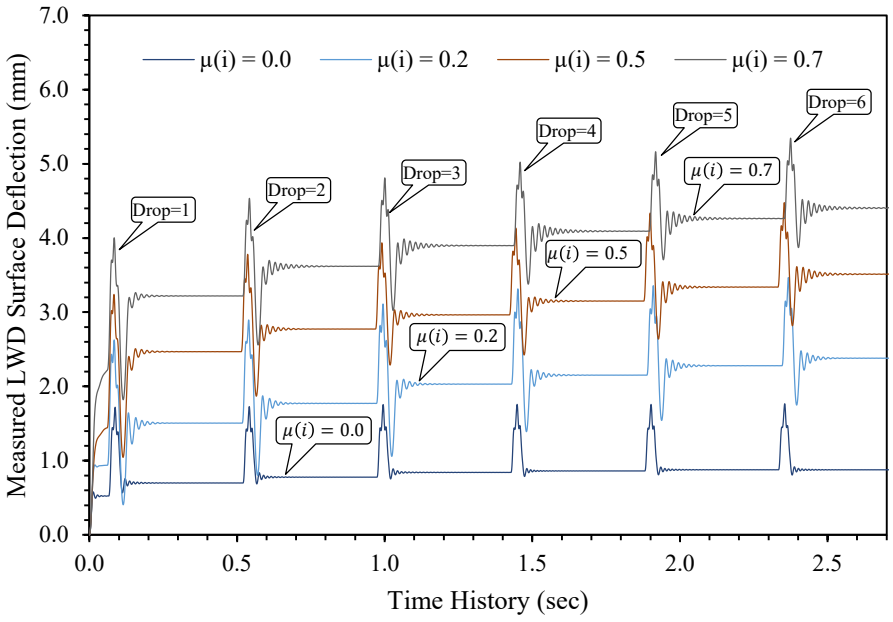

(b).

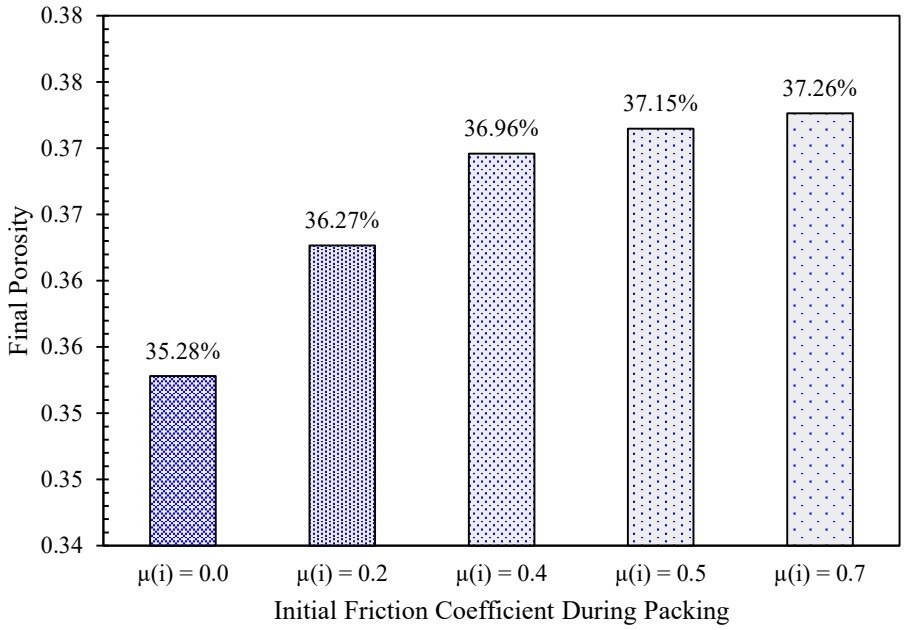

(c).

Figure 6: (a). Impact of The Sample Size and The Changes in The Initial Friction Coefficient on The Measure Surface Deflections; **(b).** Impact of The Initial Friction Coefficient on the measured Surface Deflection; **(c).** Impact of The Initial Friction Coefficient on the Final Sample Porosity

Model Validation

Once a systematic approach was identified to simulate LWD testing of OG materials in Proctor molds using DEM, the next step was to validate the model by comparing its results with those measured in the laboratory. Model validation efforts were carried out for both 'compacted' as well

as ‘uncompacted’ specimens; the details are presented in this section. As already mentioned, models with μ_i = 0 were representative of ‘compacted’ samples in the laboratory, whereas models with non-zero $\mu_i$values represented samples that were not subjected to any compactive effort in the laboratory. Figures 7a and 7b compare the LWD-measured surface deflections for the laboratory tests and the DE models. Figure 7a presents data for ‘uncompacted’ samples, whereas Figure 7b shows data for the ‘compacted’ samples. From Figure 7a shows that the average of LWD measurement drops (i.e., drops No. 4, 5, and 6) corresponding to μ_i = 0.5 closely matches the laboratory test results of the ‘uncompacted’ sample. The average deflection measured in the lab was 1.11 mm, whereas the DEM-predicted value was 1.15 mm (a 4% difference). For the compacted sample, this difference was slightly larger; the lab-measured value was 0.75 mm, whereas the DEM-predicted value was 0.88 mm (a difference of ~15%). Interestingly, the lab-measured and DEM-predicted values do not show as good for a match for the seating drops (i.e., drops No. 1, 2, and 3). The percent difference values corresponding to the seating drops for ‘uncompacted’ and ‘compacted’ samples was 15% and 14%, respectively. Except for the seating drops on the ‘uncompacted’ samples, the DEM-predicted surface deflections were always higher than those measured in the laboratory. The results discussed above clearly establish that varying the μ_i value during material genesis in DEM is a reasonable approach to simulate different levels of compaction on an OG aggregate sample. The research team is currently working on studying the effects of intermediate values of μ_i, and how they correspond to different compaction efforts in the laboratory. Results from these efforts will be presented in future manuscripts.

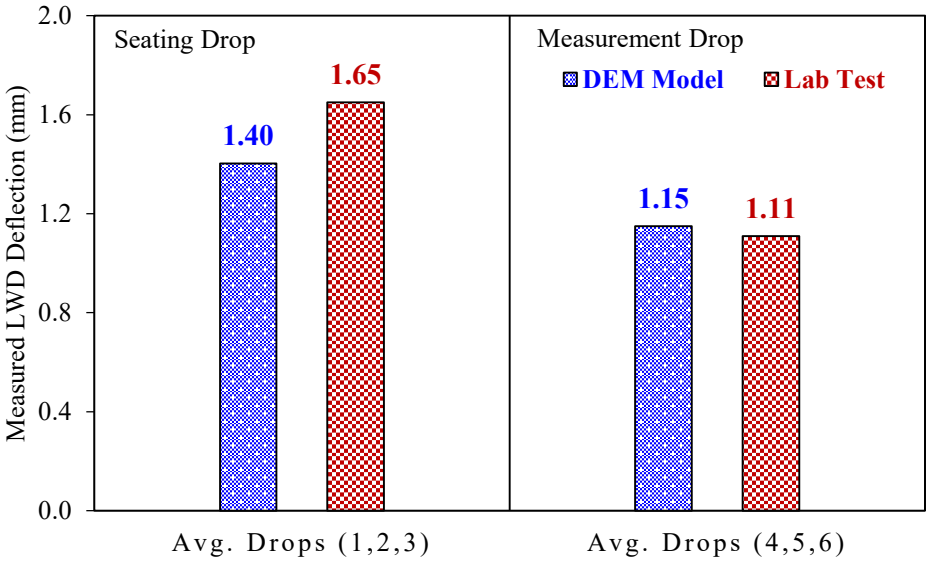

(a).

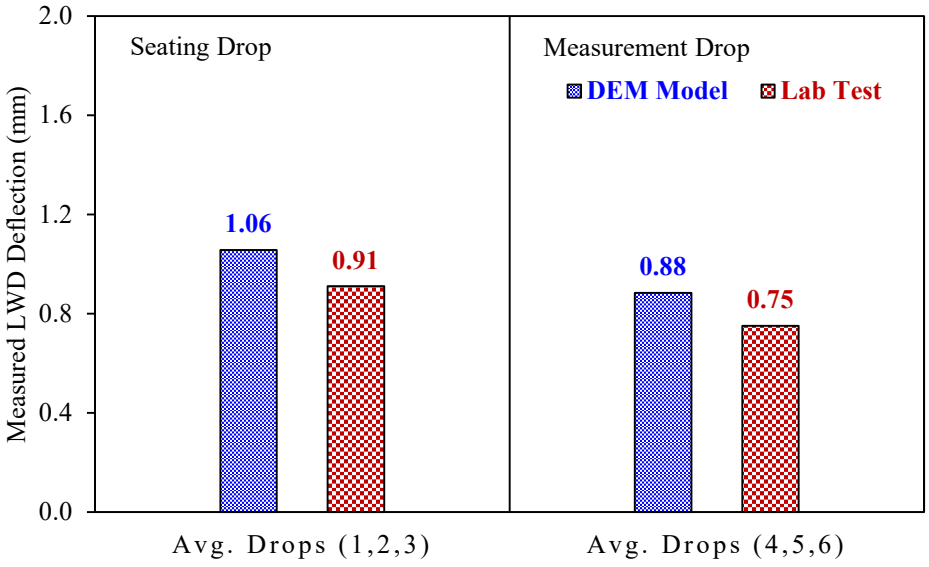

(b).

Figure 7. A Comparison Between the Numerically and Laboratory LWD-Measured Deflections of ASTM#4 Samples; **(a)** Average of Deflection for The First and Last Three Drops on Uncompacted Samples; **(b).** Average of Deflection for The First and Last Three Drops on Compacted Samples

Parametric Study on Factors Affecting OG Material Behavior

Following the model validation, parametric studies were conducted to using the DE model to study the effect of two different parameters on LWD-measured surface deflections. The primary objective in this effort was to identify factors that may play a critical role as one attempts to develop deflection-based compaction control specifications for OG aggregate materials. The two parameters considered during this parametric analysis were: (1) Final Friction Coefficient (μ_f), and (2) Modulus of Elasticity of individual aggregate particles (E_{agg}). The parametric study considered both 'uncompacted' as well as 'compacted' samples; details are presented below.

As discussed previously, the Initial Friction Coefficient (μ_f) values could be effectively used in the DE model to represent varying compaction conditions on the OG aggregate sample. Additionally, the effect of particle angularity and surface texture can be studied by altering the Final Friction Coefficient (μ_f) value. It is important to note that modern DE software packages are capable of modeling true polyhedral particles. Therefore, it is no longer necessary to use spheres to represent actual angular aggregate particles. Having said that, the LWD simulation module in the PdPkg used in the current study is capable of handling spherical particles only. Therefore, in the current research effort, the effects of aggregate angularity and surface texture on sample behavior under LWD loading are studied by altering the $\mu_f$values. The second factor considered during this parametric analysis is the aggregate particle modulus of elasticity. This is primarily aimed at capturing any differences in particle 'hardness' originating from geological differences.

Moreover, with increasing demand for marginal quality and recycled aggregates, it is important to study how aggregate materials from different sources may behave in OG aggregate layer applications. Interestingly, DEM studies reported in the literature have used a varying range of modulus of elasticity values for the aggregate particles. This range of values found in the literature was considered during the parametric study.

Figures 8 and 9 show results from parametric analyses concerning the effects of μ_f *and* E_{agg} on the response of 'uncompacted' and 'compacted' systems. Figure 8a shows that the μ_f value significantly impacts the first LWD drop on top of an 'uncompacted' sample. However, for the remaining drops, the variations become insignificant. In contrast to the effect of, the influence of μ_f, the effect of E_{agg} is substantial for each LWD drop (see Figure 8b). Similar analysis on 'compacted' samples shows that the effects of μ_f *and* E_{agg} are significant for all six LWD drops. The commonality between 'uncompacted' and 'compacted' sample behavior was that the LWD-measured surface deflection values decreased with increasing μ_f *and* E_{agg} values. From the comparisons, it is apparent that the effect of E_agg is more significant than that of μ_f.

Figure 9 shows the influence of μ_f *and* E_{agg} on permanent deformation of the synthetic granular assemblies. Given the obtained results, both μ_f *and* E_{agg} have a similarly diminishing effect on the cumulative permanent displacement. As shown in Figure 9d the permanent deformation became negative at a very high values of modulus of elasticity (i.e., for 20 and 40 GPa), indicating sample dilation. This also corresponds to instability of the compacted aggregate matrices under excessive compaction. Therefore, identification of the optimum compaction effort is essential for ensuring adequate performance of OG aggregate materials.

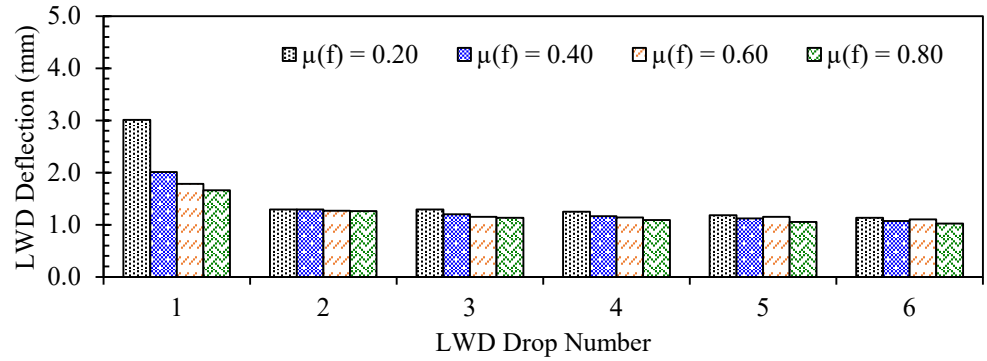

(a)

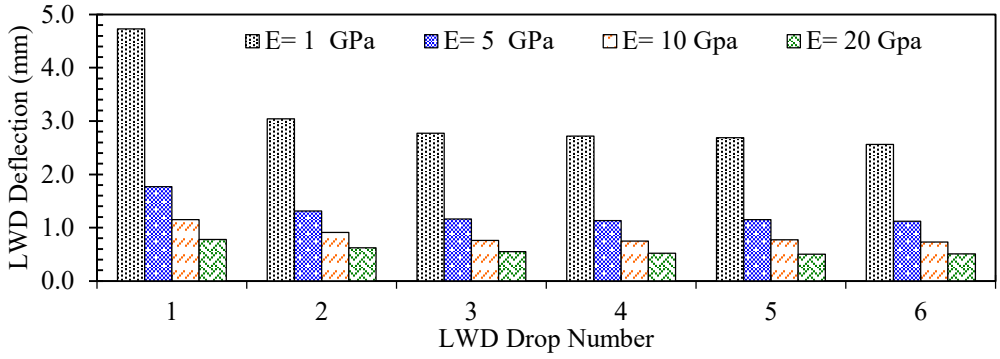

(b)

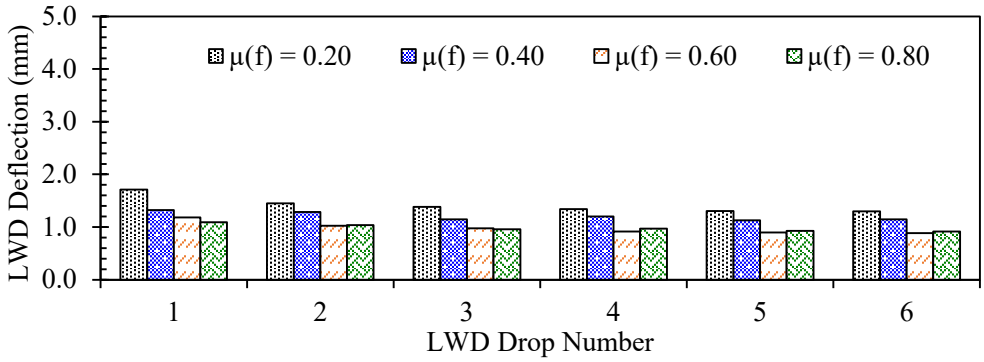

(c)

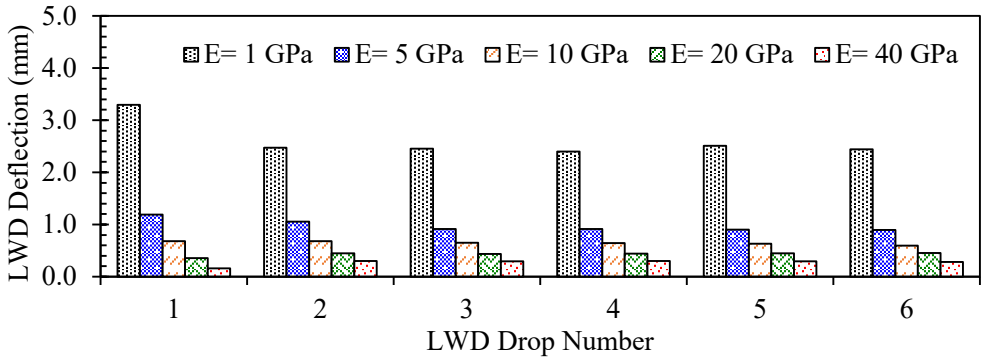

(d)

Figure 8: Measured LWD Surface Deflections: **(a**). Uncompacted Sample: Impact of Final Friction Coefficient; **(b).** Uncompacted Sample: Impact of Aggregate Stiffness; **(c**). Compacted Sample: Impact of Final Friction Coefficient; **(d).** Compacted Sample: Impact of Aggregate Stiffness.

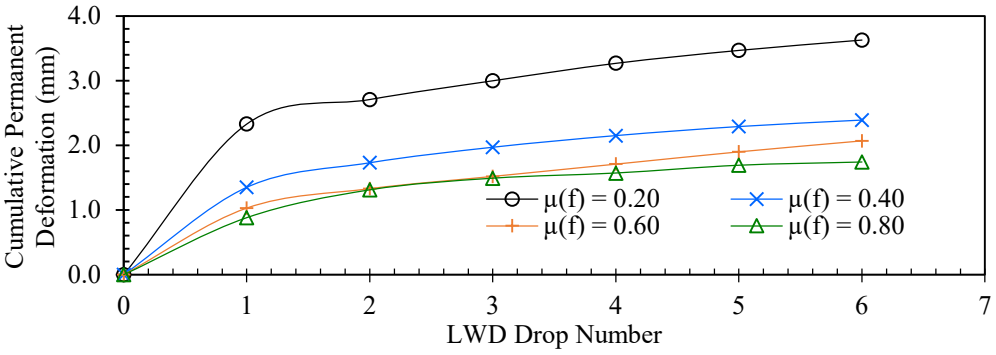

(a)

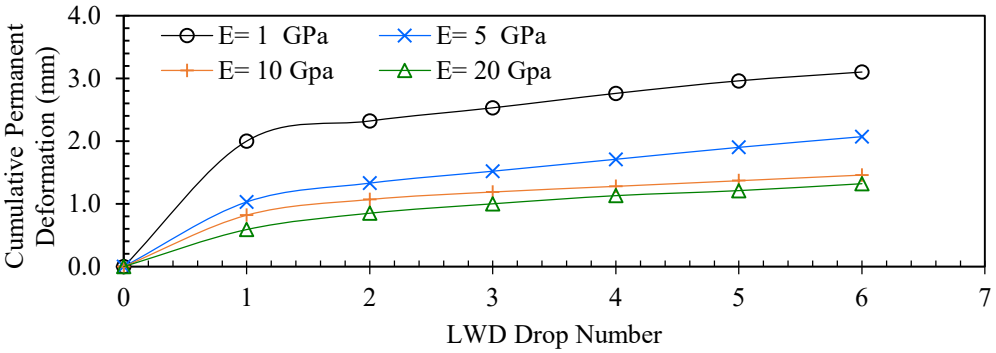

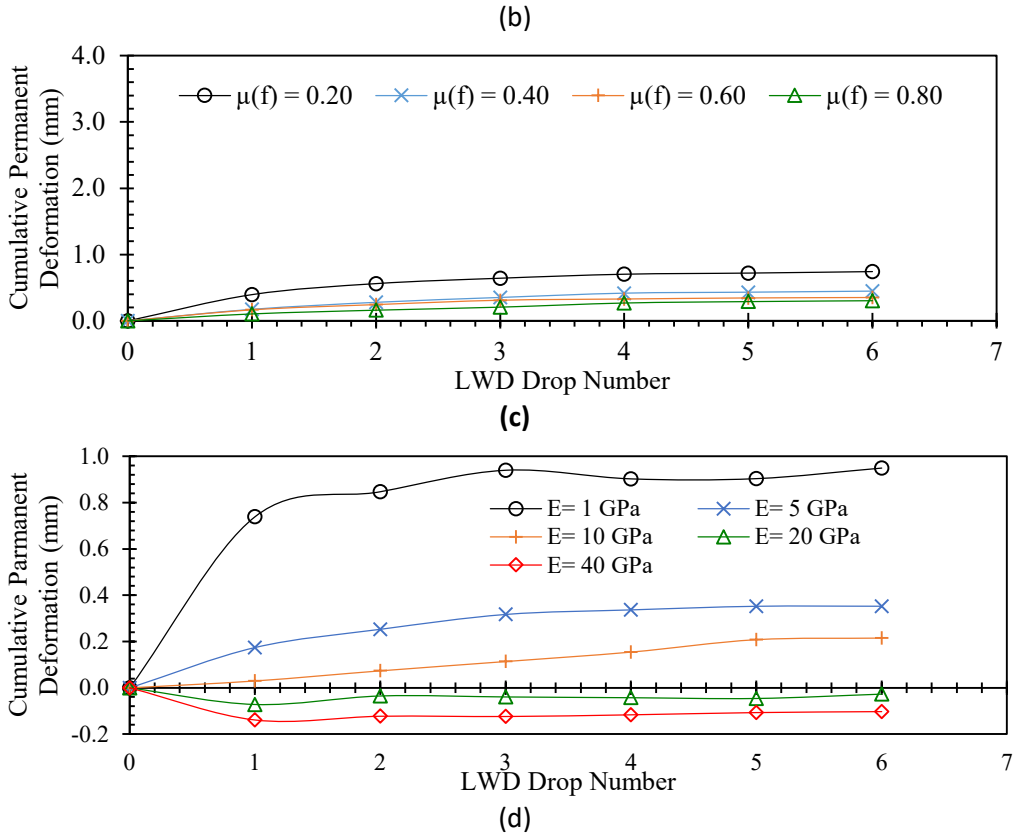

Figure 9: Measured Permanent Deformation: **(a).** Uncompacted Sample: Impact of Final Friction Coefficient; **(b).** Uncompacted Sample: Impact of Aggregate Stiffness; **(c).** Compacted Sample: Impact of Final Friction Coefficient; **(d).** Compacted Sample: Impact of Aggregate Stiffness.

Discussion of Results

The laboratory testing and numerical modeling efforts provided useful insight into the effect of degree of compaction on LWD-measured surface deflections for OG aggregate materials. Considering the laboratory test results, LWD-measured surface deflections decrease with increasing compactive efforts applied to the sample inside the mold. The numerical models showed that both inter-particle friction coefficient and modulus of elasticity of individual aggregate particles significantly affect sample response under LWD loading. As expected, the friction coefficient and modulus of elasticity parameters are inversely correlated with the LWD-measured surface deflection and permanent deformation values. However, the influence of OG aggregate particle's modulus of elasticity has a more prominent impact on sample response when compared to inter-particle friction coefficients. In addition, the numerical models also showed that a compacted sample with very hard particles (high values of E_{agg}) would exhibit dilative behavior during LWD testing. Consequently, the permanent deformation values decrease with increasing compactive effort, as long as the aggregate matrix is not 'destabilized'. In essence, this confirms that excessive compaction efforts could 'destabilize' OG aggregate matrices. Therefore, it is essential to identify the optimum amount of compaction effort for the OG aggregate materials. *The current modeling effort showed that when the LWD-measured surface deflection values for an OG aggregate material satisfying ASTM # 4 gradation specifications inside a mold is limited to a value of 0.5mm or less within the first few drops, the aggregate matrix can be said to have achieved an*

optimum level of packing. Applying further compaction effort to the sample may result in 'destabilization' of the matrix packing.

Limitations of Current Study

The current DEM modeling effort has several inherent limitations. First, in the current DEM model, OG aggregate particles have been represented using spheres. This is not a 'true' representation of an unbound granular matrix as its behavior is primarily governed by particle-to-particle interaction. In addition, the model used a modified ASTM #4 gradation, where particles larger than 37.5 mm and smaller than 19 mm were excluded from the model. This was done maximize the model computational efficiency, while at the same time keeping the model gradation close to the actual material gradation. It is important to recognize that mechanical behavior of the modified gradation may slightly differ from that for the actual material gradation. Furthermore, the current model was validated using average values of LWD seating drops and measurement drops. Therefore, LWD-measured surface deflections were not matched between laboratory and the model for each drop of the LWD mass. The behavior of the current model would be more realistic and acceptable if the model was validated for each LWD drop. However, this could not be achieved even after extensive efforts. Finally, while using the 'Boundary Contraction' procedure in the modelling of the sample, a user-defined confining pressure was applied to the material vessel. Depending on the assigned material properties, this predefined confining pressure resulted in slight changes in the final sample dimensions. In this regard, other packing procedures, such as the 'Grain Scaling', could be adopted to potentially overcome this limitation; The authors are working on modifying the numerical models to address these limitations; results from such efforts will be presented in future publications.

Acknowledgments

This research effort was sponsored by the Interlocking Concrete Pavement Institute Foundation (ICPIF). Larry Olson and Patrick Miller of Olson Engineering helped design and manufacture the scaled-up Proctor mold.

References

Dahal, B., & Mishra, D. (2020). Discrete element modeling of permanent deformation accumulation in railroad ballast considering particle breakage. Frontiers in Built Environment, 5, 145.

Eisenberg, B., Lindow, K. C., and Smith, D. R. (Eds.). (2015). "Permeable Pavements." Reston, VA, USA: American Society of Civil Engineers, ISBN 978-0-7844-7867-7.

Jibon, M., Mishra, D., and Kassem, E. (2020). "Laboratory Characterization of Fine-Grained Soils for Pavement ME Design Implementation in Idaho." Transportation Geotechnics, 25, 100395.

Lu, M., and McDowell, G. R. (2008). "Discrete element modelling of railway ballast under triaxial conditions." Geomechanics and Geoengineering: An International Journal, 3(4), 257-270.

Lu, M., and McDowell, G. R. (2010). "Discrete element modelling of railway ballast under monotonic and cyclic triaxial loading." Géotechnique, 60(6), 459-467.

Mondal, R., Rabbi, M. F., Smith, D., & Mishra, D. (2022). Compaction studies on open-graded aggregates using portable impulse plate load test devices. Construction and Building Materials, 327, 126876.

Nazarian, S., Yuan, D., and Williams, R. R. (2003a), "A Simple Method for Determining Modulus of Base and Subgrade Materials," ASTM STP No. 1437, ASTM, pp. 152-164.

Nazarian, S., Yuan, D., Tandon, V., and Arellano, M. (2003b), "Quality Management of Flexible Pavement Layers with Seismic Methods," Research Report 1735-3F, Center for Highway Materials Research, The University of Texas at El Paso, El Paso, TX.

Nazarian, S., Mazari, M., Abdallah, I., Puppala, A. J., Mohammad, L. N., and Abu-Farsakh, M. Y. (2014). Modulus-Based Construction Specification for Compaction of Earthwork and Unbound Aggregate. NCHRP Project 10-84.

Nazarian, S., Mazari, M., Abdallah, I. N., Puppala, A. J., Mohammad, L. N., and Abu-Farsakh, M. Y. (2015). Modulus-based construction specification for compaction of earthwork and unbound aggregate. Washington, DC: Transportation Research Board.

Potyondy, D. (2018) "Model-Validation Tests," Itasca Consulting Group, Inc., Technical Memorandum 2-3558-01:17TM52 (June 22, 2018), Minneapolis, MN. [ModelValidationTests.pdf]

Potyondy, D. (2019b) "Material-Modeling Support in PFC [fistPkg6.5]," Itasca Consulting Group, Inc., Technical Memorandum ICG7766-L (April 5, 2019), Minneapolis, Minnesota. [MatModelingSupport[fistPkg6.5].pdf, in fistPkgN\Documentation]

Potyondy, D. (2019c) "Hill Contact Model [version 4]," Itasca Consulting Group, Inc., Technical Memorandum ICG7795-L (April 5, 2019), Minneapolis, MN. [HillContactModel[ver4].pdf, in fistPkgN\Documentation]

Schwartz, C. W., Afsharikia, Z., & Khosravifar, S. (2017). "Standardizing Lightweight Deflectometer Modulus Measurements for Compaction Quality Assurance." (No. MD-17-SHA-UM-3-20). Maryland. State Highway Administration.

Smith, D.R. (2017). "Permeable Interlocking Concrete Pavements, 5e." Interlocking Concrete Pavement Institute (ICPI).

Smith, D. R., R. Bowers, and G. Aicken (2018). "The Lightweight Deflectometer (LWD) as an Acceptance Tool for Compacted Open-Graded Aggregates in Permeable Pavements". Proceedings of the 12th International Conference on Concrete Block Pavement; Oct. 16-19, 2018, Seoul, Korea.

Tan, D. S., Khazanovich, L., Siekmeier, J., and Hill, K. M. (2014). "Discrete Element Modeling of Effect of Moisture and Fine Particles in Lightweight Deflectometer Test." Transportation Research Record, 2433(1), 58-67.

Wang, J., Sha, A., Hu, L., and Jiang, W. (2019). "Modeling a Lightweight Deflectometer Test of Unbound Granular Materials with the Discrete Element Method." Engineering Letters, 27(1).

APPENDIX-B: PHOTOGRAPHIC RECORD OF THE CONSTRUCTION

Unprepared Subgrade

Soil Sample Collection for Laboratory Testing

Removal of Grass, Weeds

Soil Excavation

Leveling of Soil by Backhoe Loader

Leaser Level Instrument

Base-Line Marking

Indication Test cells and Transition zone by Metal Rod

Depth Checking from Base-Line

Compacting Subgrade

Prepared Subgrade

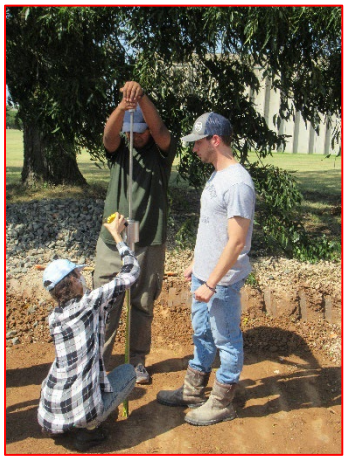

DCP Testing

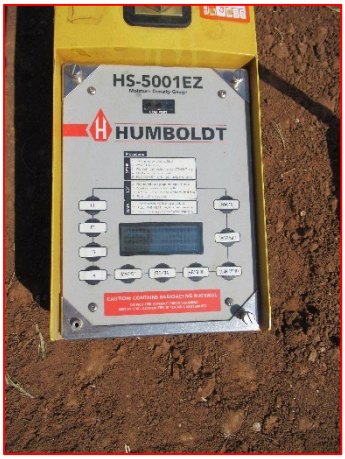

Nuclear Density Gauge

Nuclear Density testing

Geotextile Placement

Zorn LWD Testing on Subgrade

Zorn lab LWD Testing on Subgrade

Aggregate Placement and Depth Check

Compaction of 1st 4in Lift

LWD Testing on 1st Lift after Compaction

Preparing Other Test cells for Aggregate Placement

Aggregate Placement

Compaction After 2nd 6in Lift

LWD Testing after 2nd Lift (Olson)

LWD Testing after 3nd Lift (Zorn)

Zorn testing Plate

Olson Testing Plate

LWD Testing after 3nd Lift (Olson)

Placement of 4th Lift (4in ASTM#4)

LWD Testing after 4th Lift and Compacting it

Test Cell Marking

Transportation of the Excavated Soil

Used Single Steel Drum Vibratory Compactor

Breaking of the Aggregate Particle due to Over Compaction

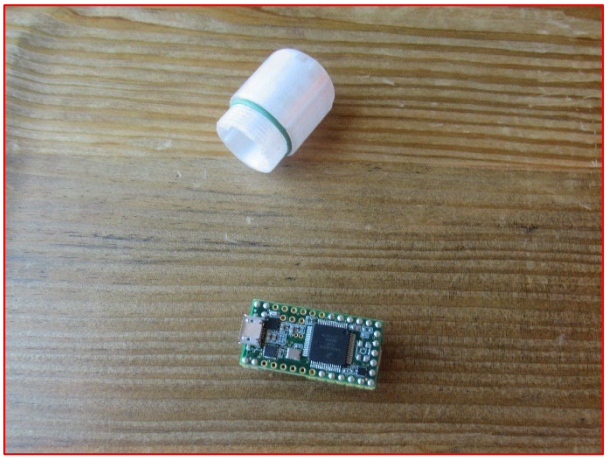

Smart-Rock

Smart-Rock Instrumentation

Geo-Cell Placement on Top of 2in Aggregate Material

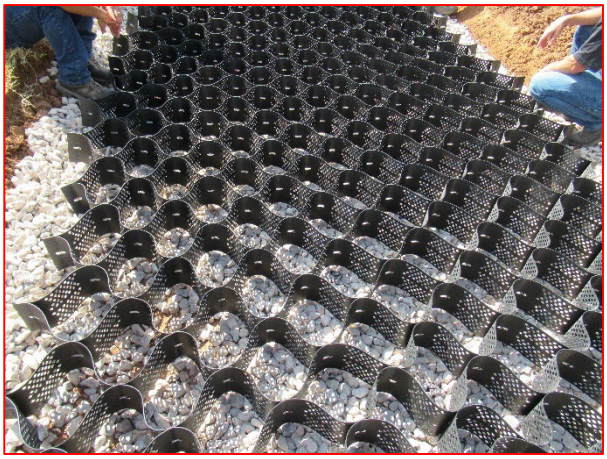

Geo-cell Opening

Placing Aggregate into the Geo-cell

Leveling the Top Surface of the Geo-Cell

LWD Testing on Geo-cell Reiforced Section (Olson)

LWD Testing on Geo-cell Reiforced Section (Zorn)

Finished Subbase and Base